การสังเคราะห์เชื้อเพลิงชนิดไอโซพาราฟินจากน้ำมันปาล์มบนตัวเร่งปฏิกิริยาวิวิธพันธุ์ชนิดกรดและเบส

นายควาง เทียน เตี่ยว

วิทยานิพนธ์นี้เป็นส่วนหนึ่งของการศึกษาตามหลักสูตรปริญญาวิทยาศาสตรดุษฎีบัณฑิต
สาขาวิชาเคมีเทคนิค ภาควิชาเคมีเทคนิค
คณะวิทยาศาสตร์ จุฬาลงกรณ์มหาวิทยาลัย
ปีการศึกษา 2559

SYNTHESIZE OF ISO-PARAFFIN FUELS FROM PALM OIL OVER HETEROGENEOUS ACID AND BASE CATALYSTS

Mr. Quang Tien Trieu

A Dissertation Submitted in Partial Fulfillment of the Requirements
for the Degree of Doctor of Philosophy Program in Chemical Technology
Department of Chemical Technology
Faculty of Science
Chulalongkorn University
Academic Year 2016

Thesis Title	SYNTHESIZE OF ISO-PARAFFIN FUELS FROM PALM OIL OVER HETEROGENEOUS ACID AND BASE CATALYSTS
By	Mr. Quang Tien Trieu
Field of Study	Chemical Technology
Thesis Advisor	Associate Professor Prasert Reubroycharoen, Ph.D.

Accepted by the Faculty of Science, Chulalongkorn University in Partial Fulfillment of the Requirements for the Doctoral Degree

.....Dean of the Faculty of Science
(Associate Professor Polkit Sangvanich, Ph.D.)

THESIS COMMITTEE

.....Chairman
(Professor Pattarapan Prasassarakich, Ph.D.)

.....Thesis Advisor
(Associate Professor Prasert Reubroycharoen, Ph.D.)

.....Examiner
(Professor Tharapong Vitidsant, Ph.D.)

.....Examiner
(Associate Professor Napida Hinchiranan, Ph.D.)

.....External Examiner
(Assistant Professor Chanatip Samart, Ph.D.)

ค ว า ง เ ที ย น เ ตี่ ย ว : การสังเคราะห์เชื้อเพลิงชนิดไอโซพาราฟินจากน้ำมันปาล์มบนตัวเร่งปฏิกิริยาวิวิธพันธุ์ชนิดกรดและเบส (SYNTHESIZE OF ISO-PARAFFIN FUELS FROM PALM OIL OVER HETEROGENEOUS ACID AND BASE CATALYSTS) อ.ที่ปรึกษาวิทยานิพนธ์หลัก: รศ. ดร. ประเสริฐ เรียบร้อยเจริญ, 123 หน้า.

งานวิจัยนี้ศึกษาเกี่ยวกับการสังเคราะห์เชื้อเพลิงไฮโดรคาร์บอนที่ประกอบด้วยพาราฟินโซ่กิ่งในปริมาณสูงและออกซิเจนในปริมาณต่ำจากน้ำมันปาล์มโดยใช้ตัวเร่งปฏิกิริยาผสมกรด-เบส ตัวเร่งปฏิกิริยาถูกนำไปวิเคราะห์ด้วยเทคนิค Nitrogen adsorption-desorption, X-ray diffraction, Hydrogen-temperature programmed reduction, CO_2 และ NH_3-temperature programmed desorption และ thermogravimetric analysis การทดสอบความว่องไวของตัวเร่งปฏิกิริยาของแข็งที่เป็นเบส (แมกนีเซียมออกไซด์, แคลเซียมออกไซด์, ซิลิกา และโซเดียมซิลิเกต) และตัวเร่งปฏิกิริยาของแข็งที่เป็นกรด (HY, H-beta, HZSM-5 และอะลูมินา) ในปฏิกิริยาดีออกซิจีเนชันของน้ำมันปาล์มด้วยเตาปฏิกรณ์แบบเซมิแบทช์ พบว่าตัวเร่งปฏิกิริยาของแข็งที่เป็นกรดและเบสที่ดีที่สุดจะถูกเลือกมาผสมกันที่อัตราส่วนปริมาตรต่าง ๆ เพื่อใช้เป็นตัวเร่งปฏิกิริยาสำหรับปฏิกิริยาดีออกซิจีเนชันของน้ำมันปาล์มที่อุณหภูมิ (400-460°C) และเวลาในการทำปฏิกิริยาที่เหมาะสม องค์ประกอบหลักในผลิตภัณฑ์ที่เป็นของเหลวที่ได้ประกอบด้วยพาราฟินโซ่ตรง, พาราฟินโซ่กิ่ง, โอเลฟินส์และอะโรแมติกส์ ในกรณีที่ใช้ตัวเร่งปฏิกิริยาของแข็งที่เป็นเบสเพียงอย่างเดียว ที่อุณหภูมิ 460°C องศาเซลเซียส โดยใช้แมกนีเซียมออกไซด์เป็นตัวเร่งปฏิกิริยาจะให้ร้อยละผลได้ของผลิตภัณฑ์ที่เป็นของเหลวมากกว่า 65% โดยน้ำหนัก ผ่านปฏิกิริยาดีคาร์บอกซิเลชันและดีคาร์โบนิเลชัน ในกรณีที่ใช้เฉพาะตัวเร่งปฏิกิริยาของแข็งที่เป็นกรดเพียงอย่างเดียว พบว่าตัวเร่งปฏิกิริยาซีโอไลต์ชนิด Beta ให้ร้อยละผลได้ของผลิตภัณฑ์ของเหลว 55% โดยน้ำหนัก ที่มีพาราฟินโซ่กิ่งปริมาณเป็นองค์ประกอบสูง อัตราส่วนตัวเร่งปฏิกิริยาผสมระหว่างแมกนีเซียมออกไซด์และ ซีโอไลต์ชนิด Beta ที่เหมาะสมคือ 3:1 ซึ่งให้ผลิตภัณฑ์ พาราฟินโซ่กิ่งในปริมาณสูง (25% และ 35% ในบรรยากาศไนโตรเจนและไฮโดรเจน ตามลำดับ)

ภาควิชา เคมีเทคนิค ลายมือชื่อนิสิต .....

สาขาวิชา เคมีเทคนิค ลายมือชื่อ อ.ที่ปรึกษาหลัก .....

ปีการศึกษา 2559

5772805823 : MAJOR CHEMICAL TECHNOLOGY

KEYWORDS: PALM OIL; DEOXYGENATION; BIO-OIL, MIXED ACID-BASE CATALYST, ISO-PARAFFIN

QUANG TIEN TRIEU: SYNTHESIZE OF ISO-PARAFFIN FUELS FROM PALM OIL OVER HETEROGENEOUS ACID AND BASE CATALYSTS. ADVISOR: ASSOC. PROF. PRASERT REUBROYCHAROEN, Ph.D., 123 pp.

This study focused on the synthesis of hydrocarbon fuel containing a high iso-paraffin and very low oxygen content from palm oil using a mixed acid-base catalyst. The catalysts were characterized by nitrogen adsorption-desorption, X-ray diffraction, hydrogen-temperature programmed reduction, carbon dioxide- and ammonia-temperature programmed desorption as well as thermogravimetric analysis. Solid base (MgO, CaO, SiO_2 and Na_2SiO_3) and solid acid (HY, H-beta, HZSM5 and Al_2O_3) catalysts were individually evaluated for their catalytic activity in a semi-batch reactor in terms of the deoxygenation level of palm oil. The best acid and alkali catalyst were then selected for mixing at different volume ratios for catalytic deoxygenation of palm oil. Finally, the reaction temperature (400–460 °C), residence time were optimized. The main components in the liquid product obtained were normal paraffins, iso-paraffins, olefins and aromatics. For the single base catalysts, a liquid yield of higher than 65 wt.% was obtained at a 460 °C using MgO catalyst, which also realized an excellent decarboxylation and decarbonylation. For the single acid catalysts, the zeolite beta catalysts reached a liquid yield of around 55 wt.% with a high iso-paraffin content. The optimal MgO: beta zeolite ratio for the acid-base hybrid catalyst was 3:1, which resulted the products with a high iso-paraffin content (25% and 35% in nitrogen and hydrogen atmosphere, respectively).

Department: Chemical Technology Student's Signature .....

Field of Study: Chemical Technology Advisor's Signature .....

Academic Year: 2016

ACKNOWLEDGEMENTS

The author would like to express his sincere thanksgiving to Assoc. Prof. Dr. Prasert Reubroycharoen, his advisor, who has dedicated his guidance and supports during author doing this project. The author also would like to acknowledge the dissertation examination committee including: Prof. Dr. Pattarapan Prasassarakich (chairman), Prof. Dr. Tharapong Vitisant (examiner), Assoc. Prof. Dr. Napida Hinchiranan (examiner) and Asst. Prof. Dr. Chanatip Samart (external examiner) for their helpful comments and suggestions. The author really appreciate the supports of Assoc. Prof. Dr. Chawalit Ngamcharussrivichai and Asst. Prof. Dr. Chaiyan Chaiya who help him characterize the samples in his research. The author would like to acknowledge Chemical Technology Department, Chulalongkorn University has created favorable conditions for the author to carry out his study. The author would like to express his gratitude to the scholarship for international graduate student in ASEAN countries from Graduate school, Chulalongkorn University. Thanks to the team of technicians and friends in the Chemical Technology Department, Chulalongkorn University who has helped author doing his project. Finally, the author would like to express his deep thanksgiving to the family who have always supported and encouraged him to have motivation to overcome difficulties.

CONTENTS

Page

Page

Page

Page

LIST OF ABBREVIATIONS

^{o}C	: Degree Celsius
CO_2-TPD	: Carbon dioxide temperature programmed desorption
NH_3-TPD	: Ammonia temperature programmed desorption
MPa	: Megapascal
LHSV	: Liquid hour space velocity
mL	: Milliliter
cm	: Centimeter
nm	: nanometer
min	: Minute
h	: Hour
g	: Gram
mmol	: Millimol
%wt	: Weight percentage
%	: Percentage
ΔH	: Enthalpy
kJ	: Kilojoule
cal	: Calorie
2θ	: Two-theta angle
GC	: Gas chromatography
TCD	: Tip to Collector Distance
FID	: Flame ionization detector
GC-MS	: Gas chromatography–mass spectrometry

BET	: Brunauer–Emmett–Teller
XRD	: X-ray diffraction
TPR	: Temperature programmed reduction
TGA	: Thermal gravity analysis
MW	: Molecular weight

LIST OF TABLE

LIST OF FIGURE

CHAPTER I:
INTRODUCTION

1.1 Background

The global energy crisis is an issue of increasing global concern because the supply of and demand for energy is becoming increasingly unbalanced, with more than 80% of current energy coming from non-renewable fossil resources, which are not globally distributed and will become scarce. Therefore, alternative energy resources have been developed in an attempt to fulfil the lack of energy resources and distribute the energy production ability more evenly across populations to match local demands with increased geopolitical independence. Diesel, currently mostly derived fossil fuel (petroleum diesel), is an important energy source that is used in diverse sectors from from agriculture to industry, in not only engines but also in power generation and as heating oil. However, the combustion of petroleum diesel produces air pollution asides from carbon particulates, due to the presence of heteroatoms, such as sulfur and nitrogen that form on combustion gaseous sulphur oxides (SO_x) and nitrogen oxides (NO_x). To resolve the energy scarcity and environmental pollution, biodiesel has been used as a partial replacement for petroleum diesel

The development of biodiesel is now into 2nd generation biofuel commercially (and 3rd generation experimentally). Initially (1st generation) biofuel was developed as bioethanol, biogas and biodiesel (as fatty acid alkyl esters), the biodiesel being produced by the transesterification of edible oil with methanol or, to a lesser extent, ethanol. However, the use of edible oils represented an economic and moral clash with food production and so 2nd generation biofuel was developed, which is produced from non-food materials, including non-edible oils and waste oil, and so this approaches a neutral carbon cycle [1]. The 2nd generation biofuel is similar in structure to the fossil derived fuel oils, including the biodiesel being similar to petroleum diesel, except, importantly, for a typically much lower N and S heteroatom content in biodiesel. One method in 2nd generation biofuel production is the deoxygenation reaction, where the oil is derived through decarboxylation, decarbonylation and

dehydration to remove the oxygen content from the oil. Noble metal catalysts yield a present excellent performance in the hydrodeoxygenation (HDO) reaction, where a hydrocarbon content of over 85% was obtained with palladium (Pd) or platinum (Pt) catalysts. However, these noble metals are expensive [2-4]. Nickel (Ni)-based catalysts were introduced as cheaper alternatives for HDO, where bimetallic Ni-molybdenum (Mo) catalysts gave a high selectivity of hydrocarbons (up to 80%) by the Ni component catalyzing the hydrogenation, HDO and hydrodecarboxylation reaction pathways [5, 6]. Likewise for Ni-cobalt (Co) bimetallic catalysts, it was proposed that the Ni catalyst mainly promoted the HDO, while the Co catalyst played the main catalytic role in hydrodecarboxylation and hydrodecarbonylation [7]. Unfortunately, either hydrodeoxygenation or hydrodecarboxylation require a critical hydrogen pressure (20-50 bars and over) and that is entirely a challenge for designation, cost together with operation.

Alkali catalysts, such as CaO and MgO, have been proposed for the deoxygenation of waste cooking oil through decarboxylation and decarbonylation without the presence of hydrogen atmosphere [8-10]. In the addition of alkali catalysts, the acidic zeolitic material catalysts exhibit good catalytic activity in the deoxygenation reaction and have been developed to produce diesel-like fuel by deoxygenation. These acid catalysts not only promoted the removal of oxygen via decarboxylation and decarbonylation reactions, as per the alkali catalysts, but also catalyzed the transformation of the hydrocarbon structure, including isomerization, alkylation and cracking to obtain high quality fuel oils [11-13].

1.2 Objective

This research was to evaluate the catalytic performance, in terms of the deoxygenation reaction, of a mixed acid-alkali catalyst to produce a high quality liquid fuel. The mixing of the selected (best performing) acid and alkali catalyst resulted in a synergistically improved deoxygenation activity and improved fuel properties. The optimal acid-base catalyst weight ratio was determined and then the reaction was optimized by evaluating the effect of the reaction temperature, pressure in a hydrogen (H_2) or

nitrogen (N_2) atmosphere, and the reactant residence time on the quality and yield of the obtained fuel oil.

1.3 Scope of the research

1. Literature review

2. Prepare necessary tools, equipment and chemicals for experiment.

3. Prepare two kinds of catalysts:

- Base catalysts:

- SiO_2, MgO, CaO: commercial catalysts

- Na/SiO_2: prepared by wet impregnation method

- Acid catalysts:

- Zeolite Y, Zeolite beta, HZSM-5, γ-Al_2O_3: commercial catalysts

- Pd/Acid catalyst: prepared by incipient wetness impregnation method

4. Characterize physicochemical properties of fresh and used catalyst: XRD, N_2 physical adsorption, TPR, NH_3-TPD, CO_2-TPD, and TGA

5. Study the production of iso-paraffinin fuels in semi-batch reactor with internal volume of 80 mL

- Temperature: 400 – 460 ^{o}C

- Gas: N_2 at 0.1 MPa, or H_2 at 0.1 – 1 MPa

- Catalysts: single catalyst, mixed base/acid catalyst at different volume ratio of 1:2, 1:1, 2:1

- LHSV: 0.36 – 0.72 hr^{-1} (volume of catalyst is kept constant at 25 mL)

6. Study on reaction mechanism of iso-paraffin synthesis

7. Analyze properties of gaseous and liquid products:

- Gas product**:** GC with TCD and FID

- Liquid product: GC FID, GC-MS, acid number, iodine Number, heating value, olefin content by sulfonic acid.

1.4 Expected results

The high quality of fuel which has high iso-paraffin and low oxygen content is expected to be obtained at the optimum reaction condition. The individual functions of basic and acid in the mixed catalyst also need to clarify in order to explain the reaction mechanism.

CHAPTER II:
THEORY AND LITERATURE REVIEWS

2.1 Biofuel from palm oil

2.1.1 Palm oil

Palm oil is a vegetable oil from palm tree (Elaeis guineensis) which is a species of palm. Similar to other vegetable oils, main compound in palm oil are triglyceride of fatty acids and it is known as the high saturated oil due to high concentration of saturated fatty acid with around 50 mol.% as revealed in table 2.1 [14]

Table 2.1 *Fatty acid composition in palm oil*

Fatty acid	Number of carbon	Formula	Percentage **(%)**
Lauric acid	$C_{12:0}$	$C_{12}H_{24}O_2$	0.8
Myristic acid	$C_{14:0}$	$C_{14}H_{28}O_2$	1.2
Palmitic acid	$C_{16:0}$	$C_{16}H_{32}O_2$	44.5
Palmitoleic acid	$C_{16:1}$	$C_{16}H_{30}O_2$	0.1
Stearic acid	$C_{18:0}$	$C_{18}H_{36}O_2$	3.8
Oleic acid	$C_{18:1}$	$C_{18}H_{34}O_2$	39.7
Linoleic acid	$C_{18:2}$	$C_{18}H_{32}O_2$	9.3
Linolenic acid	$C_{18:3}$	$C_{18}H_{30}O_2$	0.2
Arachidic acid	$C_{20:0}$	$C_{20}H_{40}O_2$	0.3
Eicosenoic acid	$C_{20:1}$	$C_{20}H_{38}O_2$	0.1

Together with coconut oil and olive oil, palm oil is one of edible vegetable oil which is used for cooking, and in certain area as Asia, Africa or South America it is a common ingredient for cooking. Recently, vegetable oil production all over the world experienced the remarkable increasing, especially in America and Brazil to satisfy

multiple demands such as: cooking oil, for making cosmetic, for emerging non-edible application. It is forecasted there will be nearly 206.8 million metric tons of vegetable oil produced on 2020 with three key product segments are: soybean, palm oil and olive (figure 2.1).

As mention before, beside used for edible purposes, palm oil also used as feed stock for biofuel production, and with the increasing of vegetable oil across the globe, palm oil is one on the most promising raw material for making alternative energy via several conversion methods such as: transesterification, hydrodeoxygenation, thermal cracking, catalytic cracking, decaboxylation.

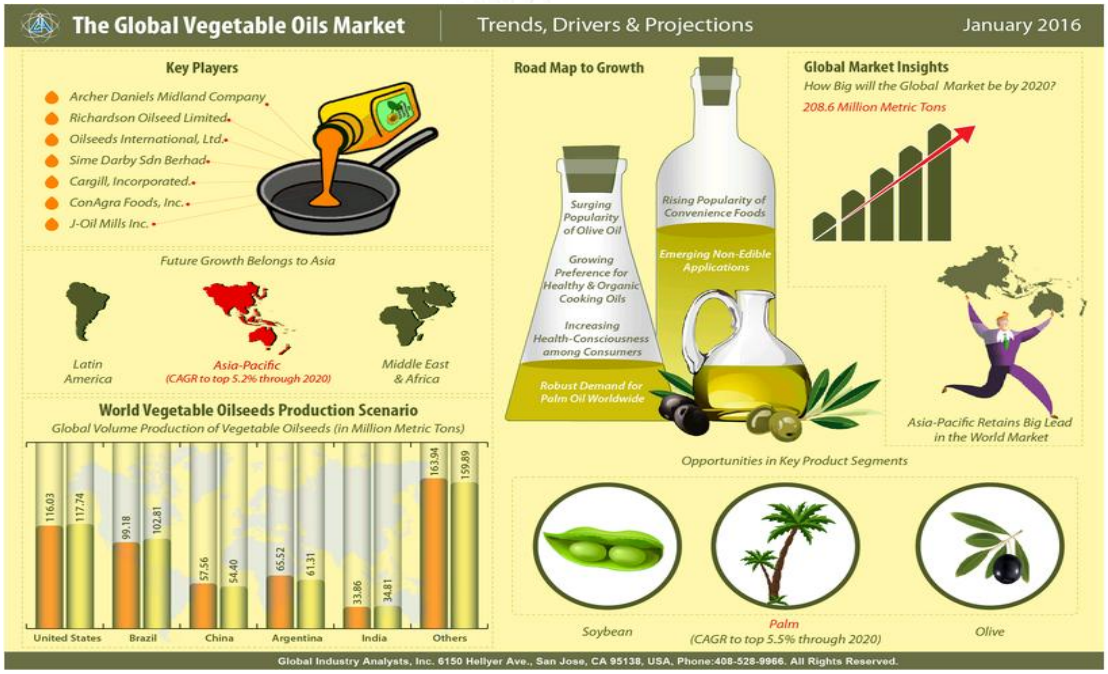

Figure 2.1 *The global vegetable oil on 2016. Source: Global industry analysts, Inc, 6150 Hellyer Ave, San Jose, CA 95138, USA.*

2.1.2 Thermal cracking

Thermal cracking is known as the oldest chemical process that is used to decompose organic compound to be smaller product compounds without the present of catalyst. In order to produce biofuel from alternative resources like vegetable, thermal cracking is also one of efficiency process that is used to convert triglyceride or fatty acid in

vegetable to into lighter products which are able to have the fuel property similar to gasoline or diesel from traditional fuel.

Due to the thermodynamic of cracking process which is favorable at high temperature, it can be carried out from 350 ^{o}C or higher depending on the expected range of product [15-21]. It was reported that at 450 – 540 ^{o}C they were able to obtain about 47 wt.% of light cycle oil and more than 21 wt.% of gasoline product from thermal cracking of canola oil in a continuous pilot plant [22]. Anyway, the increasing of temperature and residence time may cause producing various kind of side products like gas and coke due to many kind of secondary reaction occurring at extreme reaction [16, 23]. Thermal cracking of organic compounds happen follow the free radical mechanism and it has two type mode of reaction pathway as below:

a) Primary reaction: large molecules are decomposed into smaller species

$$CH_3CH_2CH_2CH_3 \longrightarrow CH_4 + CH_3CH{=}CH_2 \quad (2.1)$$

$$CH_3CH_2CH_2CH_3 \longrightarrow CH_3\text{-}CH_3 + CH_2{=}CH_2 \quad (2.2)$$

b) Secondary reaction: forming large molecules by the active of free radical group

$$CH_2{=}CH_2 + CH_2{=}CH_2 \longrightarrow CH_3CH_2CH{=}CH_2 \quad (2.3)$$

$$R.CH{=}CH_2 + R_1.CH{=}CH_2 \longrightarrow \text{coke and other products} \quad (2.4)$$

Via thermal cracking reaction, we are able to obtain lighter product in range of diesel and gasoline fraction from vegetable oil. However, by the high active of free radical group at high temperature, thermal cracking of vegetable oil is favorable to forming olefins and coke rather than paraffin or branched paraffin which are always the expectation compounds in high quality fuel.

2.1.3 Catalytic cracking

Catalytic cracking is the innovation process in the purpose of decomposition of large hydrocarbon chain or organic compound into smaller products by adding the function

of catalyst in reaction. The reaction mechanism of catalytic cracking of long chain hydrocarbon on zeolite can be described as below: [24]

- Thermal cracking:

$$nC_8H_8 \longrightarrow CH_4 + CH_3\text{-}(CH_2)_4\text{-}CH{=}CH_2 \qquad (2.5)$$

- Proton shift: (on zeolite H-Z)

$$CH_3\text{-}(CH_2)_4\text{-}CH{=}CH_2 + H\text{-}Z \longrightarrow CH_3\text{-}(CH_2)_4\text{-}CH^+\text{-}CH_3 + Z^- \qquad (2.6)$$

- Cracking C-C bond at the C^+ to form carbenium ions and olefins:

$$CH_3\text{-}(CH_2)_4\text{-}CH^+\text{-}CH_3 \longrightarrow CH_3\text{-}CH{=}CH_2 + CH_2^+\text{-}CH_2\text{-}CH_2\text{-}CH_3 \qquad (2.7)$$

The new carbenion is going to react with other paraffin molecules in the chain reaction. The reaction is terminated in case of:

- The carbenion losses a proton and converts to olefin on catalyst.

- The carbenion converts to paraffin when it picks up a hydride ion from coke.

Beside the primary cracking reaction to form smaller hydrocarbons, there are various secondary reaction due to hydrogen transfer mechanism like isomerization, or cyclisation:

- Isomerization:

Secondary cabenium ion — Tertiary carbenium ion (2.8)

- Cyclisation:

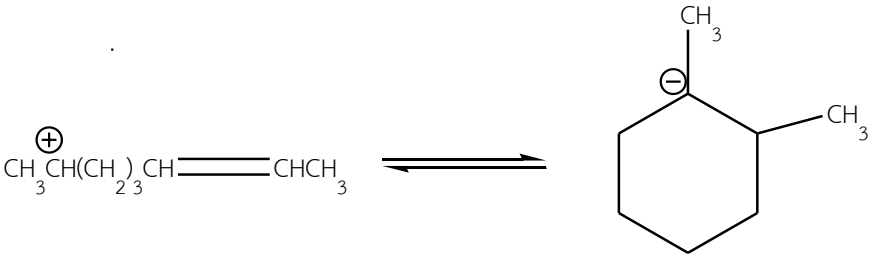

(2.9)

The final product from isomerization will be iso-paraffins while naphthenes or coke will be formed via cyclisation.

The main source supply proton for catalytic cracking reaction is commonly known as zeolite. The first generation of solid acid catalyst which had been used for cracking of petroleum residue was amorphous zeolite with high content of SiO_2 (87% SiO_2 13% Al_2O_3), then the composition of silica in catalyst had been adjusted to be lower (75%) in order to increase the acidity of catalyst which were more favorable for cracking purpose. [23]. However, high acidity also promote coke formation at high temperature beside isomerization, alkylation or cyclisation, the point is that it is necessary to balance among various kind of factors [25, 26].

Catalytic cracking has been also used to synthesize biofuel from vegetable oil because the present of catalyst can control the selectivity of desired products. According to report from [27-29], catalysts were used for cracking of vegetable oil were solid acid such as zeolite Y, HZSM-5, alumina in the range of reaction temperature from 480 to 540 °C at atmospheric pressure. The reaction pathway can be described as below:

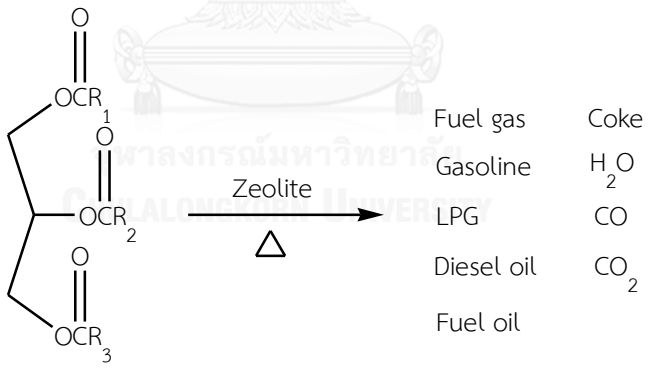

Figure 2.2 *Reaction conversion of triglyceride on zeolite catalyst*

By using catalytic cracking of vegetable, the obtained products represent the fuel property very close to with fuel from fossil resources when we are able to get high quality product like iso-paraffin, paraffin or even aromatic which are the essential component in gasoline and diesel. However, olefin still the main compounds in cracked oil and it is unexpected composition in fuel cause of its unstable oxidation ability [30-32]. In addition, high content of oxygen in biofuel which is obtained from

catalytic cracking of vegetable oil, because acid catalysts are not high selective for deoxygenation of triglyceride and fatty acid.

2.1.4 Hydrodeoxygenation

In order to produce renewable fuels with higher quality from alternative resources, hydrodeoxygenation (HDO) of bio-oil and vegetable oil has been investigated as one of the most effective technique when it is able to manufacture bio-fuel which have comparable property to original fuel from crude oil. The HDO process require an extreme hydrogen pressure and carrying out on the bi-functional catalyst which formed from noble metals and acidic supports such as: Pt/HZSM-5, Pd/HY, NiMo/γ-Al_2O_3, NiCo/γ-Al_2O_3-HZSM-5, Re-MoO_x/TiO_2 [33-35]. There are multiple reaction happen during HDO of bio-oil and vegetable oil and main expected product of this process is the mixture of hydrocarbons in the range from gasoline to gasoil which is able to use as the feed stock for bio-refining factory.

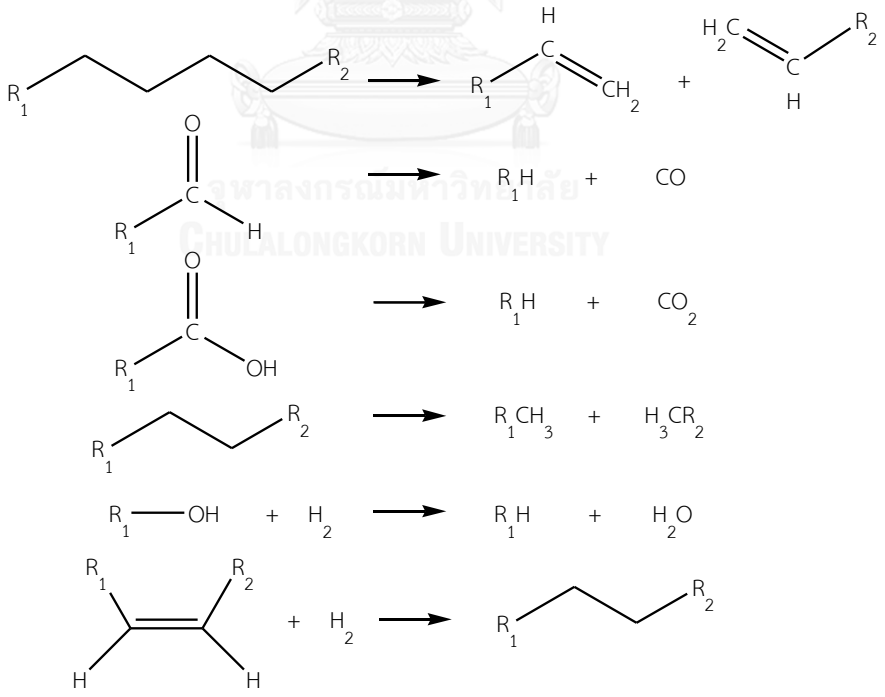

Figure 2.3 *Reactions associated with catalytic bio-oil [33]*

Figure 2.3 revealed primary reaction in HDO of bio-oil which are almost endothermic reaction and the product is promising represent low oxidation degree because almost

unsaturated compound will be hydrogenated under high hydrogen pressure. Beside primary reaction to produce hydrocarbon from oxygenate compound, the HDO of bio-oil also has various secondary reactions as below:

1) Water gas shift reaction:

$$CO + H_2O \longleftrightarrow CO_2 + H_2 \text{ , } \Delta H = -43.7 \text{ kJ/mol} \quad (2.8)$$

2) Methanation:

$$CO + 3H_2 \longleftrightarrow CH_4 + H_2O \text{ , } \Delta H = -203.7 \text{ kJ/mol} \quad (2.10)$$

3) Hydrogenation of propylene to propane

$$CH_2{=}CH\text{-}CH_3 + H_2 \longleftrightarrow C_3H_8 \text{ , } \Delta H = -125.1 \text{ kJ/mol} \quad (2.11)$$

Additionally, the liquid fuel may has higher benefit due to high content of branched hydrocarbons which are the product of hydroisomerization reaction in the same reaction condition [36]. The mechanism for hydroisomerization mechanism as in figure 2.4. There are six steps of reaction through various intermediate substances over distinct corresponding catalytic sites. The immediate olefin is formed in the first step of the process through the dehydrogenation on metal site. Then, as the high mobility of olefin, it is easy to receive the proton H^+ form acid site of acidic support to create carbocation. Skeletal believed that there is the rearrangement of a carbocation ion through a cyclo-alkyl intermediate [37] and forming the iso-paraffinic carbocation which is subsequently converted to an olefin by loss of a proton to the acid site after that. Finally, iso-olefin is hydrogennated very quickly on metal site to product the iso-paraffin product.

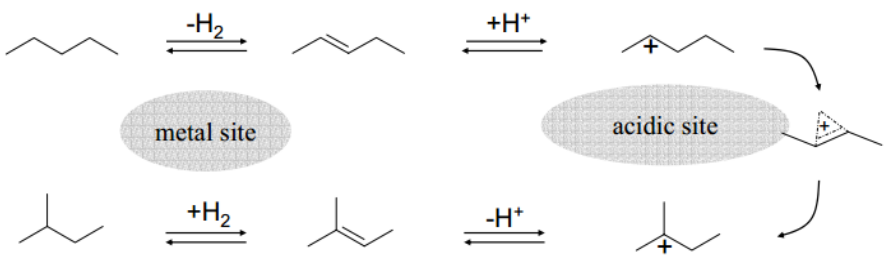

Figure 2.4 *Hydroisomerization of n-alkane over bifunctional catalyst [36]*

Although hydrodeoxygenation is able to upgrade the quality of bio-fuels because the obtained fuel is similar with that from fossil resources together with high content of branched paraffins which are the most expected compound in fuel, the reaction require very high hydrogen pressure which is the big challenge for designation and operation.

2.1.5 Decarboxylation and decarbonylation

Decarboxylation and decarbonylation of triglyceride is an effective process to produce hydrocarbons directly as the renewable fuel. Theoretically, decarboxylation reaction of fatty acid or fatty acid ester which are the chemical reaction occurring to remove (-COO-) group in fatty ester or acid to release CO_2 gas and corresponding hydrocarbon with or without the present of catalyst. This reaction can be carried out as the thermal cracking reaction when heating up fatty carboxylic acids or those ester at high temperature (normally higher than boiling point of that acid or ester). Anyway, without the present of catalyst, the selection for oxygen removal via decarboxylation and decarbonyl is not as high as the expectation of high quality fuel.

The presence of catalysts is not only able to decrease reaction temperature to minimize light hydrocarbon gas due to the thermal cracking at high temperature but it is also able to generate decarboxylation and decarbonylation reaction to eliminate oxygen in obtain fuel. There are many kinds of catalysts were studied like Pd/C, SiO_2, MgO etc. and each catalyst has particular advantages and disadvantages.

The traditional catalysts for decaboxylation of fatty acid and triglyceride is firstly novel metal like Pd. The typical mechanism for decarboxylation of acid carboxylic on Pd catalyst was referred from [38]:

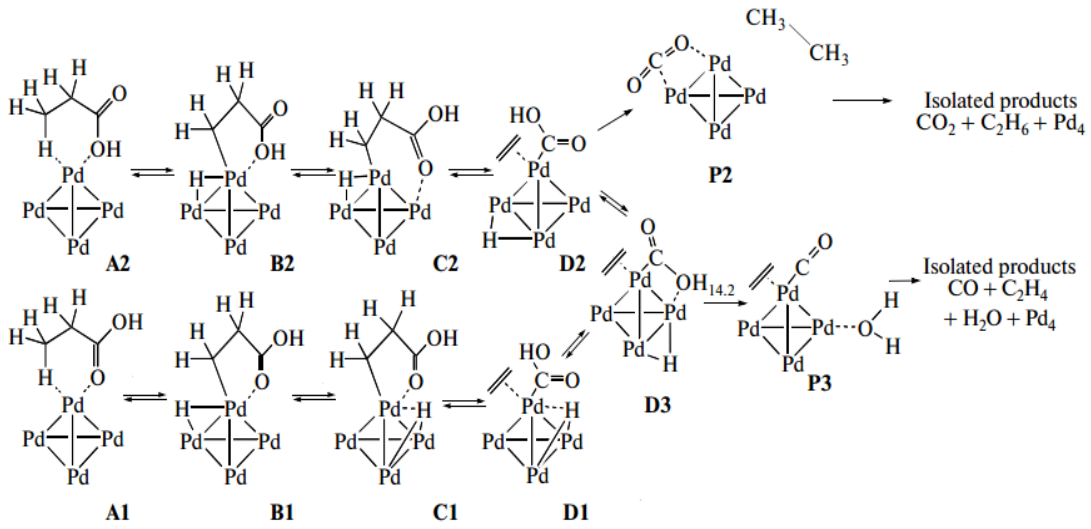

Figure 2.5 *Decarboxylation of carboxylic acid on Pd catalyst.*

However, the use of Pd for decarboxylation of fatty acid is not favorable from economic perspective due to high cost of novel metal so that it is possible to apply in industry. On the other hand, from previous research [39, 40] the Pd catalyst was deactivated very quickly and the reaction conversion could be dropped to under 10% just 10 to 20 minutes due to the coke forming on the surface of catalyst.

Recently, solid base catalysts has taken the attention of researcher when they found its ability that is able to use as the most effective catalyst for decarboxylation of fatty acid and triglyceride at soft reaction condition without the present of hydrogen. In addition, the decaboxylation and decarbonyl of fatty acid and triglyceride on base catalyst not only represent the high selective of CO_2 and CO removal but also can be low down acid value of crack oil which has been the unexpected property of fuel from pyrolysis or catalytic cracking of biomass.

Mechanism for decarboxylation on base catalysts [41]:

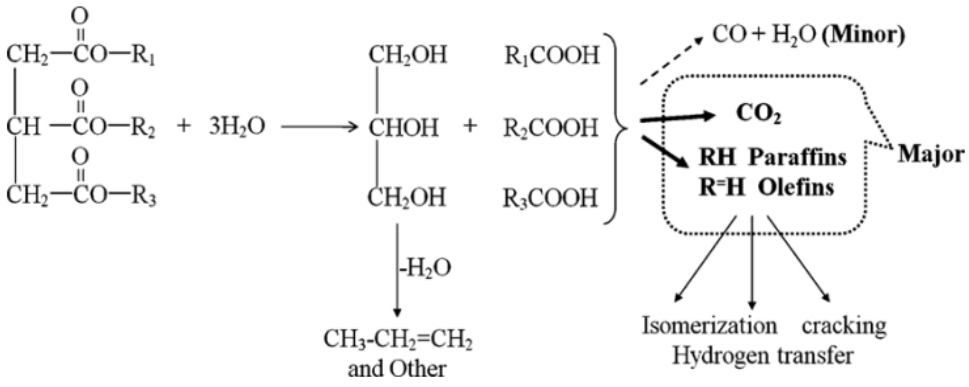

Figure 2.6 *Decarboxylation of triglyceride on MgO*

2.1.7 Catalytic characteristic

2.1.7.1 Specific surface area

The specific surface area of solid catalysts were determined by Brunauer–Emmett–Teller (BET) equation via nitrogen physical adsorption. BET analysis is known as the most common and effective technique to explain the surface morphology of solid such as surface area, pore size, pore volume, pore size distribution.

Principle:

BET analysis with nitrogen is the gas adsorbed will be conducted at boiling temperature of nitrogen (77 K), the total volume of gas absorbed versus the increase and decrease of P/P^{o} for adsorption and desorption, respectively, will be recorded for identify surface morphology of catalyst via BET equation:

$$\frac{P}{V.(P_0 - P)} = \frac{1}{V_m.C} + \frac{C-1}{V_m.C}.\frac{P}{P_0}$$

With:

P: total pressure (mmHg)

P_0: vapor pressure of adsobate at test temperature (mmHg)

V: vol. of gas adsorbed at standard (0 °C, 760 mmHg)

V_m: vol. of monolayer of gas adsorbed at standard ($cm^3.g^{-1}$)

C: constant related to $\Delta H_{ads} \sim \exp[(\Delta H_{cond} - \Delta H_{ads})/RT]$

Plotting the curve of $\frac{1}{V(P_0 - P)}$ versus P/P_0, it is easy to see that that relationship is linear in the range of pressure $0,05 < P/P_0 < 0,3$, with the slope is $\frac{C-1}{V_m.C}$ and the intercept is $\frac{1}{V_m.C}$, V_m will be determine by follow equation:

$$S_g = \frac{V_m.N.A}{M}$$

With:

S_g: surface area of adsorbent (m^2/g)

V_m: vol. of monolayer of gas adsorbed at standard ($cm^3.g^{-1}$)

N: 6.022×10^{23} (molecule/mole)

A: projected area of adsorbate (in case of nitrogen gas, A= 16,2 A^o)

M: molar weight of adsorbate (g/mol)

2.1.7.2 Acidity and basicity

In order to assess the characteristic of material's active surface, the chemical adsorption isotherm has been developed and used as the most powerful technique since 1950's [42]. Depend on which kind of active surface area that we want to know, there are three principle which are able to use to evaluate as a function of temperature namely: temperature programmed desorption (TPD), temperature programmed reduction (TPR), and temperature programmed oxidation (TPO). In case of heterogeneous acid and base catalysts, the acidity and basicity are going to test by NH_3-TPD and CO_2-TPD, respectively.

Principle of temperature programmed desorption (TPD): [42]

The sample is going to pre-heat to remove contaminate at the first step to release the solid surface, then the adsorption process of selected gas on that sample will be

carried out at certain unchanged temperature until saturation. The temperature then will be increase at the appropriate rate to desorb absorbed gas on material's surface after all remained un-adsorbed gas flushed out of system by inert gas. The desorbed gas and inert are going to observe by a TCD. According to the result from TCD signal versus definite temperature, we are able to quantity the number and strength of material active sites.

For example:

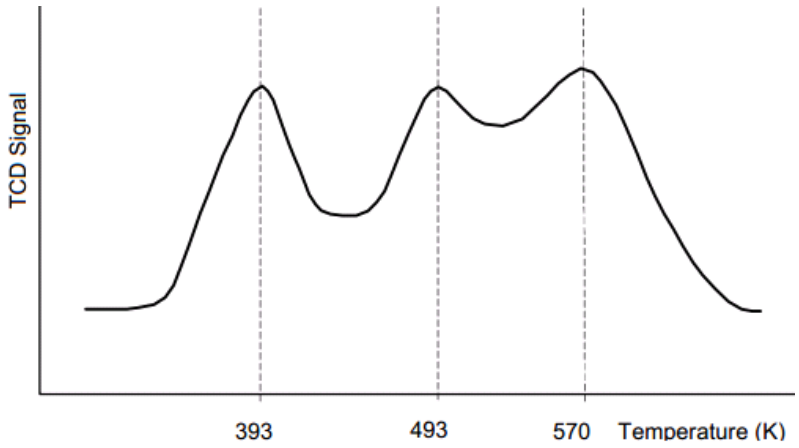

Figure 2.7 *TPD chromatogram of Hydrogen desorbing from alumina supported platinum. Three distinct adsorption bond strengths are evident.*

Figure 2.7 revealed the hydrogen TPD profile of Al_2O_3 supported Pt. It can be seen that there are three separated peaks at three distinct temperatures from low to high. Firstly, the peak at lowest temperature is 393 K which corresponds to weak active site on the surface of catalyst due to weak adsorption of hydrogen and this phenomena can be the adsorption of hydrogen with support. Secondly, at higher temperature (493 k) probably represent for the adsorption of hydrogen on Pt-alumina. Finally, the most active Pt on supports are demonstrated by hydrogen desorption at 570 K – the highest temperature in this TPD profile. Hence, according to this TPD hydrogen desorption profile, we are able to quantity the number and the strength of Pt active site and then estimate the activity of catalyst in reaction.

2.1.7.3 Crystallization properties

The powder X-ray diffraction is an analytical technique which is used for identifying crystalline phases accurately and rapidly and can also be used to quantify crystalline phases and the size of unit cell with high reliability.

Principle:

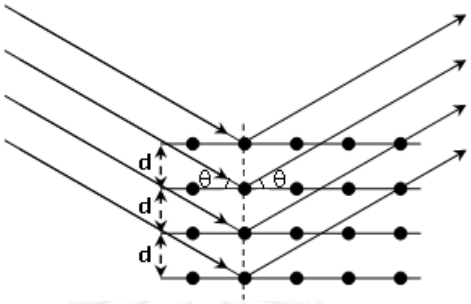

Figure 2.8 *The X-Rays are diffracted by the layers of atoms in a crystalline material.*

According to the theory of crystal structure, crystal lattices are made up of atoms or ions that are distributed steadily in space following to a definite law. The distance between the atoms (or ions) in the crystal is about a few A°, that is, in the wavelength range of the X-rays. Consider an X-ray beam with a wavelength λ projecting toward a solid crystal in the incident angle. Because the property of crystals are periodic, crystalline plan are spaced at regular intervals d, acting like diffraction gratings and producing diffraction patterns of X-rays. If we observe clusters scattering radiation by the reflecting direction (by the incident angle), the optical difference between the scattered radiations on the plan is:

$$\Delta L = 2.d.\sin\theta$$

Thus, in order to have the maximum diffraction, the incident angle must satisfy the following conditions:

$$\Delta L = 2.d.\sin\theta = n.\lambda$$

Where n is an integer

This is Vulf-Bragg's law describing the phenomenon of X-ray diffraction on crystalline and it is the basic equation for measuring X-ray wavelengths or for studying the structure of crystal lattices.

Each crystal produced by a substance has its own network and symmetry constants and therefore also has a diffraction pattern specific to that substance. On the contrary, when there is a diffraction pattern, we can also infer its crystal form.

2.1.7.4 Thermogravimetric analysis

Thermogravimetric analysis (TGA) is a thermal analysis which is commonly used to characterize physical and chemical properties of catalysts or other materials. According to the increasing of temperature of TGA analysis method, we are able to obtain information about weight loss of material due to the vaporization (moister or volatile compound on surface of material), oxidation or decomposition at high temperature. Hence, via TGA analysis we would know the chemicals content on sample which are organic or inorganic at certain temperature. In addition, in case of studying coke formation on surface of porous catalyst, we are also able to classify type of coke together with coke forming on surface of catalyst or inside the pore at appropriate temperature.

In case of investigation the chemical composition on the spent catalyst after reaction in this research, we expected to classify the organic compounds and coke formation on the surface of distinct catalyst versus different reaction condition. The spent catalysts after reaction are going to analyze in TGA analyzer to observer the weight of sample change in the range of temperature from 50 to 1000 ^{o}C. The result would be plotted by the weight loss percentage of sample versus the change of temperature.

2.2 Literature review

2.2.1 Catalytic decarboxylation on metal and heterogeneous base catalysts

P. Mäki-Arvela [39] has studied continuous decarboxylation of lauric acid in fixed bed reactor over Pd/C. In this study, they focused on the effect of catalyst mass, concentration of lauric acid in solven together with catalyst reactivation. A 5 wt.% Pd/C commercial catalyst from Aldrich was used for all experiment. The catalyst in powder

form was put in tubular reactor between sand and wool layer, and then catalyst was activated under hydrogen pressure (2 bars) at 200 °C in 2 hr. The reactions were carried out at distinct weight of catalyst, flow of lauric acid at 270 °C and 10 bars, then the gas and liquid were analyzed by GC and GC-MS, respectively. The result showed that the conversion was pretty high at initial (~65%) and declined substantially to a steady state level within 10–20 min of time-on-stream. The main reason for deactivating catalyst very quickly is coke formation on the surface of catalyst due to long contact time of lauric acid with catalyst. Unfortunately, the catalyst after reactivated by hydrogen could not be restored the activity as it was. The high light for this kind of catalyst was used in this study was able to give very high selectivity for desired hydrocarbon (undecane and undecene) which was higher than 95%.

Irina Simakova [43] was also used the same type of catalyst with [37] but in semibatch reactor and various pure fatty acids. 1 wt% of Pd/C was prepared by depositing palladium hydroxide obtained by hydrolysis of palladium chloride at pH 8–10 on mesoporous carbon. The mesoporous structure is favor for the decaboxylation with large organic compound like long chain fatty acid. The fresh and spent catalysts were characterized by specific surface area, CO-chemisorption and TEM. The reactions were carried out at 300 °C and 17 bars argon with the catalysts were reduced in inert gas following temperature program: 10 °C/min – 60 °C, hold 1 h, 10 °C/min – 300 °C and then hold 10 min at 4.8 bar. The result illustrated that the conversion on almost fatty acid were very high except C_{19} with low purity (contain sulfur) and C_{22}. It can be explained that same decarboxylation rates were got for pure fatty acids, while catalysts were poisoned and sintered with low purity fatty acids as reactants. Obviously, the catalysts were used in the decarboxylation of C_{19} and C_{22} low purity, the sintering was occurred with the rise of crystal size and decline of BET.

The decarboxylation of fatty acid on Pd was also investigated on the study of A. Dragu and partners [44]. In this study, they tried to prepare the nano-palladium catalyst supported on spherical meso-porous carbon beads (MB) and expected to obtain higher catalytic activity for deoxygenation of oleic acid via decarboxylation and decarbonylation. In order to create Pd/MB, MB would be deep into $[Pd_2(dba)_3]$ (dba:

dibenzylideneacetone) then it would be decomposed with the presence or absence of stabilizer solution such as polymer (PVP series) or triphenylphosphine (TPP series). The series of Pd/MB catalysts then characterized by TPR, TPD, XRD, XPS and HRTEM. The decarboxylation of oleic acid which was primarily used to assess the performance of obtain catalyst from preparation part would be carried out in batch and flow reactor. The presence of octadecanol and octadecane in liquid product were used to suggest the reaction mechanism whether the oleic acid was deoxygenation via both decaboxylation and decarbonylation to form corresponding alcohol and hydrocarbon. The result revealed that in case of batch reactor at 200 atm and 573 K, aromatic compounds have not been detected on Pb/MB and hydrocarbons were the main products from either decarboxylation/decarbonylation or dehydration, while in case of Pd/PVP and Pd/TPP (which were prepared under the presence of stabilizer solution) the dehydration route was not favorable for deoxygenation of oleic acid to form hydrocarbon. In flow reactor, Pd/MB demonstrated as the most efficient catalyst when it was able to give the high selectivity of octadecane (20%) and high stability when it could be maintained its performance up to 3 hours.

The nobel metal like Pd and Pt support on C or silica can be seen as the conventional catalysts for decarboxylation of fatty acid or triglyceride in vegetable oil without the presence of hydrogen. However, those catalysts are not favorable in economic aspect due to high pressure and using noble metal. Na and his partner [45] has investigated the applicability of typical base catalyst on the purpose of remove oxygen in fatty acid or triglyceride. Actually, this study was used the hydrotalcites with distinct amount of MgO for investigating decarboxylation of oleic acid in the absence of hydrogen. It was demonstrated that the oleic conversion fully depended on reaction temperature and percentage of MgO in hydrotalcites. At 300 ^{o}C the conversion of oleic acid was very low, especially in case of low content of MgO in hydrotalcites (lower than 60%), whereas at 400 ^{o}C the conversion can be reached nearly 100% (for 63 wt.% and 70 wt.% of MgO in hydrotalcites). In addition, the solid-like product can be obtained at low reaction temperature (300 ^{o}C and 350 ^{o}C) due to the saponification reaction between base MgO and fatty acid, while at 400 ^{o}C is more favor for decarboxylation

than saponification. From FT-IR analysis of product liquid fraction, the presence of oxygen was less than 1%, it means that almost oxygen was removed in term of CO_2.

In case of more applicable research, Na and partner [46] has studied the conversion of microalgal oil to hydrocarbon for transportation fuel via decarboxylation over high contained of MgO hydrotalcite (MgO : Al_2O_3 = 63 wt.% : 27 wt.%). The triglyceride has been cracked by thermal pyrolysis at 600 ^{o}C in the first step in order to obtain biooil which fatty acids with carbon number from C_{16} to C_{18} were the dominance for decarboxylation in the second step. The reaction was investigated in range of temperature from 350 ^{o}C to 400 ^{o}C and highest yield could be reached at 400 ^{o}C with 78.2 wt.% liquid hydrocarbons which were selective carbon number for C_{15} and C_{17} due to the selectivity of MgO catalyst in decarboxylation of fatty acid. In addition, the oxygen degree of liquid product was also low with just around 22%. The main reason that the reaction could not remove all oxygen in product might come from the less active oxygenate compound with hydrotalcite in pyrolysis oil such as phenolic compounds or fatty ester of alkyl acid.

In case of converting non-edible oil like Jatropha oil into renewable fuel, M. Romero [47] has been used hydrotalcite as the main catalyst for deoxygenation of Jatropha oil in batch reactor. The study has used the natural hydrotalcite namely Pural (MgO 70 wt.% and Al_2O_3 30wt.%) and has been compared the activity with commercial alumina (Puralox SBa200) in the decarboxylation of triglyceride and fatty acid. The experiments have been carried out in batch reactor under atmospheric nitrogen pressure in the range of temperature from 350 to 400 ^{o}C. The liquid products have been analyzed with FTIR to observe the oxygen content and the amount of CO and CO_2 which are the evident for oxygen removal of triglyceride via decarboxylation and decabonylation have been tested by GC with TCD detector. The result illustrated that the liquid yield could be reached 80% after 6h of reaction time and it contained very few oxygen as the expectation with about 83% hydrocarbon from C_8 to C_{18}. Consequently, the obtained product oil represented entirely high heating value (44 kJ/kg) which was absolutely closed to heating value of traditional diesel from fossil resource (46 kJ/kg in case of diesel from crude oil).

In other study M. Romero and partner has produced high quality biofuel from either waste cooking oil or non-edible oil (Jatropha curcas oil) by catalytic decarboxylation process on CaO and treated hydrotalcite MG70 [8]. The experiments have been carried out in both batch and semi-batch reactor in order to observe the influence of reactor type. Similar to previous study, the liquid product yield on batch reactor was more than 80 wt.% with about 83 wt.% hydrocarbon compounds which illustrated for high oxygen removal of triglyceride and fatty acid for both two kinds of oil. While the mean product of decarboxylation of waste cooking oil or Jatropha oil were in the range of diesel fraction and heavier in case of batch reactor, there were two fractions of liquid product which have been isolated by distillation process were light and intermediate fraction when the semi-batch reactor has been used instead. Interestingly, the oxygen content in light fraction was higher than in intermediate fraction with the hydrocarbon in light product and intermediate product were 72–80% and 85–88% respectively. However, it is experienced that CaO revealed very low catalytic performance for decarboxylation of Jatropha oil in semi-batch reactor because the short contact time was not favorable for decarboxylation of triglyceride and fatty acid on CaO.

N. A. Mijan [48] has used $Ca(OH)_2$ from natural waste shell as the main catalyst for decarboxylation of triglyceride to synthesize low oxygen content biofuel with either catalyst or raw feedstock from renewable resources. From studies before, base catalyst such as MgO and CaO have been known as the most efficient catalyst for deoxygenation of triglyceride and fatty acid via its ability in CO and CO_2 removal, the author in this work expected to use $Ca(OH)_2$ from natural waste shell in order to minimize the production cost. The waste shell has been treated the surface with both anionic and non-ionic by integration technique and obtained catalysts then have been characterized by XRD, BET and TPD-CO_2 to access its physicochemical properties. The result showed that catalyst after surfactant treatment has high specific surface area and the content large pore size with around 130 m^2/g and 18.6 nm, respectively. In addition, the derived $Ca(OH)_2$ catalyst revealed as the very strong basicity which is one of the most important property for decarboxylation on base catalyst. In decarboxylation of triolein which has been used to assess catalytic performance, the

treated $Ca(OH)_2$ showed high activity when it was able to give the triolein conversion over 44% with main compounds were hydrocarbons C17

The middle-distillate was also obtained from direct decarboxylation reaction of vegetable oil over modified MgO catalysts supported on vary carrier [41]. In this study, triglyceride from different vegetable oil such as Palm oil, Jatropha oil, Canola oil, Waste edible oil were used to monitor the applicability of MgO catalysts in decarboxylation reaction to obtain as much as possible the liquid hydrocarbon in range of diesel fraction. MgO was loaded onto commercial active carbon (wood made 1100 m^2/g) and silica gel (specific surface area 313 m^2/g) by impregnation method which dipped supports in magnesium nitrate solution, then drying and calcination. 10 wt.% of MgO catalysts were used in the reaction at 430 ^oC at atmospheric pressure and N_2 flow gas. It can be seen that the liquid hydrocarbon yield were in range of 50 wt.% to 70 wt.% on various catalysts. The carbon number of liquid product was distributed in a wide range from C_6 to C_{22} with whose peaks was from C_{10} to C_{20} (middle distillate fraction). Moreover, the hydrocarbon product which were almost paraffins and olefins illustrated the very low acid value and iodine value.

In order enhance catalytic activity in decarboxylation and decarbonylation of triglyceride to produce green hydrocarbon, T. Morgan [49]. In this study, three metal-base catalyst namely Ni-Al, Ni-MgO-Al, Mg-Al have been investigated in deoxygenation of triolein and soybean oil under atmospheric nitrogen pressure. The double layer hydroxide catalysts have been synthesized by precipitation method and the obtained catalysts have been characterized BET, TGA and TPR. The result showed that catalyst with the presence of MgO expressed better performace than Ni-Al catalyst for oxygen removal of triglyceride because the basicity of MgO was the main function for decarboxylation and decarbonylation. The adding of Ni and Al (in this case was Al_2O_3) enhanced the cracking of carbon chain of triglyceride so that the obtained liquid product would be contained hydrocarbon in the range of gasoline and light diesel fraction (C_5 – C_{17}). The kind of raw feedstock entirely affected to product composition whether soybean oil contained higher unsaturated carbon chain of fatty acid has resulted higher light product fraction and amount of coke due to higher cracking

possibility and coke formation. In the next study, E. S. Jimenez [50] has used the Ni-Al for decarboxylation of triglyceride in the presence of hydrogen in order to clarify the function of Ni metal active site together with the influence of partial hydrogen pressure to product compounds distribution. Similarly, the experience for decarboxylation of stearic acid has been carried out in semi-batch reactor with the mechanical stirring of 1000 rpm under 70 mL/min of gas flow. With the change of partial hydrogen pressure in the mixture with nitrogen from 10% to 100% at 350 °C, catalyst performed high activity in decarboxylation of stearic acid, especially when the partial hydrogen pressure increase. Ni-Al in the presence of hydrogen gas not only revealed high activity, stability, but also was amenable to regeneration. Indeed, the Ni-based catalyst recovered its activity as the fresh catalyst after it has been treat by calcination process in air, the strong base has been restored and remained stable its performance in decarboxylation of stearic acid.

2.2.2 Catalytic cracking on heterogeneous acid catalysts

In order to synthesize more valuable fuel like gasoline or diesel from heavy product (wax) from Fischer-Tropsch, V.G. Komvokis [51] has used various kind of solid acidic catalysts in catalytic cracking reaction. There were different micropore structure of zeolites such as zeolites Y, ZSM-5 and Beta have investigated to make clear its influence to conversion as well as products yield which mainly content C_2 to C_4 gases, gasoline, LCO, coke, and gasoline composition. The characterization of catalysts were indicated through XRD, BET, TPD-NH_3 and FT-IR to identify the morphology of catalysts. It can be seen that the Brönsted zeolitic acid sites were the dominant high strength which are responsible for the high cracking activity of the heavy paraffinic hydrocarbon. The reaction was carried out at 560 °C in fixed bed reactor with the feedstock was highly paraffinic hydrocarbon from F-T wax which mainly comprise C_{16}–C_{19} n-alkanes in the whole range from C_{10} to C_{35}. The result illustrated that the high wax conversion can be reached at around 88 – 95% in H-ZSM-5, H-Beta zeolites and H-Y zeolite. On H-Y and Beta zeolite was enriched n-olefins (23–25 wt.%), iso-olefins (32–35 wt.%), and branched iso-paraffins (17–18 wt.%), aromatics were very low (6.5–8.5 wt.%) whereas

on H-ZSM5 was less olefins (15 wt.% n-olefin and 24 wt.% iso-olefins) and more aromatics (15 wt.%) together with n-paraffins (23 wt.%)

In order to raise the iso-paraffinic hydrocarbons synthesized from Fischer-Tropsch (FT) process of syngas, Liu and partner have selected conventional bifunctional catalysts of novel metal and zeolite for hydroisomerization of the FT hydrocarbon [52]. On Pt/beta and Pd/beta, the product was very rich iso-paraffin with the distribution of carbon number less than 10 which demonstrated for hydrocracking reaction occur beside hydroisomerization. However, Pt/beta catalyst was deactivated very fast due to cock formation while Pd/beta was more stable with longer time on stream. The distinct performance between Pt and Pd could be explained by the different effect of CO molecules adsorption on those metal. The catalyst activity and stability not only depend on type of metal or reaction conditions but also depend on preparation method or catalyst precursors. Wang et al [53] have studied the influence of distinct Pt precursors such as $Pt(NO_3)_2$, H_2PtCl_6, and $Pt(NH_3)_4Cl_2$ on performance of Pt/ZSM-22 in hydroisomerization of n-hexadecane. With the same 0.5 wt.% Pt loading on zeolite, H_2PtCl_6 was able to form the catalyst with highest Pt dispersion together with higher activity and stability in isomerization. This phenomena was explain by the crystal orientation of Pt^o in reduce catalysts. The Pt(IV) precursors oriented the [011] plane which is buffer for forming smaller particle size and more active Pt[111].

In order to produce the alternative energy to reduce the dependence of human demand on fossil energy, more and more studies have used heterogeneous acid catalyst like zeolite to convert bi-resources into biofuel via catalytic cracking. E. Y. Emori [28] has studied the catalytic performance of commercial HZSM-5 with the molar ratio between Si/Al was 20 for cracking of soybean oil to synthesize biofuel like gasoline or light diesel. In addition, they also observed the influence of carrier gas (nitrogen and hydrogen atmosphere) on product composition. The experiments have been carried out in fixed-bed reactor and the crude soybean oil has been pumped into system at the rate of 0.07g/min while the reaction temperature has been maintained stable at 723 K in 45 minutes. The result showed that under hydrogen atmosphere more liquid product in the range of gasoline fraction has been obtained rather than with that in

the presence of nitrogen carrier gas and the mean compounds in liquid product were aromatics due to the morphology of HZSM-5 being favorable for forming aromatic compounds. It has been proposed that the catalytic cracking of either refined or unrefined soybean oil were easily deactivated in term of high acidity of HZSM-5.

Along with that trend, V. Abbasov [27] has used other type of zeolite namely Halloysite–Y as the main catalyst for catalytic cracking of waste vegetable oil in order to produce biofuel from natural renewable resources. The Halloysite–Y catalyst for reaction has been prepare by integrating commercial holloysite and commercial zeolite with the content of halloysite in the mixture was 10 wt%. The result revealed that the catalytic cracking of cottonseed oil on modification zeolite Y with halloysite showed better performance whether it has been able to give higher liquid product yield together with reducing coke formation on surface of catalyst which was known as the main factor of catalytic deactivation. Interestingly, the mixed halloysite-Y catalyst was more favorable for skeletal isomerization when the branch paraffin selectivity on modified catalyst was higher with that on traditional zeolite Y with more than 26% on halloysite-Y compare with 24.4% on single zeolite Y. This study opened the wide change for the following research which expect to create high quality of biofuel in the range of gasoline which is able to have high iso-paraffin content from direct catalytic cracking of vegetable oil.

V. Abbasov and partner has continued their work with other study in the purpose of producing green gasoline from commercial catalyst and triglyceride [29]. In the present work, authors has used the commercial catalyst for fluid catalytic cracking (FCC) with high alumina content (molar ratio Si/Al= 1) and halloysite nanotubes (HNT) for catalytic cracking of cottonseed and sunflower oils. By the addition of HNT (5–20 nm) into FCC, the main purpose of this work was to enhance liquid product yield together with gasoline and circumscription the coke formation on the surface of catalyst as well. At 500 ^{o}C of reaction temperature in fixed bed reactor, the highest conversion of oil was reached around 63% and the gasoline product fraction also got the peak about 46.5%. Those result revealed that the reaction conversion and gasoline have been slightly improved about 5% and 4%, respectively, in the comparison with the result from

previous work. In addition, the yield of coke has been significantly dropped as the expectation of this work with more than 10 wt.% less than last study. Similar to previous study, the iso-paraffin selectivity of gasoline product in case of using the 10% wt halloysite in the mixture with FCC catalyst was pretty higher when using cracking catalyst alone with 26.7% for modified catalyst and 25.1% for single catalyst.

X. Zhao modified zeolite HZSM-5 with Zn in order to improve the catalytic performance in the cracking of camelina oil reaction [54]. The difference percentage of Zn has been added onto HZSM-5 by impregnation method from 10 to 30% and then the obtained catalysts have been characterized by XRD, FT-IR, BET and TEM before testing the performance of catalysts in fixed bed reactor. The physicochemical properties of catalysts revealed that the addition of Zn on zeolite did not collapse the porous structure of zeolite and did not change the crystalline structure of HZSM-5 as well. That phenomena has been proposed that the Zn cluster located on the external surface or moving inside the pore the pore structure of zeolite. In the cracking of triglyceride reaction, 20 wt% Zn/HZSM-5 illustrated the high performance when it not only was able to give high yield of liquid crack oil with about 76% but also create higher quality fuel from vegetable oil whether cracked oil had lower viscosity, lower density, higher heating value (HHV) than the oil before reaction. The addition of metal Zn has increased the fuel properties of cracked oil significantly due to the high hydrocarbon content in liquid product which demonstrated the deoxygenation of triglyceride via decarboxylation and decarbonylation has been happened on the metal site of Zn.

H. Wan and partner have combined process for cracking and hydrotreating of waste cooking oil to synthesize high quality biofuel [55]. The commercial kaolin has been treated with HCl solution then calcined at 800 ^{o}C in 1 hour before it has been used for catalytic cracking of triglyceride step which was modeled as the FCC reaction system and carried out reaction at 700 ^{o}C. After that, the intermediate product has been condensed and hydrotreated in batch reactor on commercial CoMoS catalyst. The result revealed that the treated kaolin exhibited the excellent performance in term of deoxygenation of triglyceride and fatty acid in waste cooking oil via

decarboxylation and decarbonylation to form liquid product with high content of hydrocarbon. The result in case of traditional catalyst for fluid catalytic cracking and commercial alumina show the lower deoxygenation ability compare with treated kaolin. Hence, the combination of catalytic cracking and hydrotreating process has been able to reduce the hydrogen content in raw waste cooking oil from 87.6% to 6.6% with the hydrogen consumption (2.4 mol H_2/mol triglyceride).

CHAPTER III:

EXPERIMENTAL

3.1 Materials

All chemicals used in this study have been listed in table 3.1.

Table 3.1 *List of chemicals and sources*

Chemicals	Source
Magnesium oxide	Commercial available
Hydrochloric acid 37.0**%**	Carlo Erba
Calcium oxide 95%	Ajax Finechem
Silica 98%	Ajax Finechem
USY (Si/Al = 6)	Tosoh Corporation
Zeolite beta (Si/Al= 27)	Tosoh Corporation
HZSM-5 (Si/Al= 40)	Tosoh Corporation
Alumina 95%	Asia Pacific specialty chemicals
Sodium hydroxide 99%	Bright Chem
Palladium (II) nitrate dihydrate 99.99%	Sigma-Aldrich
Wij's solution	Panreac
Cyclohexane 99.5**%**	Merck
Potassium Iodide 99**%**	Ajax Finechem
Sodium thiosulfate pentahydrate 99%	QReC
Potassium dichromate 99**%**	QReC
Methanesulfonic acid 99.5**%**	Sigma-Aldrich
Toluene 99.8**%**	Sigma-Aldrich

Isopropanol 99.5**%**	Sigma-Aldrich
Potassium hydroxide	Ajax Finechem
Nitrogen gas **(**99.99**%** purity**)**	Praxair
Hydrogen gas **(**99.99**%** purity**)**	Praxair

3.2 Instruments and Equipments

3.2.1 Instruments and Equipment for Catalyst Preparation

1. Teflon beaker 50 mL
2. Magnetic stirrer
3. Pipette 1, 5, 10 and 20 mL
4. Water bath
5. Thermometer
6. Aluminium foil
7. Oven
8. Furnace
9. Glass beaker 100, 500 mL
10. Filter paper
11. Erlen 150, 250, 500 mL
12. Scale 5 digit
13. Dropper
14. Calcined cup
15. Volumetric flask 100, 500, 1000 mL
16. Magnetic stir bars

3.2.2 Instruments and Equipment for Catalyst Characterization

1. X-ray diffractometer (XRD) (Bruker model)

2. Ammonia (NH_3)-temperature programed desorption (Micromeristics TPD/TPR 2920 system)

3. Carbon dioxide (CO_2)- temperature programed desorption (Micromeristics TPD/TPR 2920 system)

4. Temperature programmed reduction (TPR) in quartz reactor

5. N_2 physical adsorption via BET method (Micromeristics ASAP 2020 system)

6. Thermal gravity analysis (TGA) (TGA/DSC1 Module with METTLER TOLEDO STARe system)

3.2.3 Instruments and Equipment for catalytic cracking and decarboxylation of palm oil

1. Scale 5 digit

2. Mass flow controller (KOFLOC)

3. Ball valve

4. HPLC pump

5. Thermocouple

6. Temperature controller

7. Cooling trap

8. Agitator

9. Heating tape

10. Back pressure valve

11. Flow bubble checking

12. Water trap

13. Autoclave reactor 100 bars (85 mL)

14. Gas bag

15. Pressure gauge

16. Gas Chromatography (GC) (Shimadzu GC-2014)

17. Gas Chromatography – Mass spectrometry (GCMS) (Agilent technologies, GC 7890A, MS 5975C)

3.3 Preparation and characterization of catalyst

3.3.1 Prepation of sodium silicate

Sodium silicate was prepared by wet impregnation method [56]. At first, commercial silica was put in DI water to become suspension, then aqueous sodium hydroxide was slowly added into silica suspension with the molar ratio between NaOH : SiO_2 is 2 : 1. After that, the mixture was heated to 90 ^{o}C and stirred within 2 hrs before calcined at 700 ^{o}C for 3 hours to obtain the final catalyst.

3.3.2 Preparation of Pd/zeolite by incipient wetness impregnation

Pd supported on beta zeolite was prepared by dry impregnation method. In order to make 0.5 wt% Pd on beta zeolite, the 0.01 g/ml aqueous $Pd(NO_3)_2.2H_2O$ solution was diluted before slowly dropping on beta. The obtained wet material then was dried at 120 ^{o}C to vaporize water. The adding palladium solution and drying step were repeated until all required solution has finished. Finally, precursor was calcined at 550 ^{o}C for 3 hour in air.

3.3.3 Catalytic characterization

3.3.3.1 X-Ray diffraction (XRD)

Crystal structure of both the fresh and used catalysts of catalysts were studied by X-ray powder diffraction (XRD) on X'Pert diffractometer (Bruker model) with the radiation source was Cu$K\alpha$, operating in the 2θ angle range of 5–80° with a resolution of 0.02°

3.3.3.2 Ammonia (NH_3)-temperature programed desorption (NH_3-TPD)

The acidity of acid catalysts have been characterized by ammonia temperature programmed desorption on Micromeristics TPD/TPR 2920 system. Catalysts had to be dried in oven at 100 °C overnight before it would be tested acidity by NH_3-TPD which has been operated following the temperature program as showed on figure 3.1. Obviously, the procedure could be separated into 3 region: release the surface active site of catalyst, adsorption the selected gas on catalyst and desorption by increasing temperature. At first step, catalyst has been heated from ambient temperature to 500 °C in the presence of helium as the inert carrier gas and maintain stable in 60 minutes before it has been cooled down to 50 °C. In the second step, catalyst would be treated by 10%NH_3 on helium to adsorb ammonia onto active site of catalyst at the same temperature with the end of first step and this process would be lasted within 30 minutes. After all active sites of catalyst has been saturated (as expectation in 30 minutes of adsorption), the carrier gas would be switched from mixture of 10%NH_3 on helium to purity helium in order to remove exceed NH_3 in system. At the last step, the temperature would be steadily increased to 600 °C with the heating rate was 10 °C and maintained stable in 30 minutes. The desorbed NH_3 signal would be record by TCD at corresponding temperature for determination the quantity and strength of acid site.

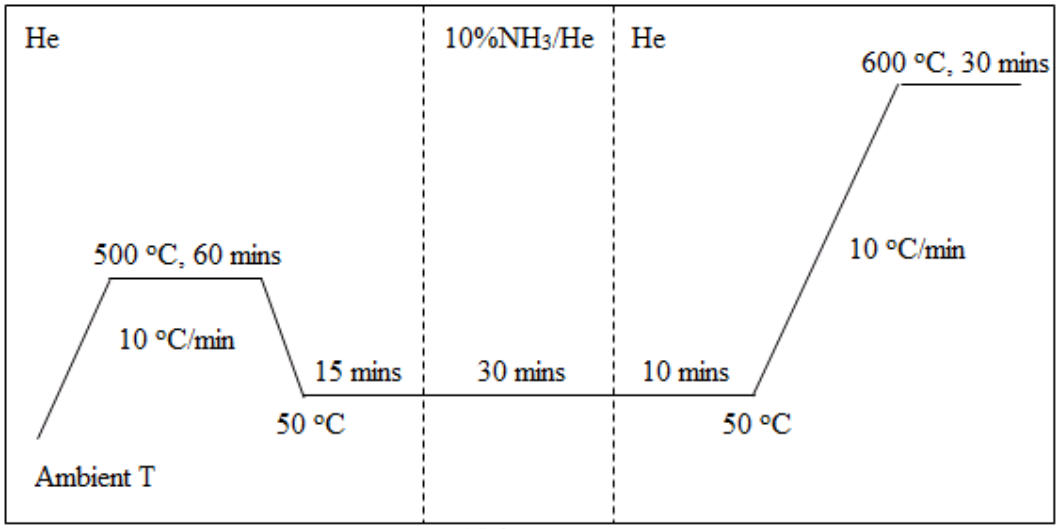

Figure 3.1 *Temperature programmed desorption for testing acid catalyst*

3.3.3.3 Carbon dioxide (CO_2)-temperature programed desorption (CO_2-TPD)

Similar to NH_3-TPD, basicity of catalysts have been tested by carbon dioxide temperature programmed desorption on Micromeristics TPD/TPR 2920 system. After drying overnight in oven, catalysts would be assessed basicity by CO_2-TPD following the temperature program revealed on figure 3.2. Catalyst would be treated surface area by the increasing of temperature to 500 °C in helium atmosphere at the first step and then cooling down to 50 °C after 120 minutes. When surface treatment has been done, the 10%CO_2/He would be flowed to system replacing to purity helium to adsorb carbon dioxide on active basic sites of catalyst until the catalyst saturated (after 30 minutes). At the last step, before the temperature was increased to 900 °C and maintained in 30 minutes to desorb and record TCD signal of desorbed CO_2, the system has also been cleared by purity helium as the inert gas. The TCD signal of CO_2 desorption would be plotted in the relation of TCD signal and temperature to determine the amount and strength of basic sites.

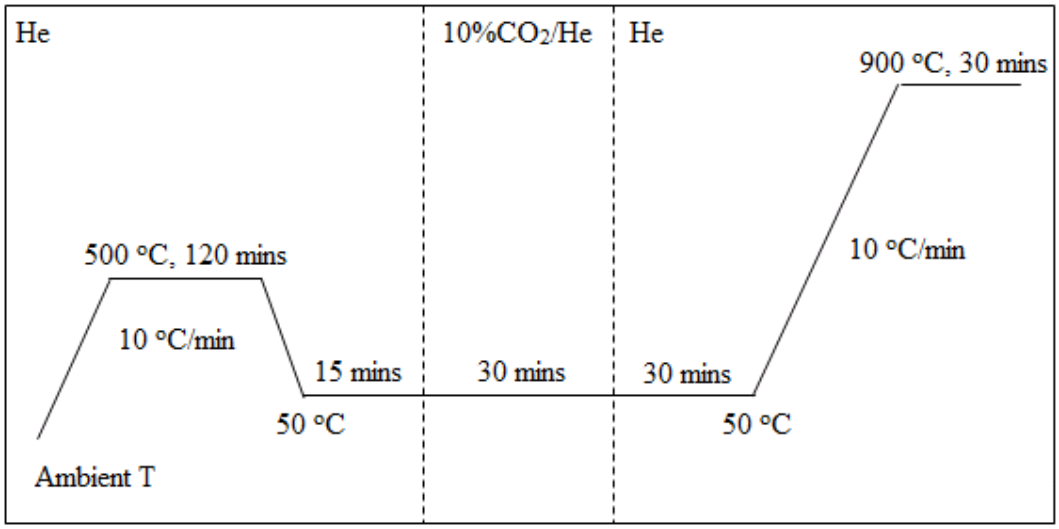

Figure 3.2 *Temperature programmed desorption for testing acid catalyst*

3.3.3.4 Temperature Program Reduction (TPR)

The reducibility of metal catalyst supported on zeolite which has been used for catalytic cracking and decarboxylation of triglyceride in the presence of hydrogen has been tested by temperature program reduction a quartz reactor. Before testing, catalyst has to be dried at 110 °C overnight to eliminate moisture on the surface of catalyst. After loading 0.1 g catalysts in to quartz reactor, the N_2 gas has been flowed over catalyst at the flow rate of 30 mL/min, then the system has been heated from ambient temperature to 100 °C with heating rate of 3 °C/min and maintained for 1 h to remove the adsorbed contaminants. After that, the system has been cooled down to 50 °C and kept in 30 min. The temperature would be increased at the last step with the heating rate of 10 °C/min to 900 °C in the flow of the 10% H_2-N_2 gas mixture at the same flow rate with previous step in order to reduce the metal oxide catalyst. The detail of temperature programmed reduction has been revealed in figure 3.3.

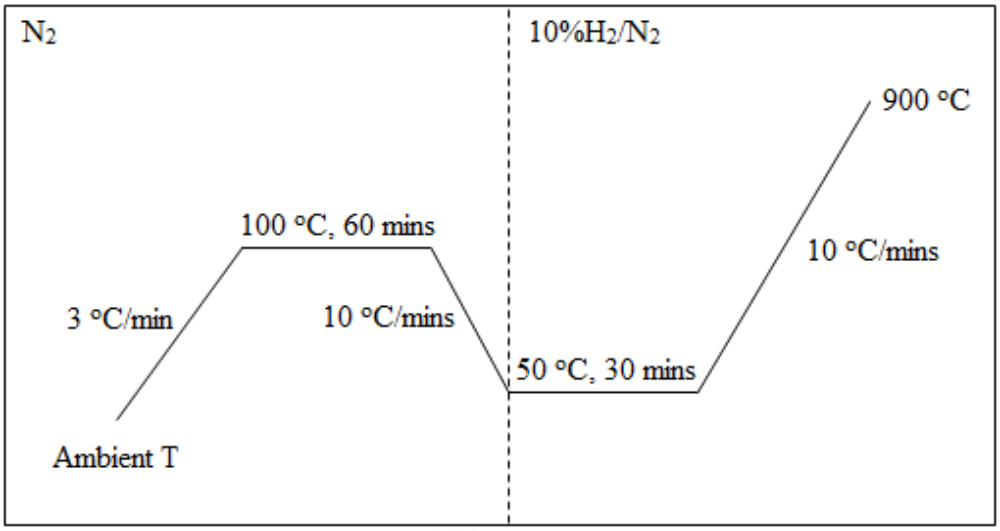

Figure 3.3 *Schematic of temperature program reduction reaction.*

3.3.3.5 N_2 physical adsorption via BET method

Specific surface area of catalysts were determined by N_2 physical adsorption via BET method (Brunauer–Emmett–Teller) on Micromeristics ASAP 2020 system.

3.3.3.6 Thermal gravity analysis (TGA)

The coke deposition on catalyst surface was investigated by thermogravimetric analysis TGA/DSC1 Module with METTLER TOLEDO STARe system at a heating rate of 10 °C/min and temperature of 21 °C in air

3.4 Testing of catalytic performance in cracking and decarboxylation of palm oil

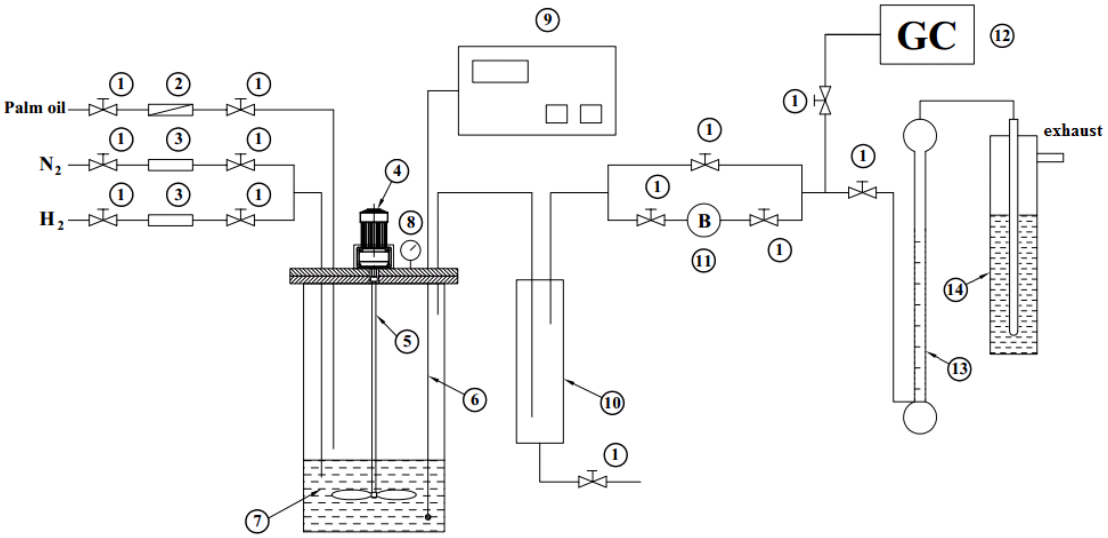

Figure 3.4 *The scheme of catalytic cracking and decarboxylation*

1. Ball valve; 2. HPLC pump; 3. Mass flow controller; 4. Motor; 5. Agitator; 6. Thermocouple; 7. Catalyst; 8. Pressure gauge; 9. Temperature controller; 10. Cooling trap; 11. Back pressure; 12. Gas chromatography; 13. Bubble flow meter; 14. Water trap

3.4.1 Experimental procedure before the reaction

1. Opening gas for gas chromatography (GC) including: hydrogen, nitrogen, oxygen, then opening GC analyzer together with computer and analytical program. Before starting to analyst gaseous product via GC, the base line of TCD and FID signal have to be stable (straight line curve on the screen)

2. The catalysts were dried in oven at 100 °C for 4 hours has been measured and re-check the weight by 5 digits scale before putting into autoclave reactor.

3. Setting up the autoclave reactor into system, make sure the all hexagonal head screw have been fixed well. Then setting up the cooling trap and connecting glass of palm oil with HPLC pump (it has been weighted before carrying out reaction), then setting up the expected oil flow rate on the volume controller of HPLC pump.

4. Opening nitrogen or hydrogen gas, then open mass flow controller and inputting the expected mass flow. The real gaseous flow have to check with bubble flow meter and compare with the setting flow on mass flow controller.

5. Preparing ice to cool down the cooling trap and agitator part as well.

6. In case of applying hydrogen pressure in reaction, the system have to be tested pressure overnight to observe whether the leak happen or not.

3.4.2 Reaction procedure

1. Setting up the reaction temperature on temperature controller together with adjusting the appropriate stirring speed of agitator and then running it.

2. Maintaining the temperature within 15 minutes once it has reached reaction temperature in order to have the stable condition before carrying out reaction

3. When everything is available for reaction, open HPLC pump and the valve connecting with reactor at the same time. Record the injecting time of palm oil, checking the flow out of reactor every 10 minutes via bubble flow meter.

4. The gaseous product (uncondensed gaseous product after cooling trap) has been analyzed by GC every 30 minutes to observer the gaseous composition especially CO and CO_2.

5. After reaction, turning of the heater and HPLC pump together with closing the connecting valve among HPLC pump and reactor, reducing the nitrogen or hydrogen gas flow to be half, and waiting until the temperature on the temperature controller point under 200 ^{o}C.

6. Turning off mass flow controller then opening cooling trap to collect liquid product. Carefully collect liquid product in the glass in order to calculate yield and analyze later.

7. When the temperature in reactor lower than 70 ^{o}C, opening reactor to collect the residue (residue is define as everything remaining in reactor after reaction except

catalyst**).** Comparing the weight of catalyst before and after reaction to know how much residue is**.** Keeping spent catalyst in desiccator to test TGA later**.**

3.4.3 Catalytic performance test

The catalytic performance on cracking and decarboxylation of palm oil to synthesize iso-paraffin fuel has been carried out in semi-batch reactor in order to investigate how the catalyst and reaction condition effect to liquid product yield, iso-paraffin and other compounds selectivity together with oxygen removal ability via CO and CO_2 yield. The experiment could be separated into two part as below:

3.4.3.1 Single catalysts

1. Effect of temperature on base catalyst (370, 400, 430 and 460 °C)

2. Effect of LHSV on base catalyst (0.36, 0.48, 0.6 and 0.72 h^{-1})

3. Effect of temperature on acid catalyst (370, 400, 430 and 460 °C)

4. Effect of LHSV on acid catalyst (0.36, 0.48, 0.6 and 0.72 h^{-1})

5. Effect of catalyst:

- Base catalysts group (decarboxylation group): SiO_2, MgO, CaO, Na_2SiO_3

- Acid catalysts group (cracking group): HZSM-5, HY, beta, alumina

3.4.3.2 Mixed catalysts

1. Effect of ratio between selected base catalyst and acid catalyst (3:1, 1:1, 1:3)

2. Effect of temperature (370, 400, 430 and 460 °C)

3**.** Effect of LHSV **(**0.36, 0.48, 0.6 and 0.72 h^{-1})

4. Effect of hydrogen pressure (0, 1, 5 and 10 bars)

5. Effect of time on stream (15, 30, 45 and 60 mins)

3.5 Analyzing of products

3.5.1 Analyzing of the gaseous products

The gaseous products have been analyzed by a Shimadzu GC-2014 gas chromatography to determine the gas composition and yield after cracking and decarboxylation of palm oil.

Table 3.2 *Optimum condition of gas chromatograph*

Carrier gas	H_2
Column	Syn-carbon, Porapak Q
Injector temperature	150 ^{o}C
Column temperature	Temperature program
	80 ^{o}C – 5 mins
	180 ^{o}C – 30 mins – rate: 10 ^{o}C/min
Detector temperature	180 ^{o}C
Detector	Thermal conduct detector (TCD)
Detector	Flame ionization detector (FID)

Formulation for calculation of yield and selectivity as below:

Molar of gaseous products:

$$n_X = \frac{A.C_{Std}.t.F}{A_{Std}.22400}$$

Where:

n_x: molar of gas X (X: CO, CO_2, CH_4, C_2H_6, C_2H_4, etc.) (mol)

A: peak area of gas X from

C_{Std}: concentration of standard gas (vol.%)

t: reaction time (s)

F: total gas flow rate after reactor (mL/min)

A_{Std}: peak area of standard gas

Yield of gaseous products:

$$Yield_X = \frac{n_X.M_X.100\%}{m_{oil}}$$

Where:

$Yield_X$: Yield of gaseous product X (wt.%)

n_X: molar of gas X (X: CO, CO_2, CH_4, C_2H_6, C_2H_4, etc.) (mol)

M_x: molecules molar weight of gas X (g/mol)

m_{oil}: total palm oil has been inputted into reactor (g)

3.5.2 Analyzing of liquid product properties

3.5.2.1 Gas chromatography – Mass spectroscopy (GC-MS)

The liquid product from catalytic cracking and decarboxylation of palm oil has been analyzed by Gas chromatography – Mass spectroscopy (GC-MS) in order to determine the selectivity of iso-paraffin and other compounds.

The selectivity of compounds in liquid product were calculated according the peak area of that compound, detail as below:

$$Selectivity_Y = \frac{A_Y.100\%}{A_{total}}$$

Where:

A_Y: peak area of substance Y in liquid

A_{total}: peak area of total substance in liquid

3.5.2.2 Acid value (ASTM D664)

The total free fatty acid in liquid product from catalytic cracking and decarboxylation of palm oil would be tested by ASTM D664. Main solvent which has been used to dissolve sample was the mixture of toluene, isopropyl alcohol (IPA) and water with the ratio by volume was toluene : IPA : water = 500 : 495 : 5. The sample after dissolving in appropriate amount of solvent would be titrated by 0.1 M potassium hydroxide in isopropanol.

3.5.2.3 Iodine number (ASTM D1959)

In order to assess the oxidation stability of liquid product which was expected as the high quality fuel, the liquid product after reaction would be analyzed by titration technique which has been absolutely followed ASTM D1959.

3.5.2.4 Total olefin content by methane sulfonic acid

The total olefin content in liquid product has been tested by analyzing liquid sample with GC FID before and after methanesulfonic acid treatment. According to that method, the chromatogram peaks of liquid sample have disappeared after treating with methanesulfonic acid would represent the olefin compounds.

3.5.2.5 Heating value (Bomb calorimeter)

One of the technique which has been used in this study to prove the oxygen content in liquid product from cracking and decarboxylation of palm oil, approximately, was total heating value which has been follow bomb calorimeter method

CHAPTER IV:
RESULTS AND DISCUSSION

4.1 Catalytic characterization

4.1.1 Textural properties

Table 4.1 *Specific surface area of catalysts*

Catalyst	BET (m^2/g)	Pore vol. (cm^3/g)	Pore size (nm)
MgO	23.13	0.026	4.561
CaO	10.48	0.042	16.043
SiO_2	140.75	0.482	13.693
Na_2SiO_3	0.16	-	-
HY	425.22	0.294	2.77
Beta	511.83	0.47	3.675
0.5% Pd/Beta	539.7	0.521	3.863
HZSM-5	291.8	0.164	2.254
Al_2O_3	254.6	0.259	4.151

Table 4.1 revealed the list of BET specific surface area together with porous properties of various catalysts which were divided into two groups: base (MgO, CaO, Na_2SiO_3 and silica) and acid (HY, Beta, HZSM-5, and alumina). It could be seen that the specific surface area of the base catalysts were relatively low, except that SiO_2 had a high specific surface area as the characteristic of porous material with about 140.75 m^2/g, the specific surface area of the catalysts MgO, CaO and Na_2SiO_3 were just 23.13, 10.48 and 0.16 m^2/g, respectively. In addition, base catalysts such as MgO, CaO and Na_2SiO_3 also showed that these were almost non-porous materials when the total porosity of

these catalysts were pretty small and it could not even be identified the pore volume and pore size on the Na_2SiO_3 catalyst. On the contrary, commercial zeolite and alumina catalysts used in this study as acid catalysts had a very large surface area ranging from 254.6 m^2/g to more than 500 m^2/g, especially surface areas of zeolite Y and zeolite beta were 425.22 and 511.83 m^2/g, respectively The peculiarity of porous materials could be clearly seen in these catalysts when the volume of porous cavities were entirely large (0.164 - 0.512 cm^3/g) and the pore size in the range of meso-porous materials (2,254 - 4,151 nm). Interestingly, the 0.5 wt.% Pd loaded on beta not only increased the surface area but also slightly rose the pore volume. Maybe, the Pd particles almost dispersed on the surface of catalyst and did not move to inside the pore of catalyst then it somehow modestly raised up the BET surface area of catalyst.

4.1.2 Acidity and basicity

a) CO_2 temperature programmed desorption:

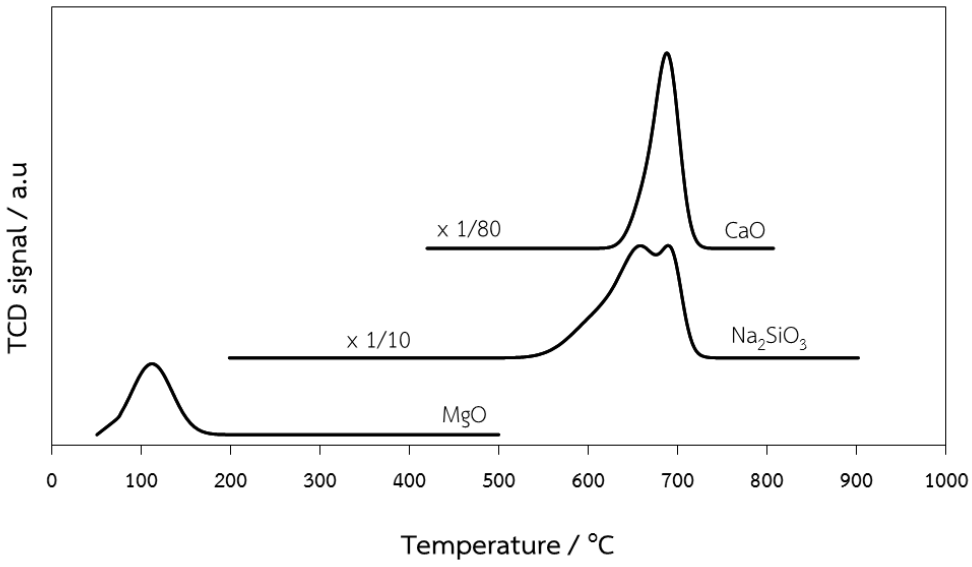

Figure 4.1 *CO_2-TPD profile of base catalysts*

Table 4.2 *The basicity of catalysts*

Catalyst	Basicity (mmol CO_2/g)	
	Weak	Strong
MgO	0.006	-
CaO	-	0.84
SiO_2	-	-
Na_2SiO_3	-	0.15

Figure 4.1 and table 4.2 illustrated the CO_2 temperature programmed desorption together with basic sites and basic strength of base catalysts. It could be seen that the desorption peaks of CaO and Na_2SiO_3 were at about 680 °C which revealed as a strong base [57, 58]. In addition, the amount of basic sites on CaO were much higher than on sodium silicate where the total CO_2 desorbed on CaO and Na_2SiO_3 was 0.84 and 0.15 mmol CO_2/g, respectively. In contrast, the desorbed peak of MgO was at very low temperature with around 120 °C and the amount of basic sites were also very few which was known as the property of weak base catalysts [59-61]. On the other hand, silica even did not show any basicity when it could not be detected CO_2 desorption peak. Actually, SiO_2 was known as a weak acid because it might have the silanol groups (S-O-H) in molecule structure. Anyway, according on the result in the study of K. Fujimoto's research group [41] silica has demonstrated the moderate ability in oxygen removal via decarboxylation and decarbonylation, so it was used as a deoxygenation catalyst in this study and listed in the same group with other bases like MgO and CaO.

b) NH_3 temperature programmed desorption

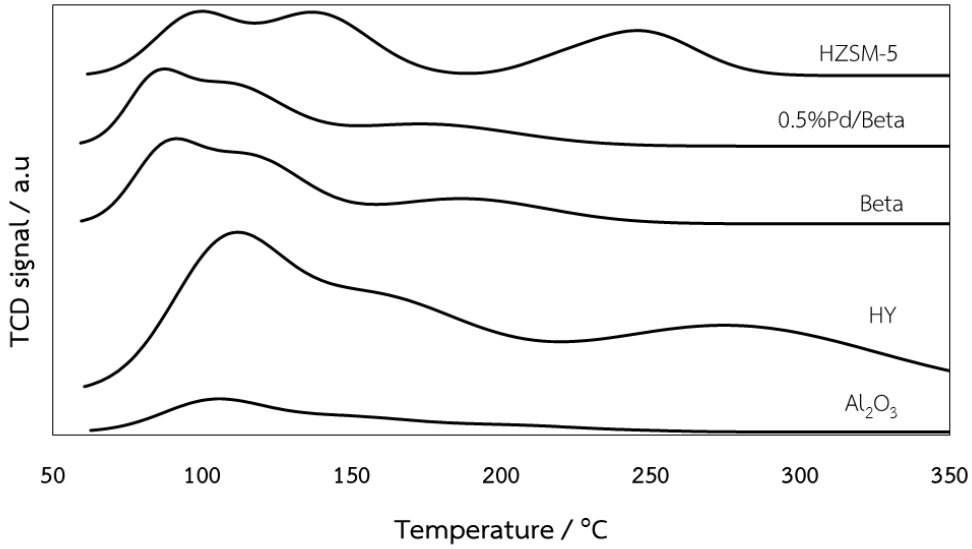

Figure 4.2 *NH_3-TPD profile of acid catalysts*

Table 4.3 *Acidity of acid catalysts*

Catalyst	Acidity (mmol NH_3/g)	
	Weak	Strong
HY	0.33	0.21
Beta	0.15	-
0.5% Pd/Beta	0.13	-
HZSM-5	0.18	-
Al_2O_3	0.06	-

Figure 4.2 and table 4.3 showed the ammonia temperature programmed desorption profile along with properties of acid sites. The amount and strength of acid sites has been determined based on the TCD signal versus the temperature increase. It can be seen that there were different peaks occurring in the temperature range of 50 to 350 ^{o}C corresponding to the strength of the acid from low to high. According to prior research, it could be seen from the range of desorption temperature whether the

desorption peaks on the left were weak acid sites whereas on the right were strong acid sites [62-65]. Apparently, HY revealed as a strongest acid in the list due to its wide range of acid sites where were distributed from low to high NH_3 desorbed temperature (weak to strong acid sites) and the total amount of NH_3-desorption was much higher the rest with 0.54 mmolNH_3/g. In reverse, alumina showed very weak acidity due to low ammonia desorbed temperature and very few acid sites on the surface of catalyst. On the other hand, zeolite beta and zeolite HZSM-5 in this study could be considered as weak acid catalysts when the acidic sites have been determined at the NH_3 desorption temperature was less than 300 °C. In addition, the total acid amount of the zeolite beta and zeolite HZSM-5 were also moderate when the total amount of ammonium desorption on those catalysts were just around 0.15 and 0.18 mmol NH_3/g, respectively. The loading of 0.5 wt.% Pd on beta had minor effect on acidity of this zeolite where the total amount of NH_3 desorption slightly dropped about 0.02 mmol NH_3/g from 0.15 to 0.13 mmol NH_3/g.

The NH_3-TPD revealed above could be used to explain for the ability to produce iso-paraffins of acid catalysts. According to the result on previous works [51], weak acid sites were favorable to obtain branch hydrocarbon rather than strong acid sites which were suitable to cracking and coking reaction. As mentioned before, the selectivity of iso-paraffins on acid catalysts was in the order of beta > HY > Al_2O_3 > HZSM-5 while acidity of acid catalyst followed by HY > HZSM-5 > beta > Al_2O_3. Although acidity of HY was higher than beta, it had lower selectivity of branched paraffins because HY had a lot of strong acid sites which promoted to cracking rather than isomerization and directly affected to iso-paraffinic selectivity. Similarly, acidity of HZSM-5 was stronger than beta zeolite, but it had very low iso-paraffin percentage because its morphology properties was appropriate for producing aromatic compounds [66-68]

4.1.3 X-ray diffraction

4.1.3.1 Base catalyst group

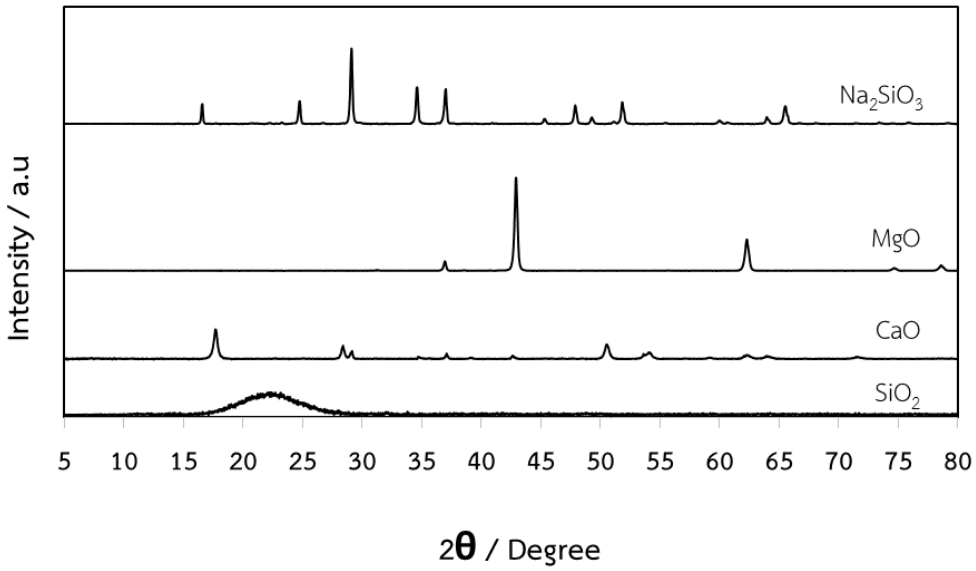

Figure 4.3 *X-ray diffraction pattern of the alkali catalysts*

The crystal structures of the catalysts were evaluated by their XRD patterns (Fig. 4.3), where the diffraction pattern of silica showed a broad peak at 2θ = 22.4, which was typical for pure silica, whereas CaO, MgO and Na_2SiO_3 presented distinctive sharp peaks. The spectra of CaO presented a mixture between $Ca(OH)_2$ and CaO, as represented by 2θ = 28.7, 50.9 and 17.8 for $Ca(OH)_2$ and at 54.6 for CaO, but both MgO and Na_2SiO_3 had characteristic peaks (2θ = 37.2, 42.9, 62.4, 74.9 and 78.8 for MgO and 2θ = 16.6, 24.8, 29.2, 34.7, 37.1, 47.9, 51.9 and 65.6 for Na_2SiO_3) without any other compounds.

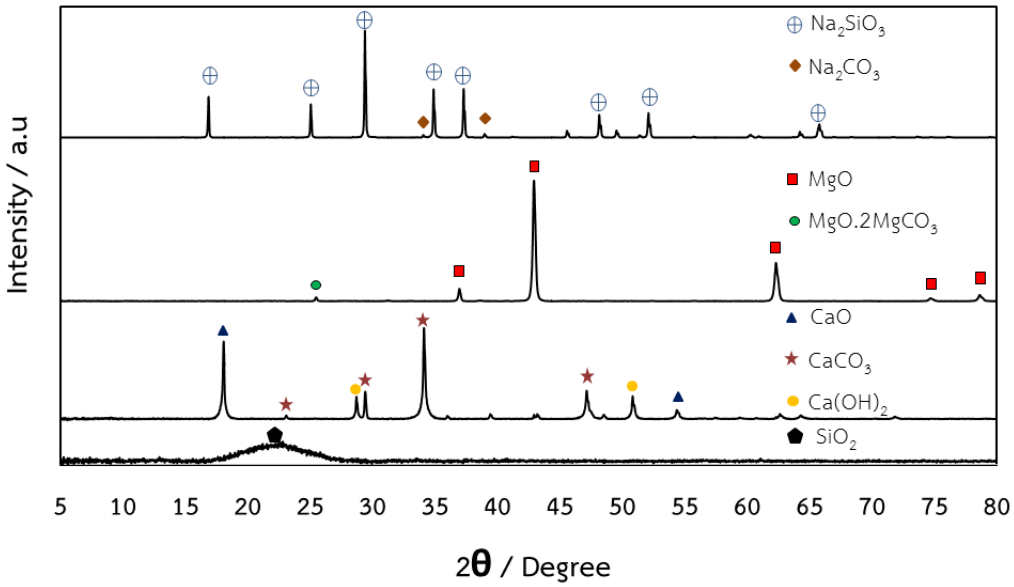

Figure 4.4 *X-ray diffraction pattern of the spent alkali catalysts*

The XRD pattern of spent catalysts was represented on figure 4.4 would be used to discuss about the mechanism of decarboxylation occurring on base catalysts. Used silica showed just only one wide peak at two theta equal to 22.45 which was the typical peak of pure SiO_2 [56] and there was no other peaks detected. On the other hand, beside the main characteristic peaks of MgO, CaO and Na_2SiO_3, there was the appearance of various kinds of peaks such as $CaCO_3$, $Ca(OH)_2$, $MgO.2MgCO_3$, and Na_2CO_3. Particularly, $CaCO_3$ was detected at two theta equal to 23.3, 29.46, 34.14, 47.19; and $Ca(OH)_2$ 28.75, 50.98 [69, 70], while magnesium oxide carbonate ($MgO.2MgCO_3$) was indicated by a small peak at around two theta equal to 25.73 [71, 72]. Similarly, There were two peaks at two theta equal to 34.47, 39.05 which was the characteristic peak of Na_2CO_3 phase [73, 74]. The common point of these catalysts was the representation of carbonate salt which may be the intermediate product of catalyst during reaction. According to the result on [41], fatty acids were able to be produced via hydrolysis of triglyceride process before reacting with base catalysts on the next step.

$$2RCOOH + MgO \longleftrightarrow (RCOO)_2Mg + H_2O \quad (4.1)$$

$$2RCOOH + CaO \longleftrightarrow (RCOO)_2Ca + H_2O \quad (4.2)$$

$2RCOOH + Na_2SiO_3 \longleftrightarrow 2RCOONa + H_2SiO_3$ (4.3)

Then:

$(RCOO)_2Mg \longleftrightarrow RCOR + MgCO_3$ (4.4)

$(RCOO)_2Ca \longleftrightarrow RCOR + CaCO_3$ (4.5)

$2RCOONa \longleftrightarrow RCOR + Na_2CO_3$ (4.6)

Base on XRD pattern of spent catalysts, the appearance of peaks related to carbonate salts on distinct used catalyst, by the way, were not similar where $CaCO_3$ revealed four clear and sharp peaks while the pattern of $MgCO_3$ and Na_2CO_3 was very faded. In detail, the CO_2 temperature desorption of MgO was very low, just around 120 ^{o}C, whereas it was up to 680 ^{o}C on CaO. That is why very few $CaCO_3$ was decomposed at reaction temperature (460 ^{o}C) and then emerged on the used catalyst as the main component. Furthermore, although sodium silicate had high CO_2 desorbed temperature, the appearance of sodium carbonate was not so clear. Na_2CO_3 properly react with H_2SiO_3 which formed before at high temperature as acid-base reaction to produce Na_2SiO_3 again.

$MgCO_3 \longleftrightarrow MgO + CO_2$ (4.7)

$CaCO_3 \longleftrightarrow CaO + CO_2$ (require very high temperature) (4.8)

$Na_2CO_3 + H_2SiO_3 \longleftrightarrow Na_2SiO_3 + CO_2 + H_2O$ (4.9)

Hence, the decarboxylation of fatty acid on base catalysts should be carried out with catalyst which its intermediate state is easy to decompose or be able to react with other intermediate compounds to return to initial circumstance.

4.1.3.2 Acid group

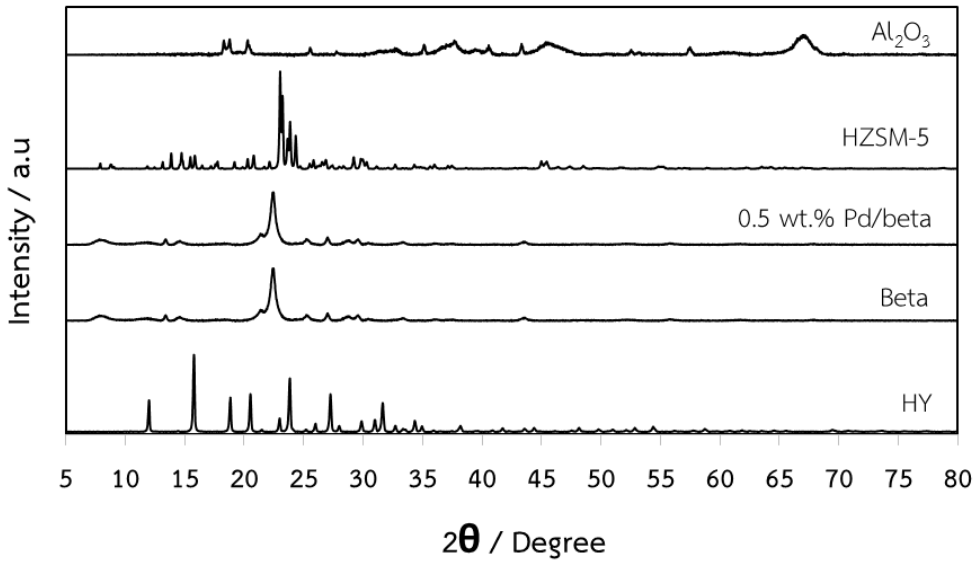

Figure 4.5 *X-ray diffraction pattern of the acid catalysts*

Figure 4.5 showed the XRD pattern of distinct acid catalysts together with Pd supported on beta catalyst. The crystal characteristic of zeolite Y were expressed through the characteristic peaks at two theta equal to 10.3, 12, 15.8, 18.8, 21, 22.9, 23.8, 25.9, 27.1, 27.9, 29.8, 30.9, 31.5, 32.5, 34.3, 35.8 and 39.3 [75, 76]. Similarly, the characteristic peaks of zeolite beta were expressed at two theta equal to 7.6, 13.4, 14.4, 21.8, 22.5, 25.4 and 27 [77, 78]. The characteristic peak of zeolite beta revealed at two theta equal to 7.9, 8.4, 22.8, 23.4 and 24 [79, 80]. The crystalline character of alumina was expressed at equivalent peaks at two theta equal to 25.3, 35, 38.5, 43.4, 52.5, 57.5, 61.1, 65.9 and 68.4 [81, 82]. In addition, the XRD pattern of 0.5 wt.% Pd supported on beta still showed the characteristic peaks of the original zeolite beta, indicating that loading Pd at 0.5 wt.% on zeolite beta catalyst did not alter the crystalline structure of zeolite beta.

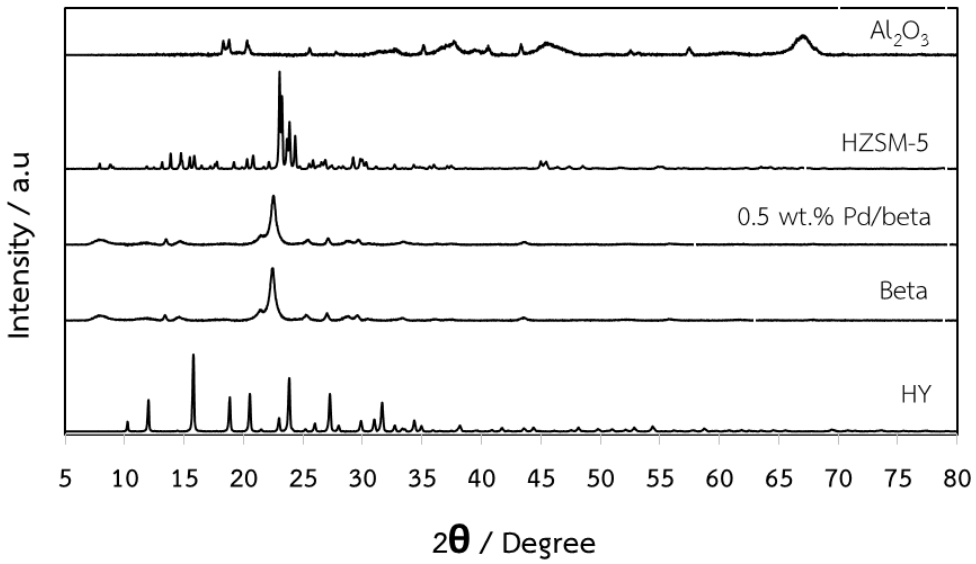

Figure 4.6 *X-ray diffraction pattern of the spent acid catalysts*

Figure 4.6 showed the XRD pattern of spent catalyst after decarboxylation and cracking of palm oil in semi-batch reactor. It could be seen that the crystalline properties of the acid catalysts after reaction have been demonstrated by characteristic peaks similar to the corresponding fresh catalysts that were shown in Figure 4.5 before, and this result demonstrated that the crystalline structure of acid catalysts almost remain unchanged after reaction compare with the original catalysts.

4.1.4 Study residue via TGA

Figure 4.7 illustrated the thermal gravimetric analysis (TGA) of spent catalysts after reaction. According to the graph on figure 4.7, the TGA profile of both base and acid catalyst were able to separate into 3 regions as followed: under 450 ^{o}C indicating the desorption of water or oil (long chain hydrocarbon or organic compounds) [83], 500 to 850 ^{o}C was the composition temperature range of coke on the catalytic surface, and coke blocked in pore of catalyst is removed at over 850 ^{o}C [84]. On base catalysts, there was no coke detected on MgO while There was about 10 wt.% of weight loss at around 700 ^{o}C on spent CaO catalyst which could be the decomposition of $CaCaO_3$ [85] beside 14 wt.% of oil desorption. Similarly, around 6.7 wt.% of surface coke decomposed on used sodium silicate and did not have oil found on this catalyst

whereas spent silica contained oil, surface coke and coke in the pore. In contrast, there was no oil remaining on acid catalyst and almost coke could not be completely remove at 1000 °C. Because of high acidity, zeolites were favorable for coke forming at reaction temperature and the worse thing for meso-porous catalysts was coke blocked in pore so that it was not able to decompose completely. There was the relation between amount of coke and NH3-TPD that total amount NH_3 desorption of zeolite was in order of HY > beta > HZSM-5> Al_2O_3 and then the order of coke removal was HY (20.3 wt.%) > beta (16.6 wt.%) > HZSM-5 (6.1 wt.%) > Al_2O_3 (3.3 wt.%). Interestingly, The coke on beta in the mixture with MgO not only remarkably decreased the amount of coke forming (from 16 wt.% to 3.5 wt.%) but also significantly dropped the coke decomposition temperature (from over 850 °C to lower than 700 °C).

According to In Hyuk Son's study [84], the coke formation on the surface of the acid catalyst depended on 2 factors namely reaction temperature and acid strength of the catalysts. Accordingly, two types of coke would be formed as amorphous carbon (formed at reaction temperatures below 400 °C) and graphite carbon (formed at 450 ° C reaction temperature). The amorphous carbon could be removed at low temperatures while graphite coke needs very high temperatures to eliminate. Moreover, in case of porous catalysts like zeolite, the formation of graphite carbon in the pore would make the catalytic recovery process was going to be extremely difficult. In addition, In Hyuk Son's study revealed that the presence of MgO would help to reduce coke formation on the surface of the catalyst, especially graphite carbon. The coke formation was known to have the presence of carbide as an important intermediates, and the presence of MgO prevents the formation of this compound and thus reduces coking on acid catalysis [84].

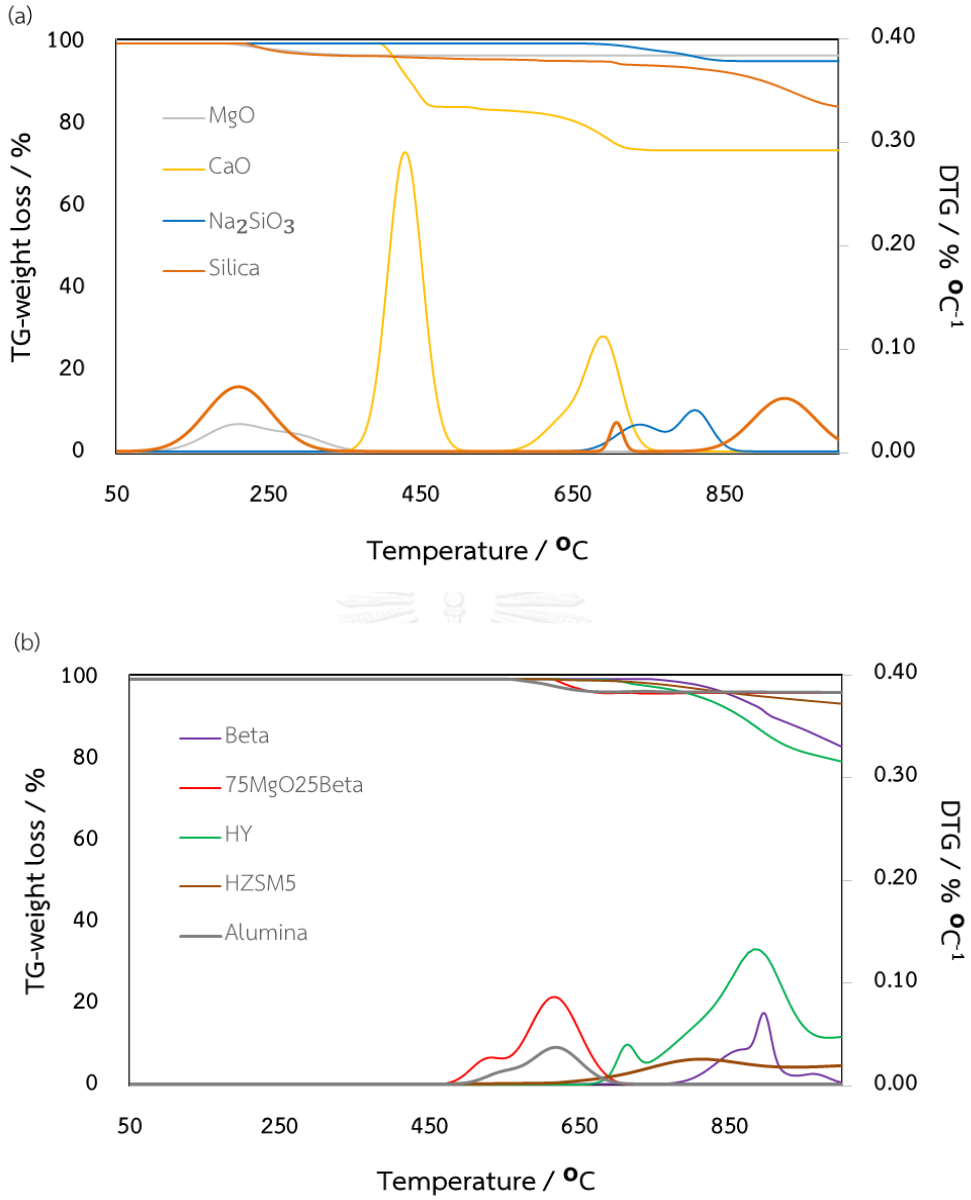

Figure 4.7 *Thermogravimetric profile of the spent (a) alkali and (b) acid catalysts*

4.1.5 Reducibility of synthesis Pd on Beta catalyst

In order to increase the selectivity of iso-paraffin in liquid product, moderate hydrogen pressure was applied for cracking reaction of palm oil and therefore novel metal supported on beta was used instead of zeolilte beta in the mixture with MgO. Figure 4.8 showed the temperature reduction profile of 0.5 wt.% Pd on beta. It was just only one peak detected at 250 °C and it could be classified as the reduction peak of bulk

PdO [86]. Moreover, the reduction of palladium oxide from Pd^{2+} to Pd^{0} at around 250 to 300 ^{o}C indicated the strong interaction between Pd species and support [87].

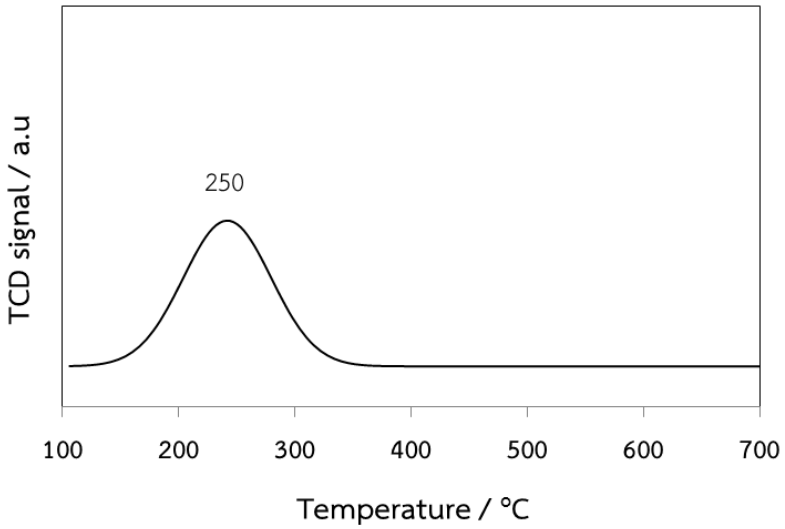

Figure 4.8 TPR profile of 0.5 wt.% Pd/beta

4.2 Catalytic performance on cracking and decarboxylation of palm oil in semi-batch reactor

4.2.1 The effect of reaction condition on yield and product selectivity

4.2.1.1 The effect of reaction temperature

Table 4.4 *Light hydrocarbon products from cracking and decarboxylation of palm oil on SiO_2 catalyst at different reaction temperature*

Products (wt.%)	Temperature (°C)		
	400	430	460
CH_4	6.0	6.4	8.0
C_2H_6	9.5	10.8	12.6
C_2H_4	5.0	6.9	9.4
C_3H_8	15.5	17.3	17.1
C_3H_6	10.2	11.9	13.1
C_3H_4	0.7	0.6	0.6
C_4H_{10}	11.5	10.4	8.9
i-C_4H_{10}	0.0	0.0	0.0
C_4H_8	20.6	18.5	15.3
n-C_5H_{12}	0.0	0.1	0.1
i-C_5H_{12}	0.0	0.1	0.0
C_5H_{10}	21.1	16.9	15.0

Reaction condition: N_2 atmosphere, temperature: 400 - 460 °C, LHSV of 0.36 h^{-1}, catalyst: SiO_2. Light hydrocarbons have been analyzed by GC FID and the compositions were calculated according to the area of corresponding GC peaks

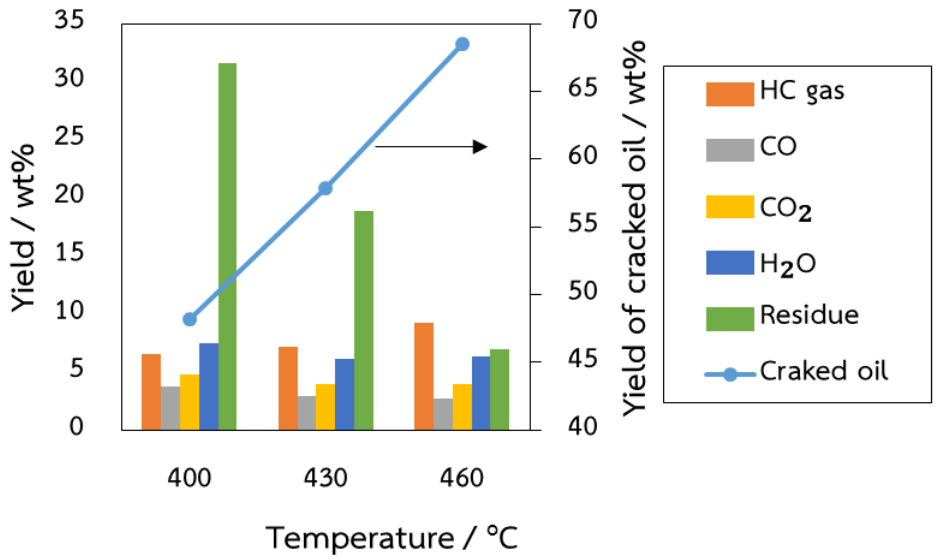

Figure 4.8 *Yield of products from cracking and decarboxylation of palm oil on SiO_2 depending on reaction temperature. Reaction condition: N_2 atmosphere, temperature: 400 - 460 °C, LHSV: 0.36 h^{-1}, catalyst: SiO_2*

Table 4.4 and Figure 4.8 show the dependence of liquid yield and percentage of light hydrocarbon products on reaction temperature. It can be seen from Figure 4.8 that the yield of liquid products increased dramatically from less than 50 wt.% to more than 65 wt% when the reaction temperature increased from 400 to 460 °C. In addition, yield of residues and gaseous hydrocarbon products of the reaction also showed a clear dependence on the temperature of the reaction when at low temperature (400 °C) the residue was the main product with about 33 wt.% while the yield of light hydrocarbons was about 6.5 wt%, and when the temperature rose to 460 °C, the composition of these two products varied markedly as the residue decreased sharply to about 7 wt.% and the gaseous product increased to more than 9 wt.%. This could be explained by the thermodynamic of the main reactions, because both cracking and decarboxylation were endothermic reaction that would be conducive to occur at high temperatures.

Table 4.4 showed that the gaseous hydrocarbons were distributed among C_1 and C_5 where the mean of products were the compounds with carbon atom number of 3 and this wass a characteristic of decarboxylation and decarbonylation of triglyceride. In addition, when the temperature rose from 400 to 460 °C, light hydrocarbon products

from C_1 to C_3 increased while products from C_4 to C_5 tend to decrease, meaning that at higher temperatures, more lighter gaseous products would be produced than heavy one.

Another thing to consider was the yield of CO and CO_2 because these two products represented for deoxygenation of triglycerides to produce products containing less oxygen. As shown in Figure 4.8, when the temperature rose from 400 to 460 ℃, total CO and CO_2 yields dropped slightly from 8.5 wt.% to 6.7 wt.%. Thus, it could be concluded that CO and CO_2 removal were more favorable at temperatures below 460 ℃; however, at temperatures under 460 ℃ the yields of liquid products are lower than expected.

Table 4.5 *Chemical composition, acid value and iodine number of liquid product from cracking and decarboxylation of palm oil depending on reaction temperature*

Temp	Selectivity %				AV[(a)]	IN[(b)]
(°C)	i-paraffins	n-paraffins	Olefins	Aromatics	(mgKOH/g)	(g I/100g)
400	18.74	27.69	52.41	1.16	78.1	93.3
430	19.08	24.28	55.34	1.30	70.5	101.7
460	17.04	23.06	58.07	1.83	73.8	111.4

Reaction condition: N_2 atmosphere, temperature: 400 - 460 °C, LHSV: 0.36 h^{-1}, catalyst SiO_2

[a] Determined by ASTM D664

[b] Determined by ASTM D1959

Table 4.5 showed the effect of temperature changes on the composition of the major liquid products from the cracking and decarboxylation of palm oil on SiO_2 catalyst along with other properties of the product such as acid value and iodine number. It could be seen that olefins were the dominant constituents of liquid products when they accounted for more than 50 wt.% and this component increased significantly when the temperature rose. Meanwhile, under the current reaction conditions,

temperature change did not change much of the other chemicals. Particularly, Isoparaffins and normal paraffin decreased slightly from 18.74% to 17.04% and 27.69% to 23.06%, respectively. In addition, aromatic compounds contributed a relatively small proportion at less than 2% to the total chemical composition in liquid product, and the change in temperature did not significantly increase the formation of these compounds.

About properties of liquid product, the cracking and decarboxylation of palm oil on SiO_2 catalyst under considered reaction condition produced the high acid value liquid product with the acid value greater than 70 mgKOH/g. On the other hand, the increase in reaction temperature from 400 to 460 °C was favorable for the cracking reaction to form more olefins compound and thus increases the iodine number of the liquid product from 93.3 to 111.4 gI/100g.

4.2.1.2 The effect of LHSV

Table 4.6 *Light hydrocarbon products from cracking and decarboxylation of palm oil on SiO_2 catalyst at different LHSV*

Products (wt.%)	LHSV (h^{-1})		
	0.36	0.48	0.6
CH_4	8.0	7.8	7.8
C_2H_6	12.6	12.5	12.3
C_2H_4	9.4	8.6	8.8
C_3H_8	17.1	17.6	16.7
C_3H_6	13.1	12.6	12.9
C_3H_4	0.6	0.9	0.5
C_4H_{10}	8.9	9.8	9.7
i-C_4H_{10}	0.0	0.0	0.0
C_4H_8	15.3	15.9	16.3
n-C_5H_{12}	0.1	0.1	0.1
i-C_5H_{12}	0.0	0.5	0.0
C_5H_{10}	15.0	13.8	14.8

Reaction condition: Reaction conditions: N_2 atmosphere, 460 °C, LHSV: 0.36 – 0.6 h^{-1}, catalyst: SiO_2. Light hydrocarbons have been analyzed by GC FID and the compositions were calculated according to the area of corresponding GC peaks

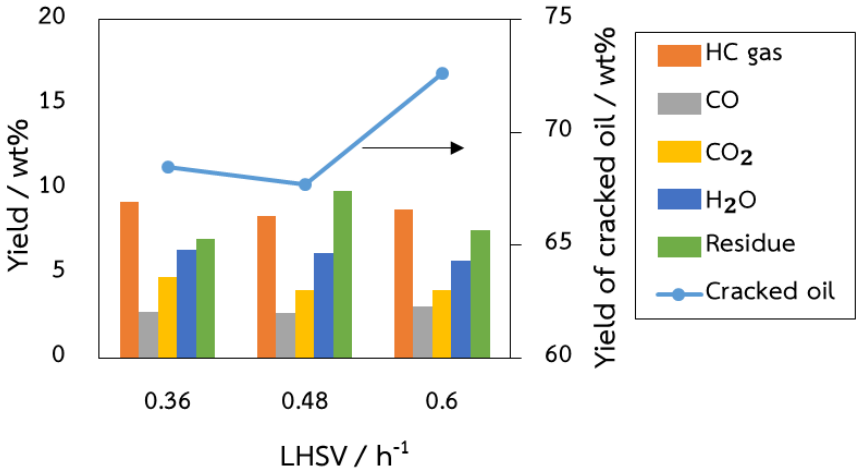

Figure 4.9 *Yield of products from cracking and decarboxylation of palm oil on SiO_2 depending on LHSV. Reaction condition: N_2 atmosphere, temperature: 460 ^oC, LHSV: 0.36 – 0.6 h^{-1}, catalyst: SiO_2*

Table 4.6 and Figure 4.9 showed the effect of LHSV on the yield of products together with the proportion of light hydrocarbon products (C_1 - C_5). Similar to Table 4.4, Table 4.6 also revealed that light hydrocarbons with carbon number equal to 3 were still the major product in the mixture with the other gaseous hydrocarbons and this phenomena has already been explained previously. The increase in LHSV from 0.36 to 0.6 h^{-1} seem to change light hydrocarbon gases propotion very few (increase or decrease about 1%). Similarly, the change of LHSV from 0.36 to 0.6 h^{-1} resulted a slight increase in the yield of liquid products from the cracking and decarboxylation of palm oil about 4 wt.% from 68.47 to 72.62 wt.%. Yield of other products varied little, only increases or decreases in small intervals (about 1 - 2 wt.%). Thus, under the consideration condition, the effect of the LHSV change on yield of products was not as much as the change of reaction temperature.

Table 4.7 *Chemical composition, acid value and iodine number of liquid product from cracking and decarboxylation of palm oil depending on LHSV*

LHSV (h^{-1})	Selectivity %				AV[(a)] (mgKOH/g)	IN[(b)] (g I/100g)
	i-paraffins	n-paraffins	Olefins	Aromatics		
0.36	17.04	23.06	58.07	1.83	73.8	111.4
0.48	18.38	24.14	56.00	1.48	76.2	115.9
0.6	19.26	23.49	55.75	1.51	75.8	108.3

Reaction condition: N_2 atmosphere, temperature: 460 ^{o}C, LHSV: 0.36 – 0.6 h^{-1}, catalyst: SiO_2

[a] Determined by ASTM D664

[b] Determined by ASTM D1959

Table 4.7 shows the effect of LHSV on the selectivity of liquid products together with acid value and iodine number. When LHSV increased from 0.36 to 0.6 h-1, the selectivity of isoparaffins increased slightly about 2% from 17.04 to 19.26%, while the olefin's selectivity decreased around 3% from 58.07% to 55.75%. This suggested that reducing the contact time of the substance with catalyst might help to improve the selectivity of isoparaffin due to the limited cracking of the products to produce more olefins. Selectivity of normal paraffin and aromatic compounds did not change significantly, increasing or decreasing less than 1%. The increase in LHSV also did not improve the high acid value and iodine number of the liquid product, the acid number was still higher than 70 mgKOH/g and the iodine index was about 110 gI/100g.

4.2.2 The influence of individual catalysts

a) Light hydrocarbons on distinct catalysts:

Table 4.8 *Light hydrocarbon products from cracking and decarboxylation of palm oil depend on type of catalysts*

Products (wt.%)	Non-cat	SiO_2	MgO	CaO	Na_2SiO_3	HY	Beta	HZSM-5	Al_2O_3
CH_4	5.6	8.0	7.9	9.6	6.4	7.2	4.1	6.2	5.0
C_2H_6	9.2	12.6	13.3	12.5	10.7	7.7	4.4	8.5	8.0
C_2H_4	8.2	9.4	10.8	10.1	6.5	1.7	3.3	4.3	4.8
C_3H_8	14.3	17.1	16.0	15.8	15.3	35.4	27.9	37.3	12.3
C_3H_6	13.6	13.1	14.3	13.7	14.6	3.5	18.3	8.8	11.2
C_3H_4	0.0	0.6	1.7	2.0	3.7	0.1	0.1	0.1	0.4
C_4H_{10}	11.2	8.9	9.3	9.6	12.2	10.7	12.5	9.4	14.3
i-C_4H_{10}	0.0	0.0	0.0	0.0	0.0	6.4	4.6	3.8	0.0
C_4H_8	23.8	15.3	12.9	12.4	13.6	7.4	7.2	9.9	15.2
n-C_5H_{12}	0.0	0.1	0.1	0.2	0.2	4.2	10.1	0.2	0.3
i-C_5H_{12}	0.0	0.0	0.0	0.0	0.0	0.2	0.9	0.1	0.7
C_5H_{10}	13.2	15.0	13.7	14.1	16.9	15.5	6.6	11.3	27.8

Reaction condition: Reaction conditions: N_2 atmosphere, 460 ^{o}C, LHSV: 0.36 h^{-1}, single catalysts. Light hydrocarbons have been analyzed by GC FID and the compositions were calculated according to the area of corresponding GC peaks

Table 4.8 illustrated the composition of light hydrocarbon on gaseous product in catalytic cracking of palm oil. It contained all saturate and unsaturated compound from C_1 to C_5 with the mean of products were C_3. This result came from the dehydration of glycerol [41, 88] and cracked long chain hydrocarbon of fatty acid. It could be seen that there was no branch gaseous paraffin detected on thermal cracking

and base catalyst whereas a minor amount of iso-C_4 and C_5 was found on zeolite and alumina. This was reasonable result because isomerization was one of the main secondary reaction in catalytic cracking reaction of long chain hydrocarbon on acid catalyst, especially zeolite [27-29].

b) Liquid product's properties from catalytic cracking and decarboxylation of palm oil on various catalysts

Table 4.9 *Yield, acid value and iodine number of reaction products from cracking and decarboxylation of palm oil depending type of catalysts*

Catalyst	Product yield (wt.%)						AV [a]	IN [b]
	Oil	HC gas	CO	CO_2	H_2O	Residue		
Palm oil	-	-	-	-	-	-	0.7	82.7
No catalyst	82.3	5.5	1.4	3.8	2.6	4.9	117.4	144.7
SiO_2	68.4	9.2	2.7	4.0	6.3	7.0	73.8	111.4
MgO	65.8	13.2	2.1	8.3	3.1	9.1	10.0	110.0
CaO	69.9	10.8	1.1	4.1	9.5	3.9	9.0	125.9
Na_2SiO_3	67.4	14.4	1.7	8.3	3.9	1.9	5.9	139.5
HY	46.6	29.3	2.5	2.1	7.4	16.2	65.5	116.5
Beta	51.8	30.2	2.2	1.6	10.6	6.6	29.4	100.0
HZSM-5	54.7	30.1	3.5	2.3	7.0	6.8	74.2	83.2
Al_2O_3	63.8	16.7	1.9	5.0	6.4	8.3	63.5	118.9

Reaction condition: Reaction conditions: N_2 atmosphere, 460 °C, LHSV: 0.36 h^{-1}, single catalysts.

[a] Acid value (mgKOH/g), Determined by ASTM D664

[b] Iodine number (gI/100g), Determined by ASTM D1959

Table 4.9 showed the products of catalytic cracking reaction of palm oil at 460 °C on two groups of commercial catalysts. The purity palm oil had very low free acid content

but high iodine number (82.7 gI/100g) due to a high amount of unsaturated ester of fatty acids such as oleic acid, linoleic acid, linolenic acid [89, 90]. The first group of catalyst was SiO_2, MgO, CaO and Na_2SiO_3 which were expected the deoxygenation function via CO and CO_2 removal, while the second group was HY, Beta, HZSM-5 and Al_2O_3 which were used to increase the branch hydrocarbon in product, especially iso-paraffin. The main products were classified as oil, gases and residue where oil was collected in cooling trap together with a minor amount of water, uncondensed gases (CO, CO_2, and light hydrocarbon from C_1-C_5), residue was everything remaining in reactor after subtracted the weight of fresh catalyst and its compositions have been illustrated and discussed by TGA before.

It could be seen that the liquid yield on the decarboxylation catalyst group in table 4.9 was over 65 wt.%, whereas at the same condition, liquid product on acid catalyst group was under 55 wt.% yield (except Al_2O_3), and HY revealed as the worse one to obtain high liquid hydrocarbon yield when its liquid yield was just 46.67 wt.%. Contrastingly, gaseous hydrocarbon products on the second group were around 16 – 30 wt.% which were higher than on the first group with just under 15 wt.%. Light hydrocarbons from C_1 to around C_5 were mainly produced by cracking hydrocarbon chain and that process was favorable on catalysts with high acidity. The pyrolysis of long chain hydrocarbon compound and on base catalysts typically occurred via radical mechanism with a lot of random reactions which was not selective to produce gaseous hydrocarbons [45, 91].

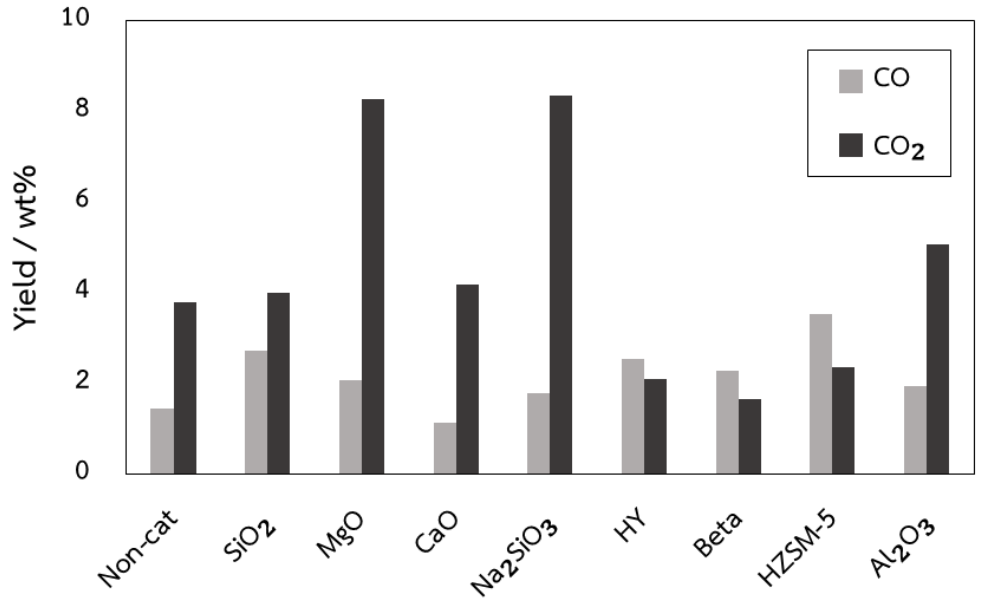

Figure 4.10 *CO and CO_2 yield from cracking and decarboxylation of palm oil on distinct catalysts*

On the other hand, there were a big difference among catalysts on yield of CO and CO_2 together with acid value which were used to evaluate the oxygen removal [41]. The result in table 4.9 and figure 4.10 showed that base group of catalyst was more appropriate than acid group on reducing oxygen due to higher CO and CO_2 yield and lower acid value whether total CO and CO_2 yield could be reached over 10 wt.% on base catalyst (MgO and Na_2SiO_3) and AV was under 10 mgKOH/g while CO and CO_2 product on acid catalyst were just around 6 wt.% and the acid value of liquid products were very high (up to 74.2 mgKOH/g on HZSM-5). This phenomena could be explain via the function of base like MgO which was able to promote the decarboxylation of vegetable oil [45]. In addition, the low oxygen content in liquid product was proved by heating value on figure 4.11 [92, 93]. It can be seen that the relationship between the amount of CO and CO_2 removal and the heating value of liquid products from the cracking and decarboxylation of triglycerides on different catalysts has been shown in Figures 4.10 and 4.11. Particularly, liquid products on catalysts with low level of oxygen removal via CO and CO_2 were going to have low heating value. MgO and Na_2SiO_3 which had higher CO and CO_2 yield than others gave the products with very high heating

value with about 10494 and 10459 cal/g, respectively, and those value were very close to heating value of original diesel fuel from fossil resource (10675 cal/g) whereas heating value on other catalysts were under 10000 cal/g because of low CO and CO_2 removal.

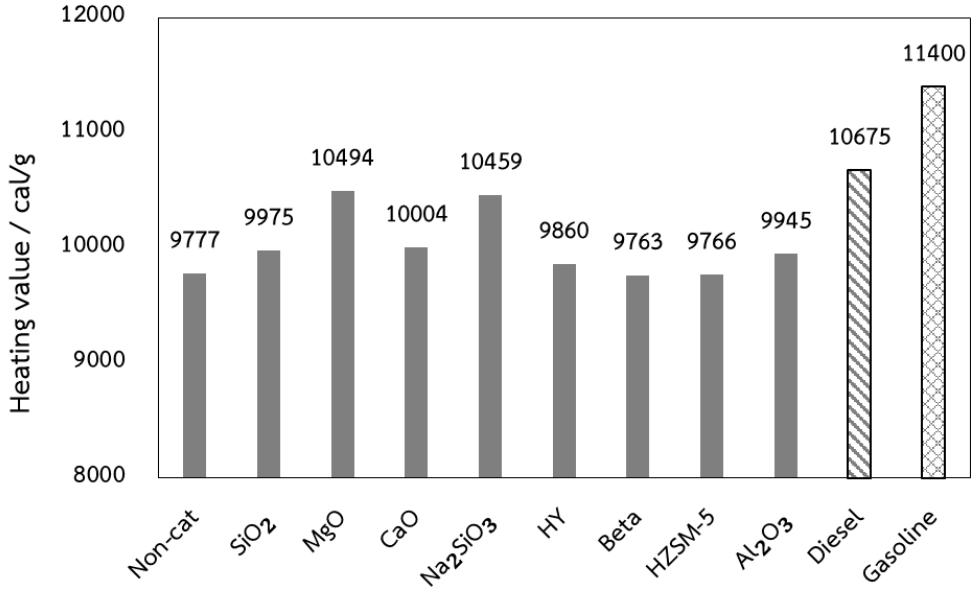

Figure 4.11 *Heating value of liquid product from cracking and decarboxylation of palm oil on distinct catalyst*

c) Product fraction and chemical composition:

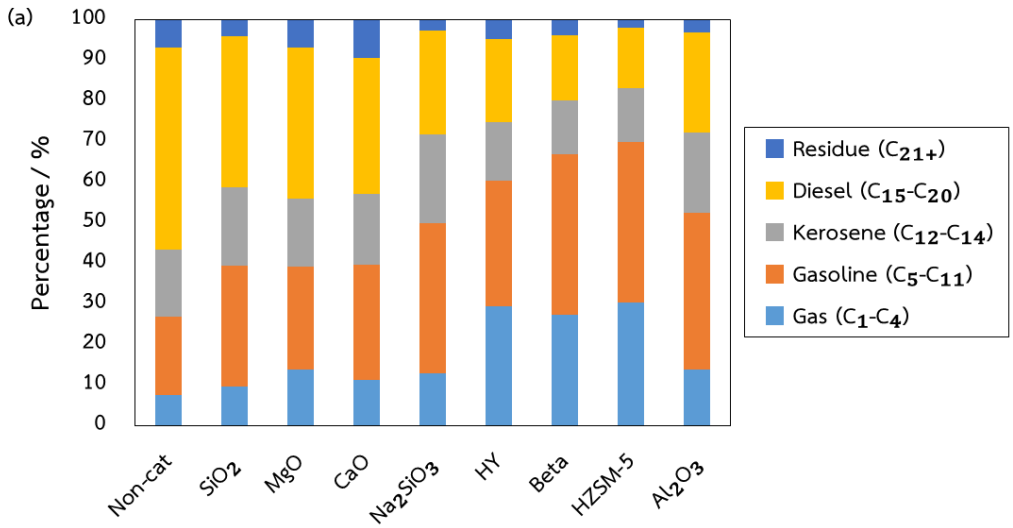

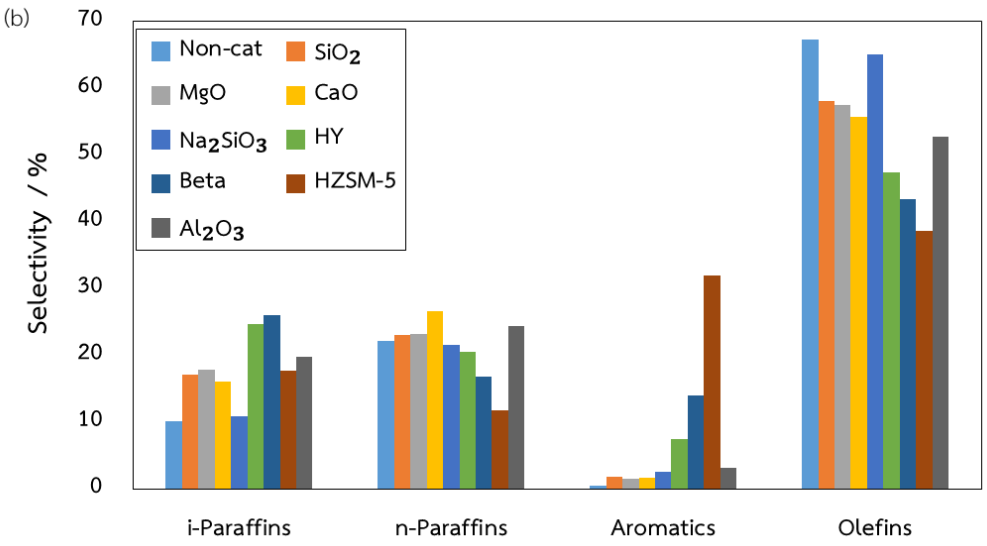

Figure 4.12 *Product fraction (a) and chemical composition (b) of liquid product from cracking and decarboxylation of palm oil on various catalysts. Reaction condition: Reaction conditions: N_2 atmosphere, 460 °C, LHSV: 0.36 h^{-1}, single catalysts*

The product distribution of the deoxygenated oil is shown in figure 4.12a, where the alkali catalysts produced a variety of hydrocarbon products because the alkali catalysts did not have any pore selectivity. The major product with the alkali catalysts was in the range of diesel oil (C_{15-20}), while that for the acid catalysts shifted to the light fraction including hydrocarbon gases (C_{1-4}) and gasoline (C_{5-11}). Moreover, the acid catalysts gave very low residue (C_{20+}) levels (less than 5%). HY, beta zeolite and HZSM-5 acid catalysts contained a large amount of acid sites that led to the strong cracking reaction, while alumina with its low acidity (0.06 mmolNH_3/g) had a poor cracking ability and so still produced a high yield of biodiesel.

Figure 4.12b revealed the main components in cracked oil of catalytic cracking of palm oil. The dominant composition in liquid fuel could be divided to four groups, namely: n-paraffins, i-paraffins, aromatic compounds and olefins. It could be seen that olefins were the major product with its selectivity was more than 40% on all type of catalyst or even thermal cracking, while aromatic compound occupied a small percentage (except on HZSM-5) and the most expected compositions in fuel were n-paraffin together with iso-paraffin contributed about 40%.

As mentioned before, main function of SiO_2, MgO, CaO and Na_2SiO_3 in this work was reduction the oxygen content in fuel via decarboxylation and decarbonylation in order to raise heating value of product. Hence, it was not surprising that the iso-paraffin products on Na_2SiO_3 was approximately similar to thermal cracking with only about 10 %. Anyway, the iso-paraffinic selectivity on SiO_2, MgO and CaO were able to reach fairly high with 17.04%, 17.86% and 16.06%, respectively. The mechanism of branch hydrocarbon production on base catalyst like MgO, CaO and Na_2SiO_3 stilled unclear, that almost occurred via random reaction of free radical group. Contrastingly, zeolites were expected to give higher iso-paraffinic selectivity due to the performance of carbenion ions which were able to shift the process to secondary reaction such as isomerization or cyclisation. Base on the result derived from figure 4.12b, the selectivity of iso-paraffin on zeolite HY and Beta were about 24.6% and 25.94%, correspondingly, while the percentage of branch paraffin on HZSM-5 and Al_2O_3 were just under 20%, approximately. In fact, the possibility to produce branched products also depended on several reason like type of acid site, amount of acid site, acid strength and textural property of catalyst and these factors have been discussed detail on TPD result before. Additionally, the morphology of HZSM-5 was favorable for production of aromatic compounds rather than iso-paraffin because of its high aromates percentage (more than 30%).

From above results, in order to synthesize fuel with high iso-paraffins and low oxygen content from triglyceride via catalytic cracking and decarboxylation, it seems the integration of MgO and Beta is going to be the most promising method because MgO is not only very good in decarboxylation and decarbonylation of triglyceride but also give a fairly ability to generate iso-paraffins in reaction while zeolite beta is the most appropriate one in group of acid catalysts to produce branched paraffins.

4.2.3 Mixed catalyst:

According to the individual positive function of MgO and zeolite beta on reducing oxygen content and promoting iso-paraffin in cracked oil, this part is going to investigate the performance of mixed catalyst which is made by physical mixing.

4.2.3.1 Effect of temperature on yield and selectivity of products

Table 4.10 *Light hydrocarbon products from cracking and decarboxylation of palm oil on mixed MgO-beta catalyst at different reaction temperature*

Products (wt.%)	Temperature (°C)			
	370	400	430	460
CH_4	0.7	1.6	2.8	3.6
C_2H_6	1.2	2.2	3.2	3.8
C_2H_4	1.4	1.8	2.4	3.2
C_3H_8	14.6	15.2	14.9	14.6
C_3H_6	8.5	11.2	12.5	15.1
C_3H_4	0.9	0.6	0.6	0.2
C_4H_{10}	9.3	13.0	13.0	13.2
i-C_4H_{10}	25.1	19.3	15.9	12.5
C_4H_8	11.2	11.6	11.6	12.0
n-C_5H_{12}	12.2	11.7	10.1	8.5
i-C_5H_{12}	0.5	0.2	0.3	0.3
C_5H_{10}	14.5	11.8	12.7	12.9

Reaction condition: Reaction conditions: N_2 atmosphere, reaction temperature: 370 - 460 °C, LHSV: 0.36 h^{-1}, ratio MgO:beta= 1:1. Light hydrocarbons have been analyzed by GC FID and the compositions were calculated according to the area of corresponding GC peaks

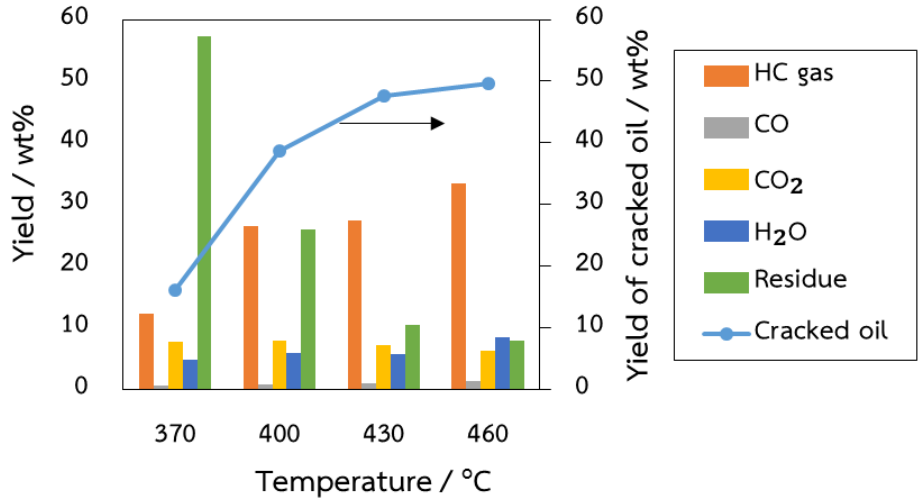

Figure 4.13 *Yield of products from cracking and decarboxylation of palm oil on mixed MgO-beta catalyst depending on reaction temperature. Reaction condition: N_2 atmosphere, reaction temperature: 370 - 460 °C, LHSV: 0.36 h^{-1}, ratio MgO : beta = 1 : 1.*

It is undeniable that temperature is the most important factors affect to yield and composition of cracked oil. Base on the result revealed on figure4.13, liquid yield significantly increased from under 20 wt.% to about 50 wt.% when temperature was raised 90 °C from 370 to 460 °C. There were a huge amount of residue (nearly 60 wt.%) and a small percentage of hydrocarbon gases (about 10 wt.%) at 370 °C due to low activity of catalyst in this condition. When the temperature was raised to 460 °C, yield of light hydrocarbon and residue had the opposite trend where the former rose to more than 30 wt% and the later collapsed about 6 time to lower 10 wt.%. On the other hand, yield of total CO and CO_2 was maintained in a narrow range from 8 to 9 wt.% although temperature changed from 370 to 460 °C. In fact, the decarboxylation and decarbonylation of fatty acid are able to occur from 300-400 °C on suitable catalyst [94], and it seems that at the reaction condition of this work, these processes were stable. However, in order to crack vegetable oil to be more benefit fuel, the higher temperature was applied.

Table 4.10 showed the composition of light hydrocarbon gases from the cracking and decarboxylation of palm oil on base-acid catalyst namely MgO-beta, depending on the

temperature change. Compared with single catalysts, the composition of light hydrocarbon products were sufficiently distributed between saturated, unsaturated, branched and non-branched C_1 through C_5. Accordingly, gas products with 3 carbon atoms were no longer the dominant products in light hydrocarbon gases, and C_4 and C_5 also accounted for a relatively large proportion. Specifically, the C_3 fraction was about 30%, the C_4 and C_5 also accounted for 37% and 21%, respectively. This indicated that the individual activity of MgO and beta in the mixture, because the C_3 hydrocarbon gases was the characterization of the decarboxylation of triglyceride on MgO catalysts while the wide range of products were able to obtain on acid catalyst due to its performance in catalytic cracking of heavy molecules. In addition, the increase of temperature also changed the fraction of light hydrocarbon gases in the trend of producing more unsaturated gas, recording the relative increased in C_2H_4 (1.8%), C_3H_6 (6.6%) and C_4H_8 (0.8%).

Table 4.11 *Chemical composition, acid value and iodine number of liquid product from cracking and decarboxylation of palm oil on mixed MgO-beta catalyst depending on reaction temperature*

Temp	Selectivity %				AV[(a)]	IN[(b)]	HV[(c)]
(°C)	i-paraffins	n-paraffins	Olefins	Aromatics	(mgKOH/g)	(g I/100g)	(cal/g)
370	13.23	17.78	62.16	6.83	-	-	-
400	17.62	18.70	56.62	7.06	7.1	120.4	10350
430	18.87	18.00	53.88	9.26	7.7	115.1	10281
460	21.97	16.30	51.17	10.57	9.9	111.1	10249

[a] Determined by ASTM D664

[b] Determined by ASTM D1959

c Determined by bomb calorimeter

The chemical composition in liquid product from cracking and decarboxylation of palm oil on mixed MgO and beta at the same ratio on table 4.11 was similar to the single

catalysts where the selectivity of olefins were the primary products with over 50%, normal and iso-paraffins contributed about 20% for each and the rest unexpected products was aromates with about 10%. Apparently, iso-paraffins and aromates had the opposite trend with olefins when the temperature increased to 460 ^{o}C from 370 ^{o}C. It could be seen from table 4.11 that the increase of branched paraffinic selectivity was nearly double from around 13% to more than 21%, and the percentage of aromatic compounds similarly slightly rose to 10% form 5%, approximately. In contrast, the amount of olefins in cracked oil moderately decreased about 11% from around 62% to 51% whereas normal paraffins maintained its selectivity at nearly 18%. Actually, the isomerization, cyclisation were favorable at high temperature in the normal pressure (atmospheric pressure) [24]. That is why secondary reactions were also accelerated besides cracking of long chain hydrocarbon at 460 ^{o}C.

The fuel properties of liquid product produced from palm oil on base-acid catalysts were also expressed in terms of acid value, iodine number and heating value in table 4.11. It could be seen that fuel had a relatively low acid index (less than 10 mgKOH / g), the increase of reaction temperature has raised the acid value but not much (from 7.1 to 9.9 mgKOH/g when the temperature rises from 400 to 460 ^{o}C). This liquid product was also suitable for using as a fuel when it had high heating value (10300 cal/g, approximately). However, liquid product had relatively high iodine index values (higher than 110 gI/100 g), which resulted in low oxidation stability.

From the above results, it could be concluded that liquid product from cracking and decarboxylation of palm oil on mixed MgO-beta catalysts had higher content of isoparaffin and less oxygen (CO and CO_2 removal with higher calorific value) than single base catalysts or acid as investigated in the previous section.

4.2.3.2 Effect of liquid hour space velocity (LHSV) on yield and selectivity of products:

Table 4.12 *Light hydrocarbon products from cracking and decarboxylation of palm oil on mixed MgO-beta catalyst at different LHSV*

Products (wt.%)	LHSV (h^{-1})			
	0.36	0.48	0.6	0.72
CH_4	3.6	3.7	4.3	4.9
C_2H_6	3.8	4.1	4.9	5.5
C_2H_4	3.2	3.5	3.5	3.7
C_3H_8	14.6	13.6	16.2	14.8
C_3H_6	15.1	16.1	14.2	14.3
C_3H_4	0.2	0.3	0.7	0.8
C_4H_{10}	13.2	13.4	12.9	13.0
i-C_4H_{10}	12.5	10.9	12.7	9.8
C_4H_8	12.0	13.1	12.4	13.1
n-C_5H_{12}	8.5	6.7	4.8	4.5
i-C_5H_{12}	0,3	0,2	0,4	0,4
C_5H_{10}	12.9	14.4	13.1	15.3

Reaction condition: Reaction conditions: N_2 atmosphere, reaction temperature: 460 ^{o}C, LHSV: 0.36 – 0.72 h^{-1}, ratio MgO:beta= 1:1. Light hydrocarbons have been analyzed by GC FID and the compositions were calculated according to the area of corresponding GC peaks

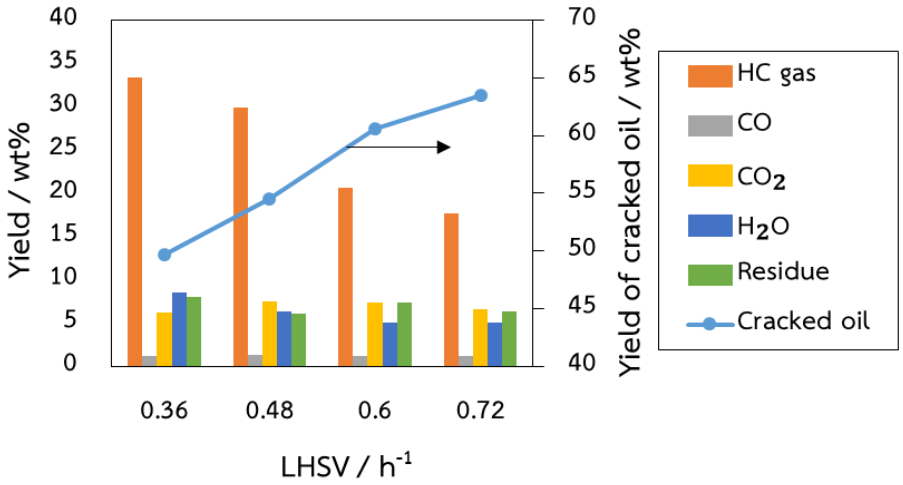

Figure 4.14 *Yield of products from cracking and decarboxylation of palm oil on mixed MgO-beta catalyst depending on LHSV. Reaction condition: N_2 atmosphere, reaction temperature: 460 °C, LHSV: 0.36 – 0.72 h^{-1}, ratio MgO : beta = 1 : 1*

Figure 4.14 showed how resident time affect to properties of product while other reactions were kept constant. When the liquid hour space velocity (LHSV) increased twice from 0.36 h^{-1} the liquid yield sharply rose nearly 15 wt.% to about 64 wt.%. Actually, a decrease of residence time would be favorable for production of heavy products instead of gaseous products. Apparently, the amount of light hydrocarbons remarkably dropped from around 33 wt.% to about 17 wt.%. On the other hand, an increase of LHSV had a subtle effect on remaining products such as CO, CO_2, water and residue. Similarly, the composition of light hydrocarbon gases shown in table 4.12 did not depend much on the change of LHSV.

Table 4.13 *Chemical composition, acid value and iodine number of liquid product from cracking and decarboxylation of palm oil on mixed MgO-beta catalyst depending on LHSV*

LHSV	Selectivity %				AV[(a)]	IN[(b)]	HV[(c)]
(h^{-1})	i-paraffins	n-paraffins	Olefins	Aromatics	(mgKOH/g)	(g I/100g)	(cal/g)
0.36	21.97	16.30	51.17	10.57	9.9	121.6	10249
0.48	21.08	17.77	52.21	8.94	10.5	118.9	10409
0.6	24.01	20.55	48.93	6.51	17.1	112.7	10318
0.72	25.92	20.38	48.06	5.64	18.1	106.1	10276

[a] Determined by ASTM D664

[b] Determined by ASTM D1959

[c] Determined by bomb calorimeter

The growth of LHSV on table 4.13 also promoted the synthesis of paraffinic compounds but constrained the formation of olefins and aromates. It could be seen that the selectivity of iso-paraffins and normal paraffins moderately increased about 4% from 22% to 26% for the former and 16% to 20% for the later, approximately. In contrast, unsaturated compounds experienced the slight decrease when LHSV doubly grew to 0.72 h^{-1} whether percentage of olefin dropped to around 48% from 51% and aromatic substances fell nearly 5%. It seems that the longer residence time was, the higher selectivity of unsaturated matters were got whereas the formation of paraffins (branched and normal) required shorter time in catalytic bulk. However, it could be seen that the acid value of liquid product increased significantly when LHSV increased. When the LHSV was 0.36 h^{-1}, the acid value was only about 10 mgKOH/g and had a sudden increase to 18.1 mgKOH/g as the LHSV increased to 0.72 h^{-1}. This could be explained that when the contact time was shorter due to the increase of LHSV, the fatty acids which have not been reacted in reaction were gone out along with the gaseous product and causing the increasing of acid value of the liquid product. In addition, In addition, it could also be seen that the heating value of liquid product

also increased slightly from 10249 cal/g to 10409 cal/g after the LHSV increased from 0.36 to 0.48 h^{-1}, but then fall down close to the initial value when LHSV increased to 0.72 h^{-1}.

4.2.3.3 Effect of ratio between MgO and zeolite beta on yield and selectivity of products

Table 4.14 *Light hydrocarbon products from cracking and decarboxylation of palm oil on mixed MgO-beta catalyst at different ratio between MgO and zeolite beta*

Products	Ratio MgO:beta		
(wt%)	3:1	1:1	1:3
CH_4	5.2	4.3	4.4
C_2H_6	6.6	4.9	5.0
C_2H_4	4.9	3.5	3.7
C_3H_8	12.2	16.2	15.8
C_3H_6	15.2	14.2	15.2
C_3H_4	1.0	0.7	0.4
C_4H_{10}	13.1	12.9	12.8
i-C_4H_{10}	6.7	12.7	11.1
C_4H_8	14.1	12.4	12.0
n-C_5H_{12}	3.1	4.8	6.1
i-C_5H_{12}	0.6	0.4	0.2
C_5H_{10}	17.1	13.1	13.3

Reaction condition: Reaction conditions: N_2 atmosphere, reaction temperature: 460 °C, LHSV: 0.6 h^{-1}, ratio MgO : beta = 3 : 1, 1 : 1, 1 : 3. Light hydrocarbons have been analyzed by GC FID and the compositions were calculated according to the area of corresponding GC peaks

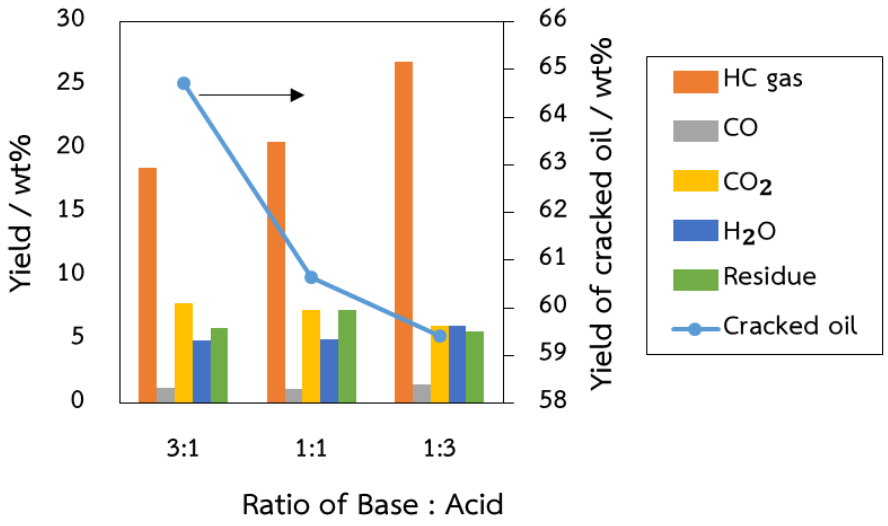

Figure 4.15 *Yield of products from cracking and decarboxylation of palm oil on mixed MgO-beta catalyst depending on ratio between MgO and zeolite beta. Reaction condition: N_2 atmosphere, reaction temperature: 460 ^{o}C, LHSV: 0.6 h^{-1}, ratio MgO : beta = 3 : 1, 1 : 1, 1 : 3*

Figure 4.15 illustrated the influence of individual catalyst in mixture of MgO and zeolite beta to yield and selectivity of products. The investigation was carried out at three different volume ratio of MgO and beta, namely 3 : 1, 1 : 1, and 1 : 3. It could be seen that liquid was able to reached nearly 65 wt.% at ratio 3 : 1 (MgO 75 vol.%, beta 25 vol.%) then it moderately dropped to 60.6 wt.% at the same initial volume of catalysts, and slightly fell to 59.4 wt.% where beta accounted for a vast majority of the mixture (75 vol.%). Similarly, yield of total CO and CO_2 subtly decreased 1.5 wt.% from 9.1 wt.% to 7.6 wt.% when the catalytic ratio of MgO and beta changed from 3 : 1 to 1 : 3. Contrastingly, a higher amount of light hydrocarbon (C_1 to C_5) were produced when the volume of beta was raised from 25 vol.% to 75 vol.%. As mentioned before, MgO played the deoxygenation via decarboxylation and decarbonylation as the main function while acid catalyst like zeolite beta promoted cracking of long chain hydrocarbon. That is why yield of cracked oil, CO and CO_2 went down when the percentage of beta in the mixture with MgO increased. On the other hand, the composition of the light hydrocarbons shown in table 4.14 revealed the clear change in percentage of iso-butane. When MgO occupied a larger proportion (3 : 1 ratio), iso-butane accounted for 6.7% and nearly doubled when the ratio of zeolite beta

increased (1 : 1 and 1 : 3 ratio). This clearly demonstrated the role of acid catalyst in enhancing selectivity of branched compounds.

Table 4.15 *Chemical composition, acid value and iodine number of liquid product from cracking and decarboxylation of palm oil on mixed MgO-beta catalyst depending ratio between MgO and zeolite beta*

Ratio (MgO/beta)	Selectivity %				AV[(a)] (mgKOH/g)	IN[(b)] (g I/100g)	HV[(c)] (cal/g)
	i-paraffins	n-paraffins	Olefins	Aromatics			
3 : 1	24.99	20.48	49.77	4.76	10.0	111.8	10424
1 : 1	24.01	20.55	48.93	6.51	17.1	114.9	10318
1 : 3	23.47	18.84	49.09	8.60	20.9	111.6	10154

[a] Determined by ASTM D664

[b] Determined by ASTM D1959

c Determined by bomb calorimeter

On the other hand, the change of individual MgO and beta in the mixture had the minor effect to the selectivity of main expected compounds in liquid product (table 4.15). Specifically, the selectivity of iso-paraffins and normal paraffins experienced the slight decrease from about 25% to 23.5% for the former and from 20.5% to 18.8% for the later when the amount of MgO drop to 25% from 75% in the mixture. Whereas, percentage of aromates sharply increased nearly twice from 4.8% to 8.6% and the selectivity of olefins was stable at around 49% in case of decreasing ratio MgO over beta. In addition, when MgO occupied a greater proportion of the mixture with zeolite beta (3 : 1), the properties of liquid products were better. Specifically, the acid value and heating value of the liquid product were 10 mgKOH/g and 10424, respectively, at ratio MgO:beta equaled to 3 : 1, whereas at 1 : 3 ratio (zeolite beta accounted for more weight) acid value liquid product was 20.9 mgKOH/g and heating value was 10154 cal/g. Apparently, the best ratio of MgO and beta was 3 : 1 whether it is able to give remarkable liquid yield as well as oxygenation removal due to high oxygen removal

via high CO and CO_2 yield together with high selectivity of branch paraffinic compounds.

4.2.3.4 Effect of hydrogen pressure on yield and selectivity of products

Table 4.16 *Light hydrocarbon products from cracking and decarboxylation of palm oil on mixed MgO-beta catalyst at different hydrogen pressure*

Products (wt%)	Hydrogen pressure (MPa)			
	0	0.1	0.5	1
CH_4	5.2	10.5	11.8	10.1
C_2H_6	6.8	15.0	14.8	14.1
C_2H_4	4.9	9.9	6.9	3.2
C_3H_8	10.4	17.2	21.0	29.3
C_3H_6	15.7	21.6	12.0	9.8
C_3H_4	1.0	0.9	0.3	0.2
C_4H_{10}	13.6	10.3	10.3	14.5
i-C_4H_{10}	4.3	7.8	5.6	11.5
C_4H_8	15.6	4.2	6.5	6.4
n-C_5H_{12}	0.7	0.8	0.3	0.2
i-C_5H_{12}	0.8	1.7	0.9	0.4
C_5H_{10}	21.1	0.1	9.6	0.2

Reaction condition: Reaction conditions: hydrogen pressure: 0 – 1 MPa, reaction temperature: 460 ^{o}C, LHSV: 0.6 h^{-1}, ratio MgO : beta = 3 : 1. Light hydrocarbons have been analyzed by GC FID and the compositions were calculated according to the area of corresponding GC peaks.

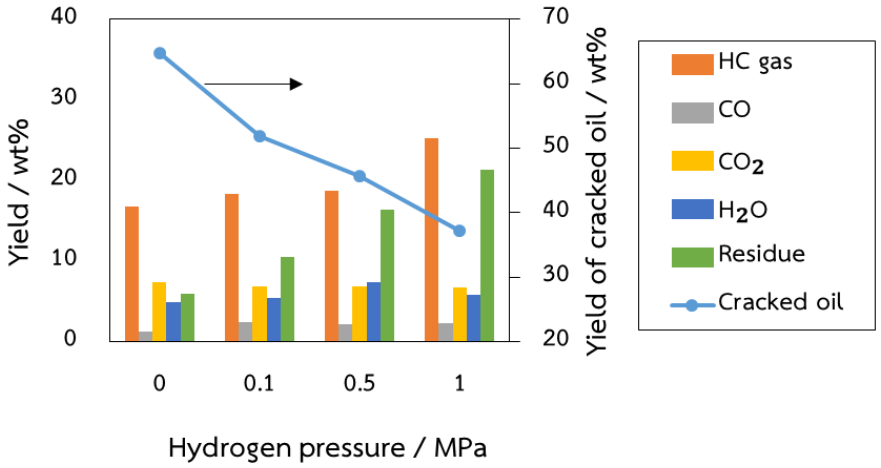

Figure 4.16 *Yield of products from cracking and decarboxylation of palm oil on mixed MgO-beta catalyst depending on hydrogen pressure. Reaction condition: hydrogen pressure: 0 – 1 MPa, reaction temperature: 460 ^{o}C, LHSV: 0.6 h^{-1}, ratio MgO : beta = 3 : 1*

From the above results, the fuel in range of gasoline and diesel with the selectivity of iso-paraffins was about 25% on mixed 75 vol.% MgO and 25 vol.% beta catalyst. In order to push up the selectivity of branch paraffin, this part would observe the effect of hydrogen pressure on liquid product composition. However, this study was not aimed to use hydrogen for hydrodeoxygenation at high pressure, it was simply used to promote the isomerization process during the cracking reaction of long chain hydrocarbon at partial hydrogen pressure around 1 MPa [95]. So, the modified 0.5 wt.% Pd on beta was used instead of zeolite beta in the mixture with MgO and the investigated hydrogen pressure was replaced to nitrogen in range of pressure from 0 to 10 bars.

Base on the result on figure 4.16, the cracked oil yield rapidly went down from 64.76 wt.% to 37.14 wt.% when hydrogen pressure was steeply increased from 0 to 10 bars. Obviously, high pressure was favorable for the cracking and coking reaction cause of the increase of gaseous hydrocarbons and residue products. However, the present of hydrogen did not have much effect on deoxygenation on MgO due to the total CO and CO_2 yield remained stable at 9 wt.%, approximately. On the other hand, the presence of hydrogen gas at different pressures also changed the composition of light

hydrocarbon gases (Table 4.16). Firstly, increasing the pressure from 0 to 1 MPa made more light gases in the mixture of gaseous hydrocarbons whether the percentage of gases from C_1 to C_3 increased while from C_4 to C_5 decreased markedly. Typically, the total percentage of C_3 gas had risen significantly from 27.1% to 39.3%, while total C_5 emissions have decreased remarkably from 22.6% to 0.8% since the pressure increased from 0 to 1 MPa. Secondly, the presence of hydrogen in the reaction slowed down the proportion of unsaturated gases. Particularly, the percentage of C_3H_6 and C_4H_8 decreased by 5.9% and 9.2%, respectively, when the hydrogen pressure increased from 0 to 1 MPa.

Table 4.17 *Chemical composition, acid value and iodine number of liquid product from cracking and decarboxylation of palm oil on mixed MgO-beta catalyst depending hydrogen pressure*

Pressure	Selectivity %				AV[(a)]	IN[(b)]	HV[(c)]
(MPa)	i-paraffins	n-paraffins	Olefins	Aromatics	(mgKOH/g)	(g I/100g)	(cal/g)
0	31.33	17.24	47.75	3.68	14.2	108.3	10352
0.1	35.32	18.48	39.12	7.07	9.3	91.6	10331
0.5	25.38	25.73	39.69	9.21	6.8	94.6	10397
1	19.13	31.84	38.75	10.28	6.2	89.7	10328

[a] Determined by ASTM D664

[b] Determined by ASTM D1959

c Determined by bomb calorimeter

In addition, hydrogen pressure had the apparent effect on composition of liquid product. According to the graph on table 4.17, the iso-paraffins selectivity reached the peak at 35.32% when hydrogen pressure was raised to 1 bar, then it sharply declined to 25.38% and 19.13% at 5 and 10 bars, correspondingly. By contrast, the selectivity of normal paraffins and aromatic compounds had the same upward trend whether the former significantly rose over 14% from 17.24% to 31.84% and later moderately went

up to 10.28% from 3.68%. It could be seen that the application of high pressure hydrogen for cracking and decarboxylation of palm oil on base-acid mixture catalysts did not achieve the desired results. By applying hydrogen gas to the reaction, a 0.5 wt.% Pd/beta catalyst was used instead of the zeolite beta, unfortunately, at high pressures in this reaction the coking process occurred rapidly causing the catalyst deactivation and could not support for reaction any longer. That was why at 0.1MPa the results were pretty good when the iso-paraffin selectivity was over 35% but then dropped very quickly to less than 20% at 1 MPa and the yield of the liquid product also dropped significantly to below 40 wt.%. Anyway, it could be seen that the presence of hydrogen increased the fuel quality of liquid product when acid value and iodine number decreased.

Table 4.18 *Selectivity of iso-paraffin in deoxygenated oil with different hydrogen pressures*

H_2 pressure (MPa)	iso-paraffin selectivity (%)	Percentage (%)	
		C_{6-14}	C_{15+}
0	31.33	27.77	72.23
0.1	35.32	70.33	29.67
0.5	25.38	95.22	4.78
1.0	19.13	94.92	5.08

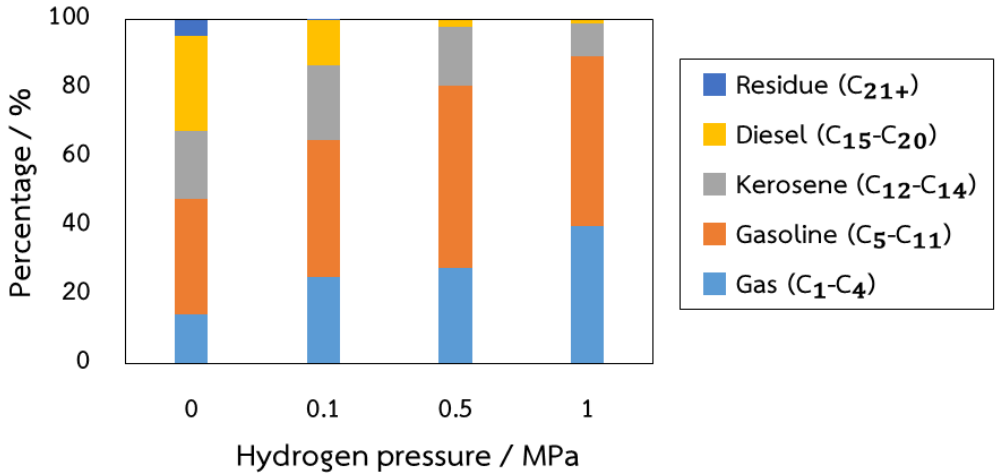

Figure 4.17 *Product fraction of liquid cracked oil from cracking and decarboxylation of palm oil on mixed MgO-beta catalyst depending on hydrogen pressure. Reaction condition: hydrogen pressure: 0 – 1 MPa, reaction temperature: 460 ^{o}C, LHSV: 0.6 h^{-1}, ratio MgO : beta = 3 : 1*

The result in table 4.18 revealed that the selectivity of iso-paraffins concentrated in the range of carbon number C_{15}+ at atmospheric hydrogen pressure with its percentage being more than 70%. Nevertheless, when the pressure steeply increased to 0.1, 0.5 and 1 MPa, the iso-paraffinic selectivity switched to lighter product fraction (C_6 to C_{14}). The reason was the product fractions distribution have been shifted to gasoline range (figure 4.17) where C_5 to C_{11} were the main hydrocarbons. In fact, the isomerization reaction was favorable for the long chain hydrocarbons whereas high hydrogen pressure, at over 2 MPa, favored short chain counterparts [89, 96, 97]. Anyway, the high hydrogen pressure was not the objective of this study, so the most suitable hydrogen pressure for mixed 75 vol.% MgO and 25 vol.% beta modified 0.5 wt.% Pd was 1 bar in order to obtain acceptable iso-paraffinic selectivity.

4.2.3.5 Effect of time on stream selectivity of products

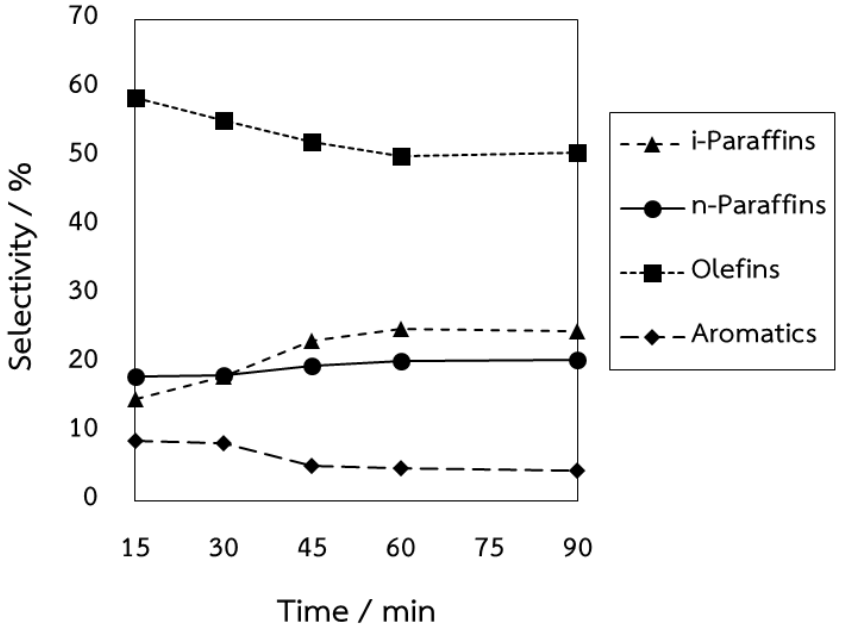

Figure 4.18 *Chemical composition of liquid cracked oil from cracking and decarboxylation of palm oil on mixed MgO-beta catalyst depending on reactoin time. Reaction condition: N_2 atmosphere, reaction temperature: 460 ^oC, LHSV: 0.6 h^{-1}, ratio MgO : beta = 3 : 1*

Figure 4.18 showed the effect of reaction time on selectivity of key compounds in liquid products from the cracking and decarboxylation of palm oil. Generally, it could be seen that in the first 60 minutes the selectivity of olefins and aromatics had the same downward tendency, while iso-paraffins and paraffins tended to increase. In the first 15 minutes, olefins were produced a lot and accounted for nearly 60% then it dropped dramatically to about 50% after 60 minutes. Similarly, at first 30 minutes the selectivity of the aromatics was about 8.5% before dropping by nearly half to remain about 4.2% at the 60th minute. On the contrary, only about 17% iso-paraffin in liquid product within the first 15 minutes and then increased significantly to nearly 25% after 60 minutes. It has been observed the same trend with iso-paraffins but the selective paraffins increased less with only 2.5% from 18% to 20.5% in the same period. From 60 minutes onwards, the ratio of substances in liquid products seem to be unchanged.

Those results may help to predict the mechanism of the reaction because there are a lot of oleofins have been produced in the initial stages, while in the early stages there are not many branched paraffins have been created. The reduction in proportion of olefins after reaction time has been longer almost corresponds to an increase of iso-paraffins selectivity. Thus, it is proposed that the olefins will be converted carbenium after absorbing proton H^+ from zeolite catalyst and converted to tattiary carbenium to produce iso-paraffin as the secondary reaction.

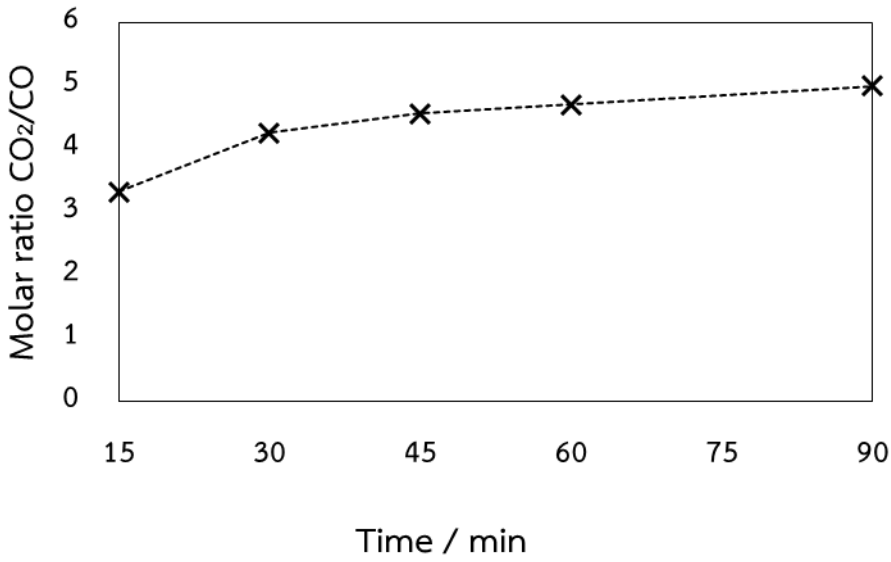

Figure 4.19 *Ratio between CO_2 and CO from cracking and decarboxylation of palm oil on mixed MgO-beta catalyst depending on reactoin time. Reaction condition: N_2 atmosphere, reaction temperature: 460 ^oC, LHSV: 0.6 h^{-1}, ratio MgO : beta = 3 : 1*

Figure 4.19 showed the influence of reaction time on ratio between CO_2 and CO in the cracking and decarboxylation of palm oil on mixed MgO-beta catalyst. The relationship between CO_2 and CO was able to be used to predict the mechanism of decarboxylation reaction on the MgO catalyst. It could be seen that the ratio of CO_2 and CO in the first 15 minutes of reaction at about 3.3, then increased significantly to around 4.3 in 30 minutes, then increased gradually to about 5 after 90 minutes. This result could be predicted for the MgO-triglyceride intermediate state. As discussed before in the XRD pattern of base catalysts part, MgO would probably react with fatty

acids to form the salt of fatty acids before decomposition to form $MgCO_3$ which would be decomposed by heat to release CO_2 and MgO.

4.3 Propose reaction mechanism

The mechanism of iso-paraffin production reaction from triglyceride in palm oil on mixed base-acid catalysts will be proposed base on composition of products after reaction and the change of components in liquid product by time under optimal reaction conditions. Triglycerides are converted into branched hydrocarbons in the cracking and decarboxylation reactions on the mixed MgO-beta catalyst can be divided into three main stages:

a) Hydrolysis triglyceride forming FFA

Major products of the reaction included cracked oil, gaseous products (CO, CO_2 and light hydrocarbons from C_1 to C_5), residue and water. It can be seen that the cracking and decarboxylation of palm oil in case of non-catalyst (pyrolysis) or on base catalysts, acid catalysts and a mixed base-acid catalyst there are always an amount of water present in result about 2.5 wt.% to more than 10 wt.%, whereas palm oil are virtually water-free (or just moisture content). The only possibility in this case is that water is generated from the dehydration process of fatty acids or glycerol. Table 4.9 also showed that palm oil had a very low acid value (0.7 mgKOH/g) which indicated that the raw material had very little fatty acid content, whereas the liquid products of the reaction have high acid. Particularly, the liquid product from reaction carried out on base catalyst had acid value from 6 to 10 mgKOH/g, on acid catalyst was over 30 mgKOH/g and on mixed MgO-beta catalyst was about 10 mgKOH/g. Thus, in the reaction a fatty acids have been produced and this result was similar to the study from Tani research group [41]. The proposed mechanism for this case which fatty acids have been formed is that the triglycerides in palm oil have been hydrolyzed to produce fatty acids and glycerol, detail as below:

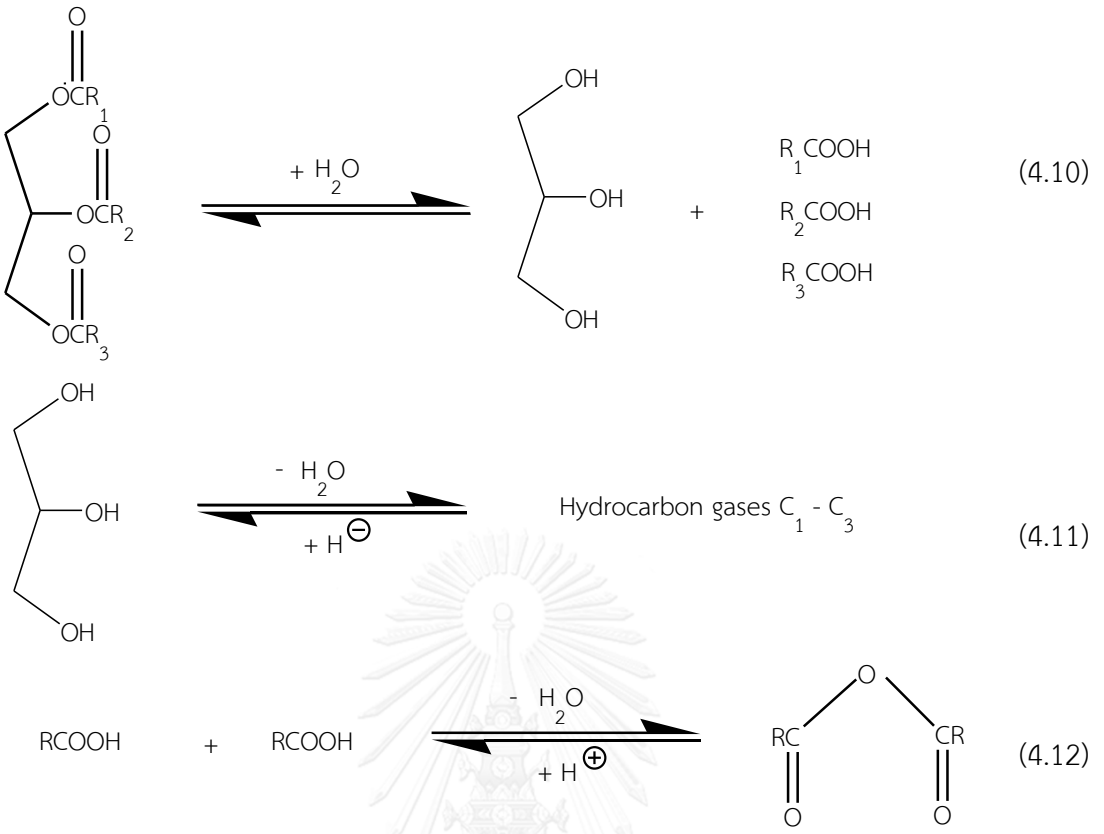

b) Intermediate state of MgO:

The role of MgO catalyst is clearer in this stage when triglycerides have been hydrolyzed to free fatty acids. Accordingly, MgO will react with free fatty acids to form a salt of Mg with fatty acids, and this is considered to be the most important intermediate product in the decarboxylation of triglycerides. The exist of intermediate product in decarboxylation between Caxium and fatty acid was discused in the research of Brown [98]. As discussed before, the ratio of CO_2 and CO depending on time could prove the existence of an intermediate product of MgO and triglyceride (in this case free fatty acids) which would transform into $MgCO_3$ and released a large ketone molecular as the secondary intermediate product. In addition, the XRD pattern of MgO catalyst after the reaction had the presence of the $MgCO_3$ compound which could be seen as an evidence for that hypothesis. On the other hand, the CO_2-TPD of MgO exhibited a peak at about 100 °C indicated that $MgCO_3$ was difficult to sustain at reaction temperature (460 °C). Therefore, $MgCO_3$ would be decomposed to release

CO_2 and recover MgO catalyst for the next reaction [99]. This process can be described as follows:

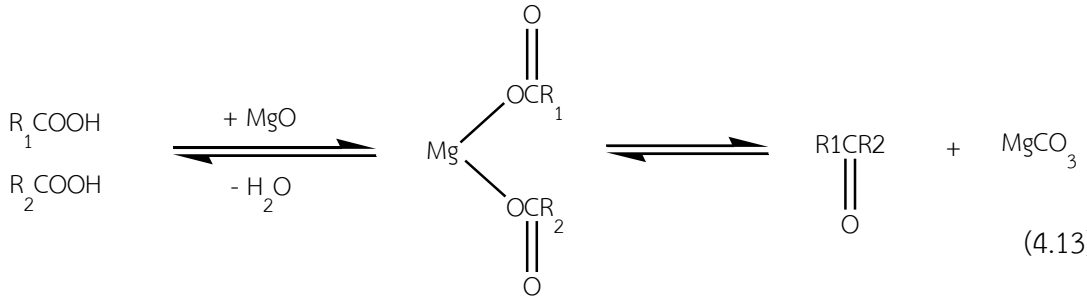

(4.13)

c) Iso-paraffin forming:

In this stage, the role of zeolite beta will be a catalyst for the cracking and isomerization of large ketone intermediate molecular [99]. As mentioned before, the olefins in the initial stage which might be from the thermal cracking process would absorb proton H^+ forming carbenium. Then, carbenium would form a variety of products in which the major role was to crack large molecules into smaller molecules, or to convert into higher order carbenium to produce side products secondary reaction such as isomerization and cyclisation [24].

(4.14)

Cracking:

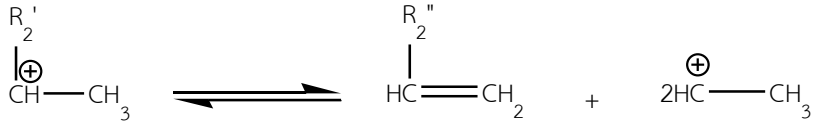

(4.15)

The carbenium transpose to higher order carbenium:

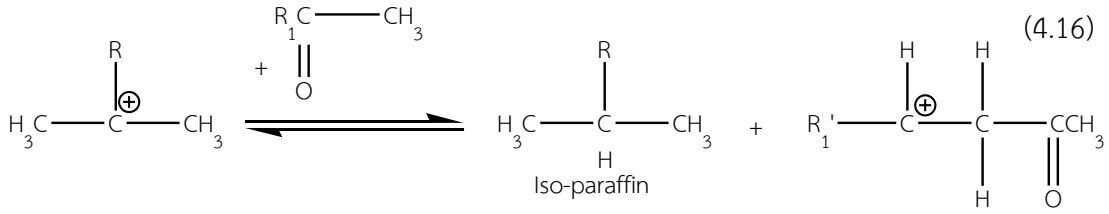

(4.16)

New carbenium would attack to other carbon chain or release proton H^+ back to catalyst [100]. So, the summarization for all stages from triglyceride to iso-paraffin can be described as below:

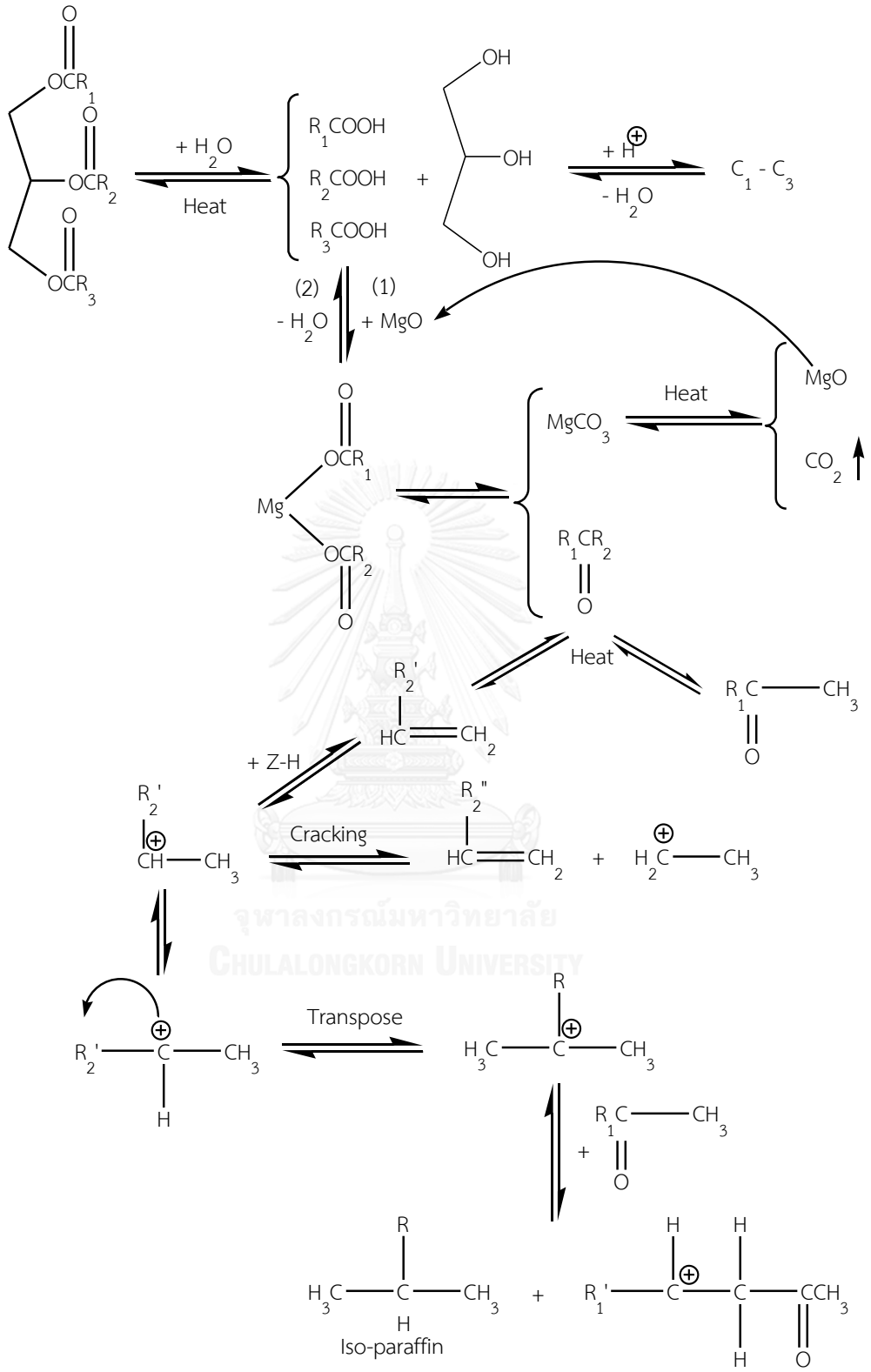

Figure 4.20 *Mechanism for synthesis of iso-paraffin from palm oil mixed MgO-beta*

CHAPTER V:
CONCLUSION AND RECOMMENDATION

5.1 Conclusion

Through the study on synthesis of iso-paraffin fuels from palm oil over heterogeneous catalytic acid and base catalysts in semi-batch reactors with the desirability of producing an alternative fuel with high branched paraffins and low oxygen content, the author has following conclusions:

1) Among the base catalysts studied, MgO was the most suitable catalyst for the conversion of palm oil into low oxygen content fuel because it had high performance on deoxygenation process via decarboxylation and decarbonylation in the range of reaction temperature from 430 to 460 ℃.

2) The acid catalysts used to enhance iso-paraffin content in liquid products showed that the acidity of the catalyst had a significant effect on the selectivity of iso-paraffin. Accordingly, catalysts had medium acid strength like zeolite beta were more suitable for increasing the selectivity of iso-paraffin.

3) In order to create an effective catalyst for converting triglycerides into low-oxygen and high-content iso-paraffin based, the integration of MgO (base catalyst) and zeolite beta (acid catalyst) revealed the good result. It could be seen that, MgO and beta performed their own functions distinctly in the mixture and do not collapse each other. Typically, the liquid product obtained from the palm oil transformation reaction in semi-batch reactor on mixed MgO-beta catalyst had high iso-paraffin and low oxygen content (high CO and CO_2 removal together with high heating value)

4) In nitrogen atmosphere, liquid product yields could be obtained up to 65 wt% at reaction conditions as following: temperature= 460 ^{o}C, LHSV= 0.6 h^{-1}, ratio MgO : beta = 3 : 1. The iso-paraffin selectivity of the product under optimal reaction conditions was 25% and the heating value was 10424 cal/g which was very close to that of traditional diesel (10675 cal/g).

5) In this study, hydrogen has been tested at low pressures (less than 1 MPa) to increase selectivity of branched paraffins in liquid products and 0.5 wt% Pd/beta catalyst has been used instead of beta in the mixture with MgO. Under optimum conditions, iso-paraffin selectivity of liquid product could be about 35% at hydrogen pressure of 0.1 MPa. However, at higher hydrogen pressures (0.5 and 1 MPa), the results were not as expected, yield of liquid product was significantly reduced, and iso-paraffin was also reduced and this phenomena has been predicted by coke formation very quickly on surface of catalyst and cause the catalyst deactivation.

5.2 Recommendation

The author has some suggestions for the future work on this topic:

1) To evaluate the oxygen content of liquid products in this study, the author used the relative comparison of the total yield of CO and CO_2 together with heating value of liquid products. However, in order to have more accurate conclusion, liquid products need to be analyzed the oxygen content by CHN analysis and compared with the raw materials.

2) The application of hydrogen in the same reactor at high pressures to increase the selectivity of isoparaffin in liquid product did not obtain the expected results. The author suggests separating the hydrogenation process into other reactor following the cracking and decarboxylation of palm oil in a semi-batch reactor.

REFERENCES

1. S. N. Naik, V. G. Vaibhav, K. R. Prasant, and K. D. Ajay, *Production of first and second generation biofuels: A comprehensive review.* Renew Sust Energ Rev **14 (2010**) 578–597.

2. N. S. Larissa, C. P. F. Isabel, P. S. Fabiana, and M. D. P. Vânya, *Biokerosene and green diesel from macauba oils via catalytic deoxygenation over Pd/C.* Fuel **164 (2016**) 329–338.

3. E. Meller, U. Green, Z. Aizenshtat, and Y. Sasson, *Catalytic deoxygenation of castor oil over Pd/C for the production of cost effective biofuel.* Fuel **133 (2014**) 89–95

4. M. S. Zanuttini, C. D. Lago, C. A. Querini, and M. A. Peralta, *Deoxygenation of m-cresol on Pt/γ -Al_2O_3 catalysts.* Catal Today **213 (2013**) 9–17.

5. D. Kubicka and L. Kaluza, *Deoxygenation of vegetable oils over sulfided Ni, Mo and NiMo catalysts.* Appl Catal A: Gen **372 (2010**) 199–208.

6. P. Songphon, K. Worapon, Y. Hiroshi, T. Tomohiko, K. Kunlanan, L. Navadol, and A. Suttichai, *Oil extracted from spent coffee grounds for bio-hydrotreated diesel production.* Energy Convers Manage **126 (2016**) 1028–1036.

7. Z. Haiping, L. Hongfei, and Z. Ying, *The role of cobalt and nickel in deoxygenation of vegetable oils.* Appl Catal B: Environ **160–161 (2014**) 415–422.

8. M. J. A. Romero, A. Pizzi, G. Toscano, G. B. Busca, B. Bosio, and E. Arato, *Deoxygenation of waste cooking oil and non-edible oil for the production of liquid hydrocarbon biofuels.* Waste Manage **47 (2016**) 62–68.

9. M. N. Asikin, H. V. Lee, J. C. Juana, A. R. Noorsaadahb, A. M. A. G. Abdulkareem, and Y.Y. Taufiq, *Waste clamshell-derived CaO supported Co and W catalysts for renewable fuels production via cracking-deoxygenation of triolein.* J Anal Appl Pyrol **120 (2016**) 110–120.

10. M. N. Asikin, H. V. Lee, Y. H. Taufiq, J. C. Juana, and N. A. Rahman, *Pyrolytic–deoxygenation of triglyceride via natural waste shell derived $Ca(OH)_2$ nanocatalyst.* J Anal Appl Pyrol **117 (2016**) 46–55.

11. H. Konstantin, A. Matthias, P. Rebecca, and F. H. Wolfgang, *Deoxygenation and cracking of free fatty acids over acidic catalysts by single step conversion for the production of diesel fuel and fuel blends.* Appl Catal B: Environ **174–175 (2015**) 383–394.

12. L. Peter, H. Pavol, H. Marcela, and H. Aleš, *Conversion of rapeseed oil via catalytic cracking: Effect of the ZSM-5 catalyst on the deoxygenation process.* Fuel Process Technol **134 (2015**) 223–230.

13. M. G. José, D. Eduardo, and Ignacio, *Deoxygenation of m-toluic acid over hierarchical x zeolite.* Catal Commun **78 (2016**) 55–58.

14. W. Kiatkittipong, S. Phimsen, K. Kiatkittipong, S. Wongsakulphasatch, N. Laosiripojana, and S. Assabumrungrat, *Diesel-like hydrocarbon production from hydroprocessing of relevant refining palm oil.* Fuel Processing Technology **116 (2013**) 16–26.

15. C. C. K. Barreto, C. C. Oliveira, G. G. Souza, P. A. Z. Suarez, and J. C. Rubim, *Evaluation of the stability during storage of a diesel-like fuel obtained by the pyrolysis of soybean oil.* biomass and bioenergy **3 7 (2012**) 4 2-4 8.

16. W. Seames, Y. Luo, I. Ahmed, T. Aulich, A. Kuba ́tova, J. Sta ́vova, and E. Kozliak, *The thermal cracking of canola and soybean methyl esters: Improvement of cold flow properties.* biomass and bioenergy **34 (2010**) 939-946.

17. A. L. F. Santos, D. U. Martins, O. K. Iha, R. A. M. Ribeiro, R. L. Quirino, and P. A. Z. Suarez, *Agro-industrial residues as low-price feedstock for diesel-like fuel production by thermal cracking.* Bioresource Technology **101 (2010**) 6157–6162.

18. B. V. D. Beld, E. Holle, and J. Florijn, *The use of pyrolysis oil and pyrolysis oil derived fuels in diesel engines for CHP applications.* Applied Energy **102 (2013**) 190–197.

19. H. Lappi and R. Alén, *Pyrolysis of vegetable oil soaps—Palm, olive, rapeseed and castor oils.* Journal of Analytical and Applied Pyrolysis **91 (2011**) 154–158.

20. Y. Luo, I. Ahmed, A. Kubátová, J. Šť ávová, T. Aulich, S. M. Sadrameli, and W. S. Seames, *The thermal cracking of soybean/canola oils and their methyl esters.* Fuel Processing Technology **91 (2010**) 613–617.

21. R. R. Gil, R. P. Girón, M. S. Lozano, B. Ruiz, and E. Fuente, *Pyrolysis of biocollagenic wastes of vegetable tanning. Optimization and kinetic study.* Journal of Analytical and Applied Pyrolysis **98 (2012**) 129–136.

22. J. Fimberger, M. Swoboda, and A. Reichhold, *Thermal cracking of canola oil in a continuously operating pilot plant.* Powder Technology **(2016**) In Press, Corrected Proof.

23. J. G.Speight, *Thermal cracking of petroleum*. Natural and Laboratory Simulated Thermal Geochemical Processes. 2003: Springer Science Business Media.

24. M. A. Fahim, T. A. Al-Sahhaf, and A. Elkilani, *Fundamentals of Petroleum Refining*. 2010, The Netherlands: Elsevier. 516.

25. F. Zhoub, Y. Gao, G. Wu, F. Ma, and C. Liu, *Improved catalytic performance and decreased coke formation in post-treated ZSM-5 zeolites for methanol aromatization.* Microporous and Mesoporous Materials **240 (2017**) 96–107.

26. Q. Chen, J. Zhang, B. Pan, W. Kong, Y. Chen, W. Zhang, and Y. Sun, *Temperature-dependent anti-coking behaviors of highly stable Ni-CaO-ZrO_2 nanocomposite catalysts for CO2 reforming of methane.* Chemical Engineering Journal **320 (2017**) 63–73.

27. V. Abbasov, T. Mammadova, N. Andrushenko, N. Hasankhanova, Y. Lvov, and E. Abdullayev, *Halloysite–Y-zeolite blends as novel mesoporous catalysts for the cracking of waste vegetable oils with vacuum gasoil.* Fuel **117 (2014**) 552–555.

28. E. Y. Emori, F. H. Hirashima, C. H. Zandonai, C. A. O. Bravo, N. R. C. F. Machado, M. Heloisa, and N. O. Scaliante, *Catalytic cracking of soybean oil using ZSM5 zeolite.* Catalysis Today **(2016**) (article in press).

29. V. Abbasov, T. Mammadova, N. Aliyeva, M. Abbasov, N. Movsumov, A. Joshi, Y. Lvov, and E. Abdullayev, *Catalytic cracking of vegetable oils and vacuum gasoil with commercial high alumina zeolite and halloysite nanotubes for biofuel production.* Fuel **181 (2016**) 55-63.

30. S. M. Sadrameli, *Thermal/catalytic cracking of liquid hydrocarbons for the production of olefins: A state-of-the-art review II: Catalytic cracking review.* Fuel **173 (2016**) 285–297.

31. X. Zhao, L. Wei, S. Cheng, Y. Cao, J. Julson, and Z. Gu, *Catalytic cracking of carinata oil for hydrocarbon biofuel over fresh and regenerated Zn/Na-ZSM-5.* Applied Catalysis A: General **507 (2015**) 44–55.

32. A. Ishihara, D. Kawaraya, T. Sonthisawate, K. Kimura, T. Hashimoto, and H. Nasu, *Catalytic cracking of soybean oil by hierarchical zeolite containing mesoporous silica-aluminas using a Curie point pyrolyzer.* Journal of Molecular Catalysis A: Chemical **396 (2015**) 310–318.

33. L. Xiangping, G. Chena, C. Liua, W. Mac, B. Yanc, and J. Zhang, *Hydrodeoxygenation of lignin-derived bio-oil using molecular sieves supported metal catalysts: A critical review.* Renewable and Sustainable Energy Reviews **71 (2017**) 296–308.

34. I. T. Ghampson, G. Pecchi, J. L. G. Fierro, A. Videlad, and N. Escalona, *Catalytic hydrodeoxygenation of anisole over Re-MoOx/TiO_2 and Re-VOx/TiO_2 catalysts.* Applied Catalysis B: Environmental **208 (2017**) 60–74.

35. A. Gutierrez, E. M. Turpeinen, T. R. Viljava, and O. Krause, *Hydrodeoxygenation of model compounds on sulfided CoMo/γ -Al_2O_3 and NiMo/γ -Al_2O_3 catalysts; Role of sulfur-containing groups in reaction networks.* Catalysis Today **285 (2017**) 125–134.

36. C. Woltz, *Kinetic studies on alkane hydroisomerization over bifunctional catalysts*, in *Lehrstuhl für Technische Chemie II*. 2005, Technische Universität München: Germany.

37. V. M. Benitez, C. A. Querini, N. S. Fõ Âgoli, and R. A. Comelli, *Skeletal isomerization of 1-butene on WOx/ɣ-Al_2O_3.* Applied Catalysis A: General **178 (1999**) 205-218.

38. A. S. Berenblyum, T. A. Podoplelova, R. S. Shamsiev, E. A. Katsman, and V. Ya. Danyushevsky, *On the mechanism of catalytic conversion of fatty acids into hydrocarbons in the presence of palladium catalysts on alumina.* Petroleum Chemistry **51 (2011**) 336–341.

39. P. M. Arvela, M. Snåre, K. Eränen, J. Myllyoja, and D.Yu. Murzin, *Continuous decarboxylation of lauric acid over Pd/C catalyst.* Fuel **87 (2008**) 3543–3549.

40. E. Sari, M. Kim, S. O. Salley, and K. Y . S. Ng, *A highly active nanocomposite silica-carbon supported palladium catalyst for decarboxylation of free fatty acids for green diesel production: Correlation of activity and catalyst properties.* Applied Catalysis A: General **467 (2013**) 261–269.

41. H. Tani, T. Hasegawa, M. Shimouchi, K. Asami, and K. Fujimoto, *Selective catalytic decarboxy-cracking of triglyceride to middle-distillate hydrocarbon.* Catalysis Today **164 (2011**) 410–414.

42. P. A. Webb, *Introduction to Chemical Adsorption Analytical Techniques and their Applications to Catalysis*. 2003, Georgia: Micromeritics Instrument Corp.

43. I. Simakova, O. Simakova, P. M. Arvela, and D. Y. Murzin, *Decarboxylation of fatty acids over Pd supported on mesoporous carbon.* Catalysis Today **150 (2010**) 28–31.

44. A. Dragu, S. Kinayyigit, E.J. G.Suárez, M. Florea, E. Stepan, S. Velea, L. Tanase, V. Collière, K. Philippot, P. Granger, and V.I. Parvulescu, *Deoxygenation of oleic acid: Influence of the synthesis route of Pd / mesoporous carbon nanocatalysts ontotheir activity andselectivity.* Applied Catalysis A: General **504 (2015**) 81–91.

45. J. G. Na, B. E. Yi, J. N. Kim, K. B. Yi, S. Y. Park, J. H. Park, J. N. Kim, and C. H. Ko, *Hydrocarbon production from decarboxylation of fatty acid without hydrogen.* Catalysis Today **156 (2010**) 44–48.

46. J. G. Na, J. K. Han, Y. K. Oh, J. H. Park, T. S. Jung, S. S. Han, H. C. Yoon, S. H. Chung, J. N. Kim, and C. H. Ko, *Decarboxylation of microalgal oil without hydrogen into hydrocarbon for the production of transportation fuel.* Catalysis Today **185 (2012**) 313–317.

47. M. Romero, A. Pizzi, G. Toscano, A. A. Casazza, G. Busca, B. Bosio, and E. Arato, *Preliminary experimental study on biofuel production by deoxygenation of Jatropha oil.* Fuel Processing Technology **137 (2015**) 31–37.

48. N. Asikin-Mijan, H.V. Lee, Y.H. T. Yap, J.C. Juan, and N.A. Rahman, *Pyrolytic–deoxygenation of triglyceride via natural waste shell derived $Ca(OH)_2$ nanocatalyst.* Journal of Analytical and Applied Pyrolysis **117 (2016**) 46–55.

49. T. Morgan, E. S. Jimenez, A. E. H. Ware, Y. Ji, D. Grubb, and M. Crocker, *Catalytic deoxygenation of triglycerides to hydrocarbons over supported nickel catalysts.* Chemical Engineering Journal **189–190 (2012**) 346–355.

50. E. S. Jimenez, T. Morgan, J. Shoup, A. E. H. Ware, and M. Crocker, *Catalytic deoxygenation of triglycerides and fatty acids to hydrocarbons over Ni–Al layered double hydroxide.* Catalysis Today **237 (2014**) 136–144.

51. V.G. Komvokis, S. Karakoulia, E.F. Iliopoulou, M.C. Papapetrou, I.A. Vasalos, A.A. Lappas, and K.S. Triantafyllidis, *Upgrading of Fischer–Tropsch synthesis bio-waxes via catalytic cracking: Effect of acidity, porosity and metal modification of zeolitic and mesoporous aluminosilicate catalysts.* Catalysis Today **196 (2012**) 42-55.

52. Z. W. Liu, X. Li, K. Asami, and K. Fujimoto, *Iso-paraffins synthesis from modified Fischer–Tropsch reaction—Insights into Pd/beta and Pt/beta catalysts.* Catalysis Today **104 (2005**) 41–47.

53. Y. Wang, Z. Tao, B. Wu, J. Xu, C. Huo, K. Li, H. Chen, Y. Yang, and Y. Li, *Effect of metal precursors on the performance of Pt/ZSM-22 catalysts for n-hexadecane hydroisomerization.* Journal of Catalysis **322 (2015**) 1–13.

54. X. Zhao, L. Wei, S. Cheng, Y. Huang, Y. Yu, and J. Julson, *Catalytic cracking of camelina oil for hydrocarbon biofuel over ZSM-5-Zn catalyst.* Fuel Processing Technology **139 (2015**) 117–126.

55. H. Lin H. Wang, P. Feng, X. Han, Y. Zheng *Integration of catalytic cracking and hydrotreating technology for triglyceride deoxygenation.* Catalysis Today **In Press, Corrected Proof**

56. G. P. Maniam, N. Hindryawati, M. R. Karim, and K. F. Chong, *Transesterification of used cooking oil over alkali metal (Li, Na, K) supported rice husk silica as potential solid base catalyst.* Engineering Science and Technology, an International Journal **17 (2014**) 95-103.

57. M. Wang, T. Wei, Y. Sun, and B. Zhong, *Effect of the amount of base site on catalytic behavior of cao for synthesis of dimethyl carbonate from propylene carbonate and methanol.* Fuel Chemistry Division Preprints **47 (2002**) 88-89.

58. L. Li, K. Quan, J. Xu, F. Liu, S. Liu, S. Yu, C. Xie, B. Zhang, and X. Ge, *Liquid Hydrocarbon Fuels from Catalytic Cracking of Waste Cooking Oils Using Basic Mesoporous Molecular Sieves K_2O/Ba-MCM-41 as Catalysts.* ACS Sustainable Chem. Eng. **1 (2013**) 1412–1416.

59. C. Xu, D. I. Enache, R. Lloyd, D. W. Knight, J. K. Bartley, and G. J. Hutchings, *MgO Catalysed Triglyceride Transesterification for Biodiesel Synthesis.* Catal Lett **138 (2010**) 1-7.

60. J. Puriwat, W. Chaitree, K. Suriye, S. Dokjampa, P. Praserthdam, and J. Panpranot, *Elucidation of the basicity dependence of 1-butene isomerization on MgO/Mg(OH)$_2$ catalysts.* Catalysis Communications **12 (2010**) 80–85.

61. C. Chizallet, H. Petitjean, G. Costentin, H. Lauron-Pernota, J. Maquet, C. Bonhomme, and M. Che, *Identification of the OH groups responsible for kinetic basicity on MgO surfaces by 1H MAS NMR.* Journal of Catalysis **268 (2009**)

62. X. Guo, X. Wang, J. Shen, and C. Song, *Shape-selective synthesis of 4,4′-dimethyl-biphenyl over modified ZSM-5 catalysts.* Catalysis Today **93–95 (2004**) 411–416.

63. S. Gao, X. Zhu, X. Li, Y. Wang, S. Xie, S. Du, F. Chen, P. Zeng, S. Liu, and L. Xu, *Direct amination of isobutylene over zeolite catalysts with various topologies and acidities* Journal of Energy Chemistry **(2017**) In Press, Accepted Manuscript

64. D. He, D. Chen, H. Hao, J. Yu, J. Liu, J. Lu, G. Wan, S. He, K. Li, and Y. Luo, *Enhanced activity and stability of Sm-doped HZSM-5 zeolite catalysts for catalytic methyl mercaptan (CH_3SH) decomposition.* Chemical Engineering Journal **317 (2017**) 60–69.

65. W. Choopun and S. Jitkarnk, *Catalytic activity and stability of HZSM-5 zeolite and hierarchical uniform mesoporous MSU-SZSM-5 material during bio-ethanol dehydration.* Journal of Cleaner Production **135 (2016**) 368–37.

66. S. Tamiyakul, W. Ubolcharoen, D. N. Tungasmita, and S. Jongpatiwut, *Conversion of glycerol to aromatic hydrocarbons over Zn-promoted HZSM-5 catalysts.* Catalysis Today **256 (2015**) 325–335.

67. K. Ding, Z. Zhong, J. Wang, B. Zhang, M. Addy, and R. Ruan, *Effects of alkali-treated hierarchical HZSM-5 zeolites on the production of aromatic hydrocarbons from catalytic fast pyrolysis of waste cardboard.* Journal of Analytical and Applied Pyrolysis **(2017**) In Press, Corrected Proof

68. C. Yang, M. Qiu, S. Hu, X. Chen, G. Zeng, Z. Liu, and Y. Sun, *Stable and efficient aromatic yield from methanol over alkali treated hierarchical Zn-containing HZSM-5 zeolites.* Microporous and Mesoporous Materials **231 (2016**) 110–116.

69. R. Molinder, T. P. Comyn, N. Hondow, J. E. Parkerc, and V. Dupont, *In situ X-ray diffraction of CaO based CO_2 sorbents.* Energy Environ. Sci. **5 (2012**) 8958–8969.

70. S. Vichaphund, V. Sricharoenchaikul, and D. Atong, *Industrial waste derived CaO-based catalysts for upgrading volatiles during pyrolysis of Jatropha residues.* Journal of Analytical and Applied Pyrolysis **124 (2017**) 568–575.

71. J. Fagerlund, J. Highfieldb, and R. Zevenhoven, *Kinetics studies on wet and dry gas–solid carbonation of MgO and $Mg(OH)_2$ for CO_2 sequestration.* RSC Advances **2 (2012**) 10380–10393.

72. B. R. Vahid and M. Haghighi, *Biodiesel production from sunflower oil over MgO/MgAl2O4 nanocatalyst: Effect of fuel type on catalyst nanostructure and performance.* Energy Conversion and Management **134 (2017**) 290–300.

73. B. Zhao, D. Jiang, and Y. Xie, *Dispersion of Na_2CO_3 on Al_2O_3 and the threshole effect in flue-gas desulfurization.* Fuel **81 (2002**) 1565-1568.

74. H. E. Çamurlu, *Effect of Na2CO3 on hexagonal boron nitride prepared from urea and boric acid.* Ceramics International **37 (2011**) 1993–1999.

75. W. Lutz, *Zeolite Y: Synthesis, Modification, and Properties—A Case Revisited.* Advances in Materials Science and Engineering **2014 (2014**) 1-20.

76. A. Choudhary, B. Das, and S. Ray, *Encapsulation of a Ni salen complex in zeolite Y: an experimental and DFT study.* Dalton Trans **44 (2015**) 3753-3763.

77. S. Rajendra, I. Nobuhiro, F. Shin-ichiro, and A. Masahiko, *Dealumination of Zeolite Beta Catalyst under Controlled Conditions for Enhancing Its Activity in Acylation and Esterification.* Catalysis Letters **130(3-4) (2009**) 655-663.

78. M. Tangestanifard and H. S. Ghaziaskar, *Methylation of toluene with methanol in sub/supercritical toluene using H-beta zeolite as catalyst.* The Journal of Supercritical Fluids **113 (2016**) 80–88.

79. A. S. A. Dughaithe and H. D. Lasa, *HZSM-5 Zeolites with Different SiO_2/Al_2O_3 Ratios. Characterization and NH_3 Desorption Kinetics.* Ind. Eng. Chem. Res. **53 (40) (2014**) 15303–15316.

80. X . H. Vu, R. Eckelt, U. Armbruster, and A. Martin, *High-Temperature Synthesis of Ordered Mesoporous Aluminosilicates from ZSM-5 Nanoseeds with Improved Acidic Properties.* Nanomaterials **4 (2014**) 712-725.

81. S. Cava, S. M. Tebcherani, I. A. Souza, S. A. Pianaro, C. A. Paskocimas, E. Longo, and J. A. Varela, *Structural characterization of phase transition of Al_2O_3 nanopowders*

obtained by polymeric precursor method. Materials Chemistry and Physics **103 (2007**) 394–399.

82. Y. Jian-hong, S. You-yi, G. Jian-feng, and X. Chun-yan, *Synthesis of crystalline γ -Al2O3 with high purity, .* Trans. Nonferrous Met. Soc. China **19 (2009**) 1237-1242.

83. W. Kiatkittipong, K. Yoothongkham, C. Chaisuk, P. Praserthdam, S. Goto, and S Assabumrungrat, *Self-Etherification Process for Cleaner Fuel Production.* Catal Lett **128 (2009**) 154–163.

84. I. H. Son, S. J. Lee, I. Y. Song, W. S. Jeon, I. Jung, D. J. Yun, D. W. Jeong, J. Shim, W. Jang, and H. Roh, *Study on coke formation over Ni/γ -Al_2O_3, Co-Ni/γ -Al_2O_3, and Mg-Co-Ni/γ -Al_2O_3 catalysts for carbon dioxide reforming of methane.* Fuel **136 (2014**) 194-200.

85. H. Gu, D. Cao, J. Wang, X. Lu, Z. Li, C. Niu, and H. Wang, *Micro-CaCO3 conformal template synthesis of hierarchical porous carbon bricks: As a host for SnO2 nanoparticles with superior lithium storage performance.* Materialstoday energy **4 (2017**) 75–80.

86. M. A. Aramendı, V. Borau, J. C. Colmenares, A. Marinas, J. M. Marinas, J. A. Navı, and F. J. Urbano, *Modification of the photocatalytic activity of Pd/TiO_2 and Zn/TiO_2 systems through different oxidative and reductive calcination treatments.* Applied Catalysis B: Environmental **80 (2008**) 88–97.

87. H. Jiang, X. Yu, R. Nie, X. Lu, D. Zhou, and Q. Xia, *Selective hydrogenation of aromatic carboxylic acids over basic N-doped mesoporous carbon supported palladium catalysts.* Applied Catalysis A: General **520 (2016**) 73–81.

88. J. G. Na, J. K. Han, Y. K. Oh, J. H. Park, T. S. Jung, S. S. Han, H. C. Yoon, S. H. Chung, J. N. Kim, and C. H. Ko, *Decarboxylation of microalgal oil without hydrogen into hydrocarbon for theproduction of transportation fuel.* Catalysis Today **185 (2012**) 313–317.

89. Q. Liu, H. Zuo, Q. Zhang, T. Wang, and L. Ma, *Hydrodeoxygenation of palm oil to hydrocarbon fuels over Ni/SAPO- 11 catalysts.* Chinese Journal of Catalysis **35 (2014**) 748–756.

90. T. Haryatia, Y. B. C. Man, A. Asbi, H. M. Ghazali, and L. Buan, *Determination of Iodine Value of Palm Oil by Differential Scanning Calorimetry.* Journal of the American Oil Chemists' Society **74(8) (2015**) 939-942.

91. C. M.R. Prado and N.R. A. Filho, *Production and characterization of the biofuels obtained by thermal cracking and thermal catalytic cracking of vegetable oils.* J. Anal. Appl. Pyrolysis **86 (2009**) 338–347.

92. M. Gülüm and A. Bilgin, *Density, flash point and heating value variations of corn oil biodiesel–diesel fuel blends.* Fuel Processing Technology **134 (2015**) 456–464.

93. I. K. Hong, J. R. Lee, and S. B. Lee, *Fuel properties of canola oil and lard biodiesel blends: Higher heating value, oxidative stability, and kinematic viscosity.* Journal of Industrial and Engineering Chemistry **22 (2015**) 335–340.

94. A. C. Knipe and W. E. Watts, *Oganic reaction mechanism.* John wiley and Sons **(1997**) 70-72.

95. Z. W. Liu, X. Li, K. Asami, and K. Fujimoto, *Selective production of iso-paraffins from syngas over Co/SiO_2 and Pd/beta hybrid catalysts.* Catalysis Communications **6 (2005**) 503–506.

96. E. F. Iliopoulou, E. Heracleous, A. Delimitis, and A. A. Lappas, *Producing high quality biofuels: Pt-based hydroisomerization catalysts evaluated using BtL-naphtha surrogates.* Applied Catalysis B: Environmental **145 (2014**) 177–186.

97. S. V. Konnov, I. I. Ivanov, O. A. Ponomareva, and V. I. Zaikovskii, *Hydroisomerization of n-alkanes over Pt-modified micro/mesoporous materials obtained by mordenite recrystallization.* Microporous and Mesoporous Materials **164 (2012**) 222–231.

98. B. R. Brown, *The mechanism of thermal decarboxylation.* Q. Rev. Chem. Soc. **5 (1951**) 131-146.

99. M. Shimouchi H. Tani, H. Haga, K. Fujimoto, *Development of Direct Production Process of Diesel Fuel from Vegetable Oils.* Journal of the Japan Institute of Energy **90 (2011**) 466-470.

100. I. Shimada, R. Imai, Y. Hayasaki, H. Fukunaga, N. Takahashi, and T. Takatsuka, *Increasing Octane Value in Catalytic Cracking of n-Hexadecane with Addition of *BEA Type Zeolite.* Catalysts **5 (2015**) 703-717.

APPENDIX

Appendix A

Calculation for Preparation of 0.5wt%Pd/beta catalyst

0.5wt%Pd/beta catalyst was prepared by impregnation method

Using the palladium nitrate as a precursor $Pd(NO_3)_2.2H_2O$

In order to synthesize 10 g of catalyst:

Therefore weight of Pd = 10 x 0.5/100 = 0.05 g

$Pd(NO_3)_2.2H_2O$ (MW = 266.46 g/mol) and Pd (MW = 106.42 g/mol)

Therefore weight of $Pd(NO_3)_2.2H_2O$ = 266.46 x 0.05/106.42 = 0.125 g

Calculation for Preparation of Na_2SiO_3

Sodium silicate was prepared by wet impregnation method

Using SiO_2 and NaOH as the precursors. The molar ratio between SiO_2 and NaOH is 1:2

Basic: 2 g of SiO_2

SiO_2 (MW = 60.08 g/mol); NaOH (MW = 40 g/mol)

Therefore weight of NaOH = 2 x 40 x 2/60.08 = 2.67 g

Calculation of yield CO and CO_2

Area Standard 1%CO = 496,2 1%CO_2 = 558,2

Reaction conditions: Temperature 460 ^{o}C, time: 2.5 hours, catalyst: MgO

Time (min)	Flow rate (ml/min)	Area TCD	
		CO	CO_2
30	25	3046,1	12277,4
60	25	3942,7	11967,1
90	25	4049	12031,3
120	25	4149,6	11742,2
150	25	2581,4	2579,3

Mole of CO gas = (Area CO/Area std CO) x 1% x time (min) x flow rate/22400

Mole of CO_2 gas = (Area CO_2/Area std CO_2) x 1% x time (min) x flow rate/22400

Then

Time (min)	Flow rate (ml/min)	mole TCD	
		CO	CO_2
30	25	0.002055	0.007364
60	25	0.00266	0.007178
90	25	0.002732	0.007217
120	25	0.0028	0.007043
150	25	0.001742	0.001547

Therefore

Mole of CO gas = 0.002055 + 0.00266 + 0.002732 + 0.0028 + 0.001742= 0.01199 mol

Mole of CO_2 gas = 0.007364 + 0.007178 + 0.007217 + 0.007043 + 0.001547 = 0.03035 mol

Weight of CO gas= 0.01199 x 28 = 0.336 g

Weight of CO gas= 0.03035 x 44= 1.335 g

Total palm oil inputted to reaction: 15.97 g

Yield of CO= 0.336 x 100/15.97 = 2.1 wt%

Yield of CO_2= 1.335 x 100/15.97 = 8.4 wt%

Calculation for acid amount (base on NH_3-TPD result)

Standard: HUSY

TCD area: 6.02

Acidity: 1.04 mmolNH_3/g

Hence:

Acidity of catalyst = [area of fit peaks] x 1.04/6.02

Catalyst	TCD area		
	Weak	Average	Strong
Al_2O_3	0.37	0.00	0.00
HY	0.12	0.21	0.21
Beta	0.11	0.04	0.00
Pd-Beta	0.09	0.04	0.00
HZSM5	0.12	0.06	0.00

Then:

Acidity of Al_2O_3 = 0.37 x 1.04/6.02 = 0.06 mmolNH_3/g

Acidity of HY = (0.12 + 0.21 + 0.21) x 1.04/6.02 = 0.54 mmolNH_3/g

Acidity of Beta = (0.11 + 0.04) x 1.04/6.02 = 0.16 mmolNH_3/g

0.5wt%Pd/beta = (0.09 + 0.04) x 1.04/6.02 = 0.14 mmolNH_3/g

HZSM-5 = (0.12 + 0.06) x 1.04/6.02 = 0.17 mmolNH_3/g

Calculation for base amount (base on CO_2-TPD result)

Standard: Dolomite

TCD area: 36.32

Basicity: 10.83 mmolNH_3/g

Hence:

Basicity of catalyst = [area of fit peaks] x 10.83/36.32

Catalyst	TCD area		
	Weak	Average	Strong
MgO	0.02	0.00	0.00
CaO	0.00	0.00	2.83
Na_2SiO_3	0.00	0.00	0.49
SiO_2	0.00	0.00	0.00

Then:

Basicity of MgO = 0.02 x 10.38/36.32 = 0.01 mmolCO_2/g

Basicity of CaO = 2.83 x 10.38/36.32 = 0.84 mmolCO_2/g

Basicity of Na_2SiO_3 = 0.49 x 10.38/36.32 = 0.15 mmolCO_2/g

Appendix B

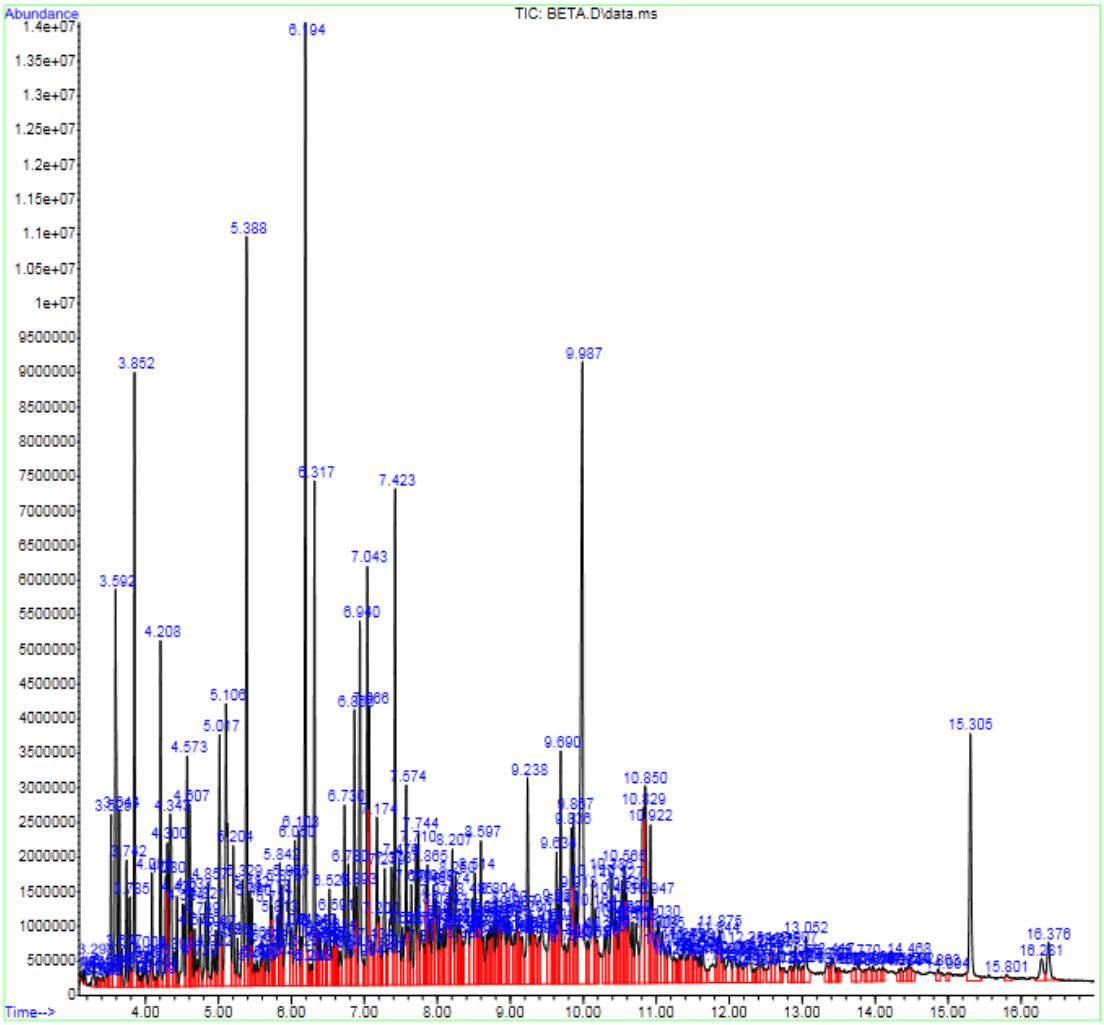

Figure B-1 GC-MS chromatogram of cracked oil from deoxygenation of palm oil on MgO catalyst

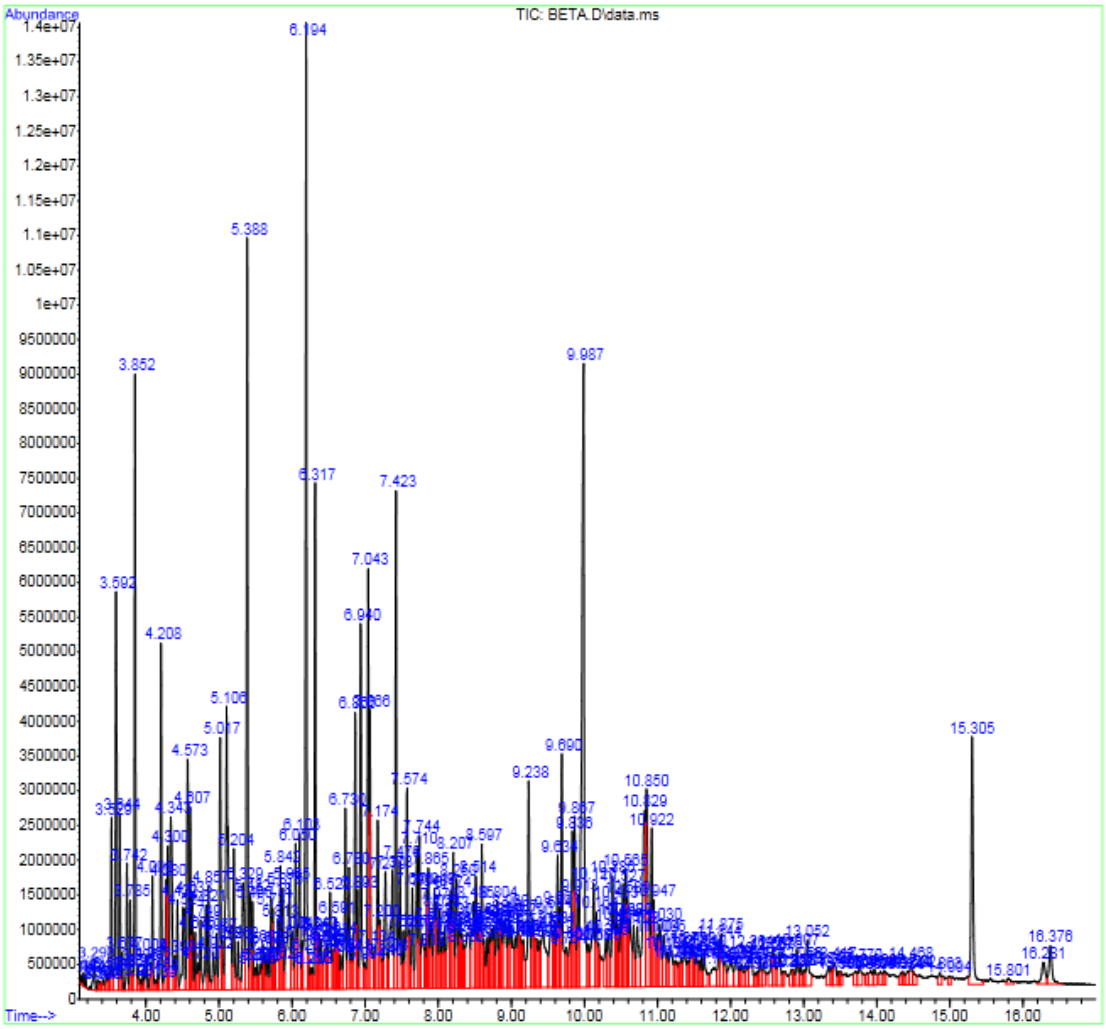

Figure B-2 GC-MS chromatogram of cracked oil from deoxygenation of palm oil on zeolite beta catalyst

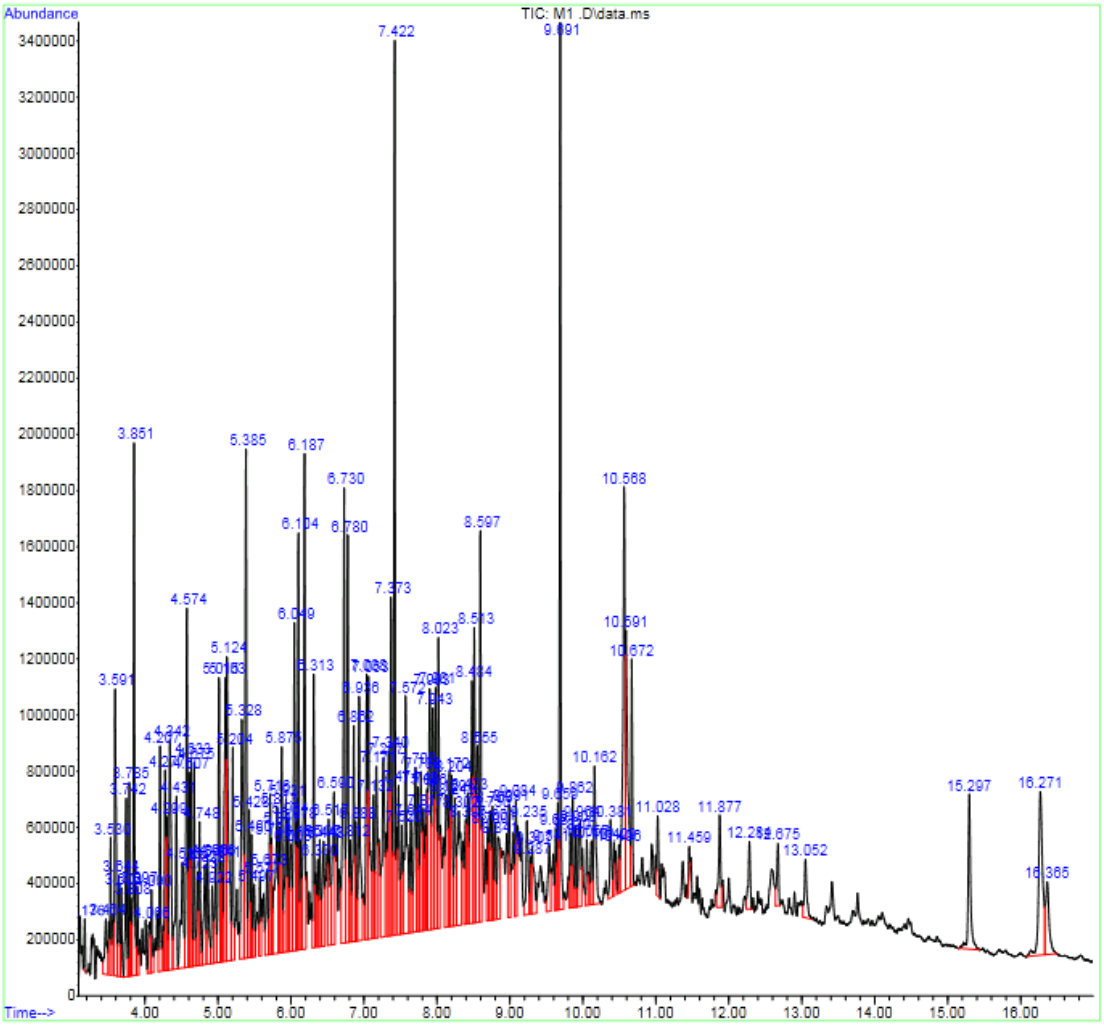

Figure B-3 GC-MS chromatogram of cracked oil from deoxygenation of palm oil on mixed 75%MgO 25% beta catalyst

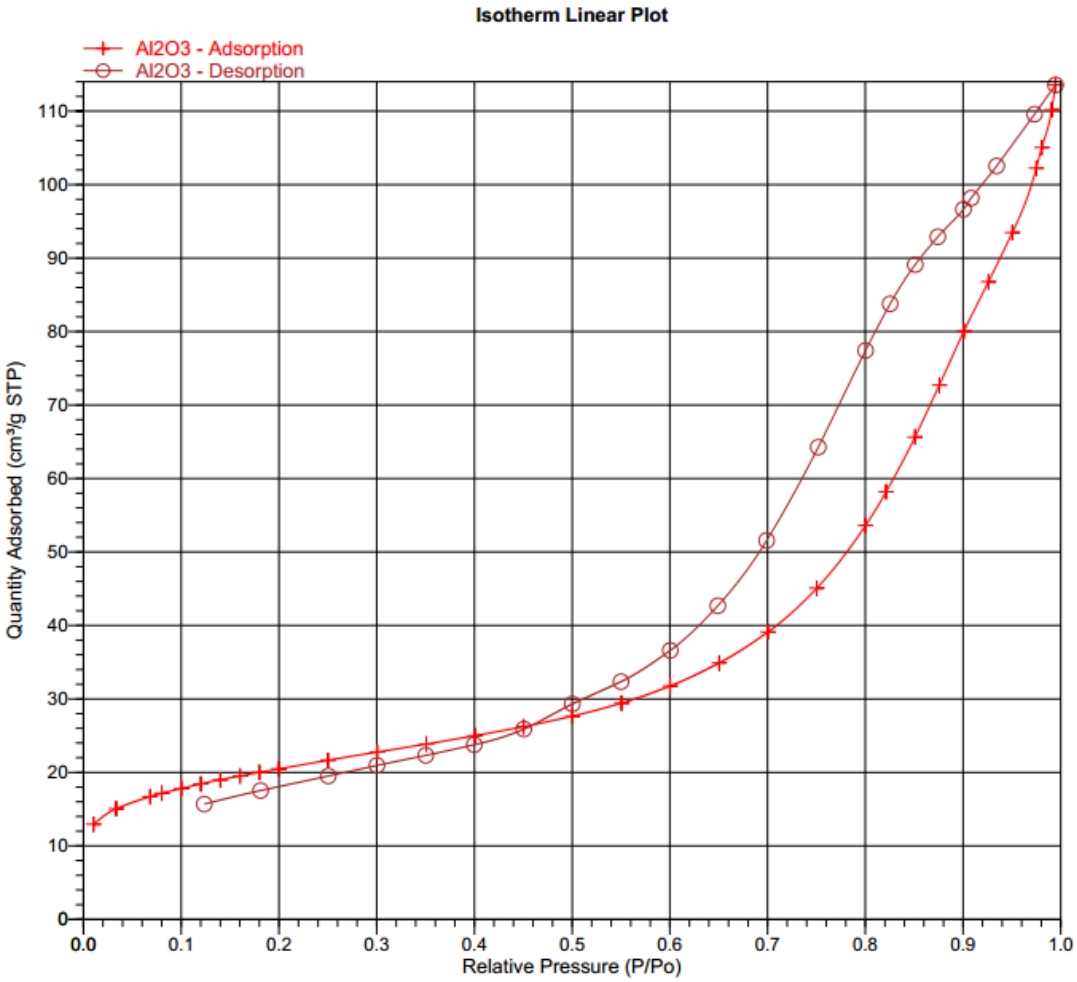

Figure B-4 Isotherm Linear plot of Al_2O_3

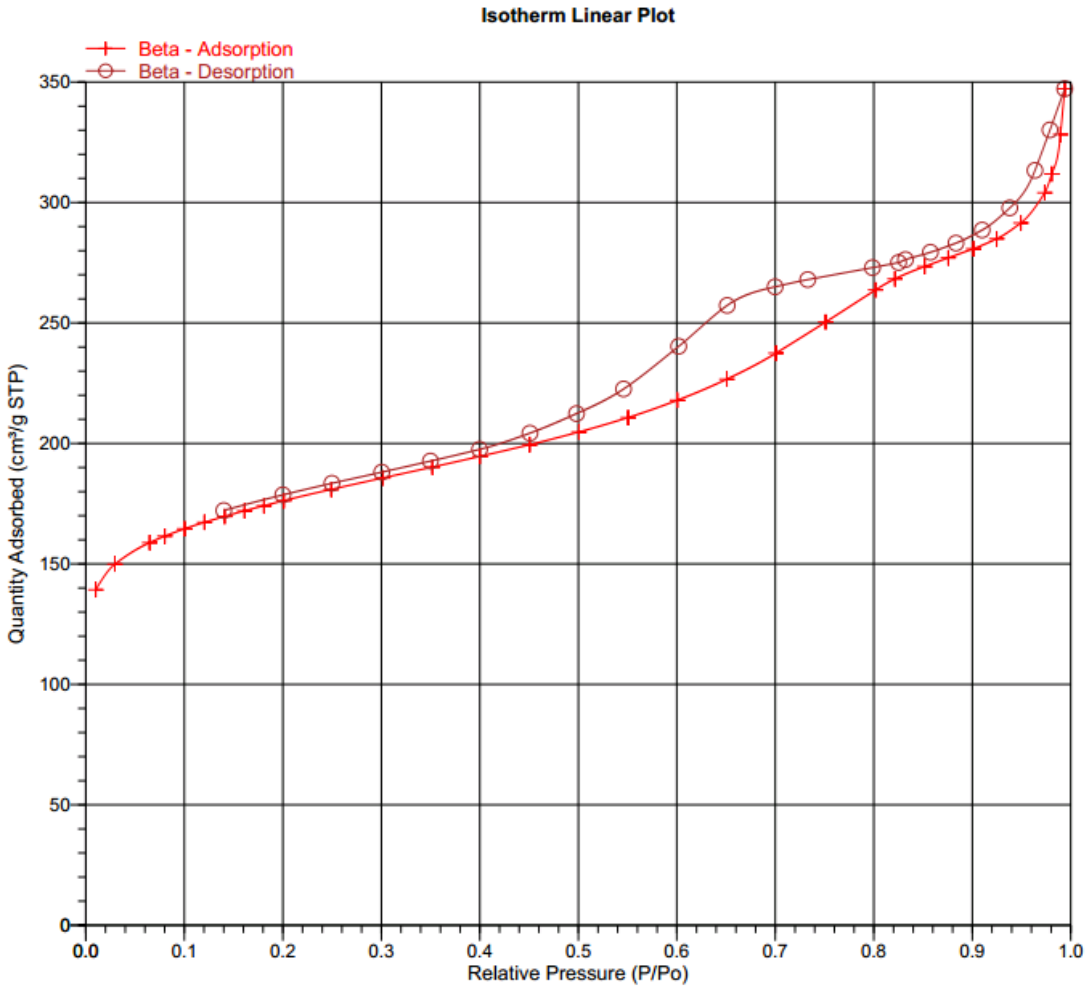

Figure B-5 Isotherm Linear plot of zeolite beta

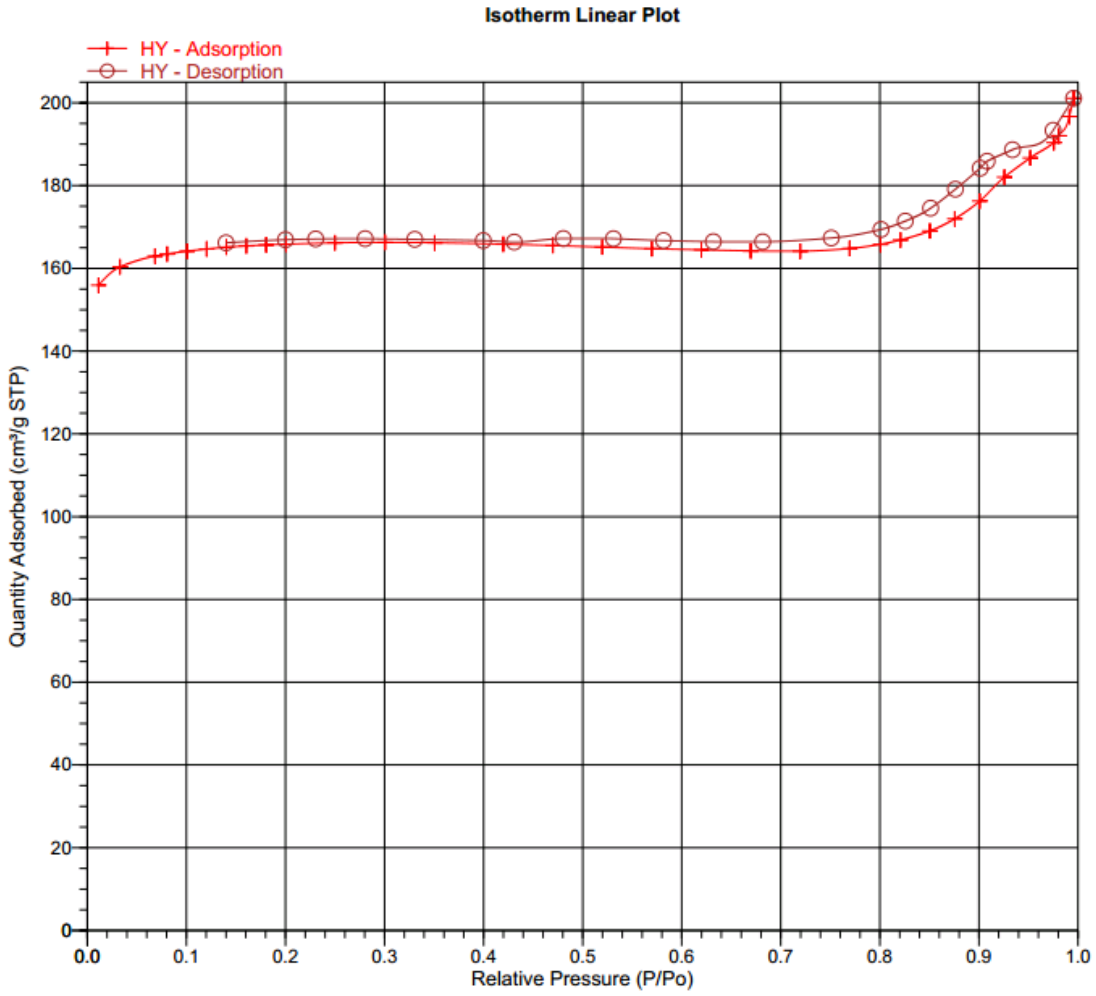

Figure B-6 Isotherm Linear plot of zeolite HY

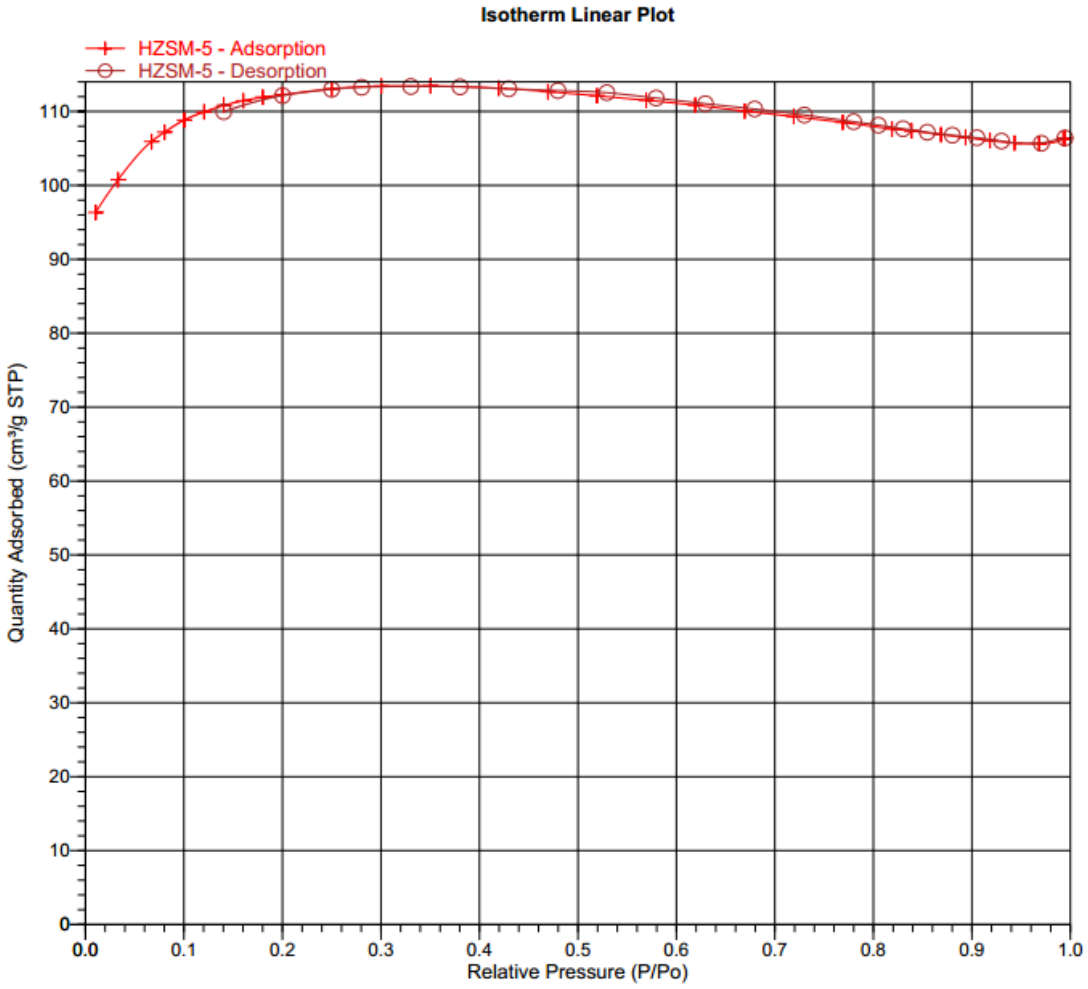

Figure B-7 Isotherm Linear plot of zeolite HZSM-5

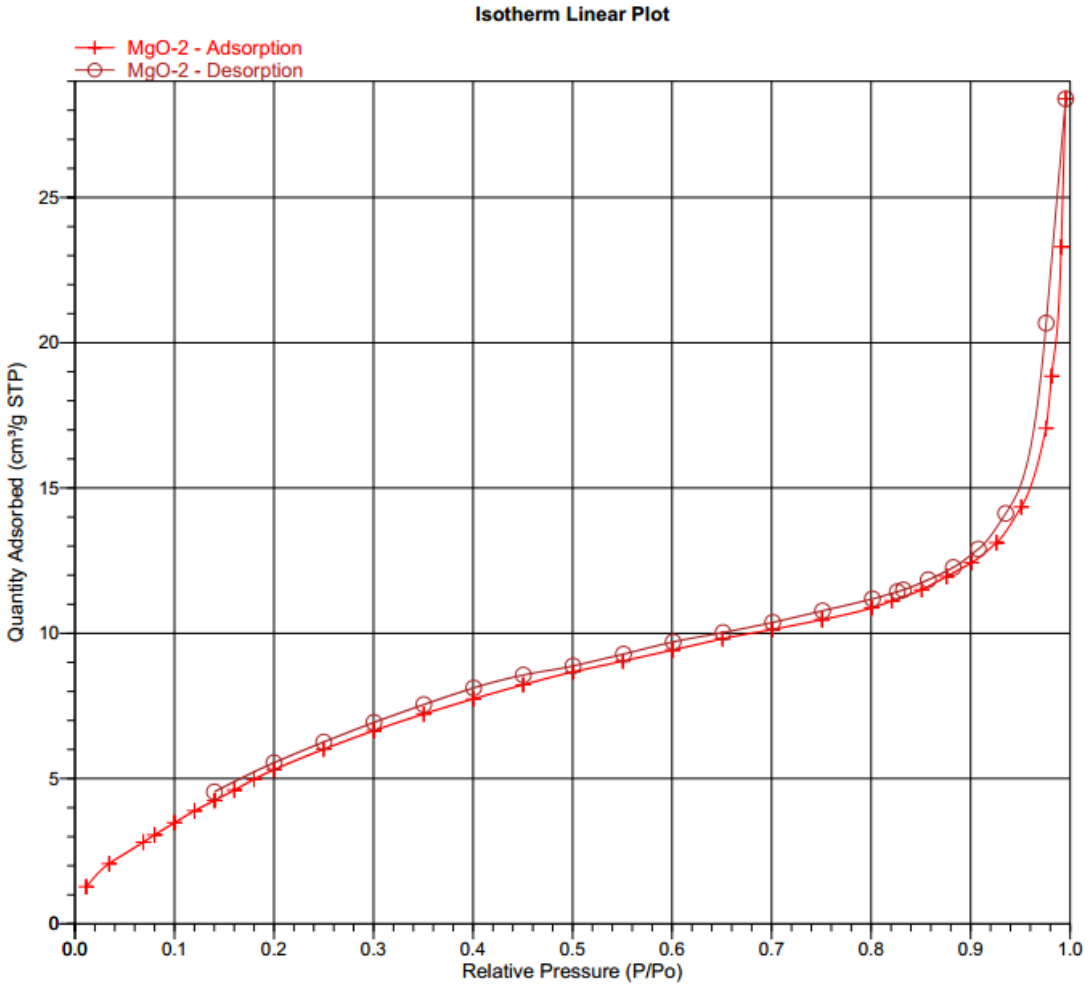

Figure B-8 Isotherm Linear plot of MgO

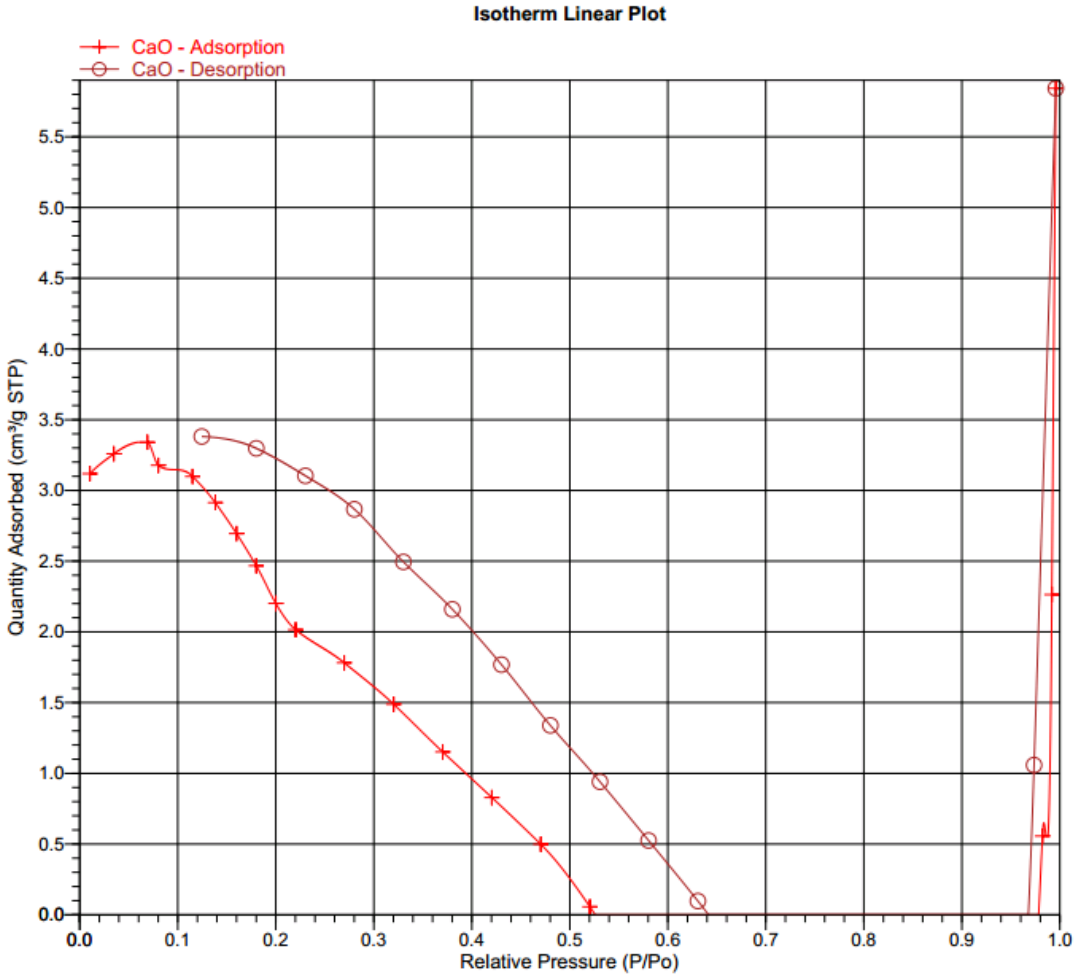

Figure B-9 Isotherm Linear plot of CaO

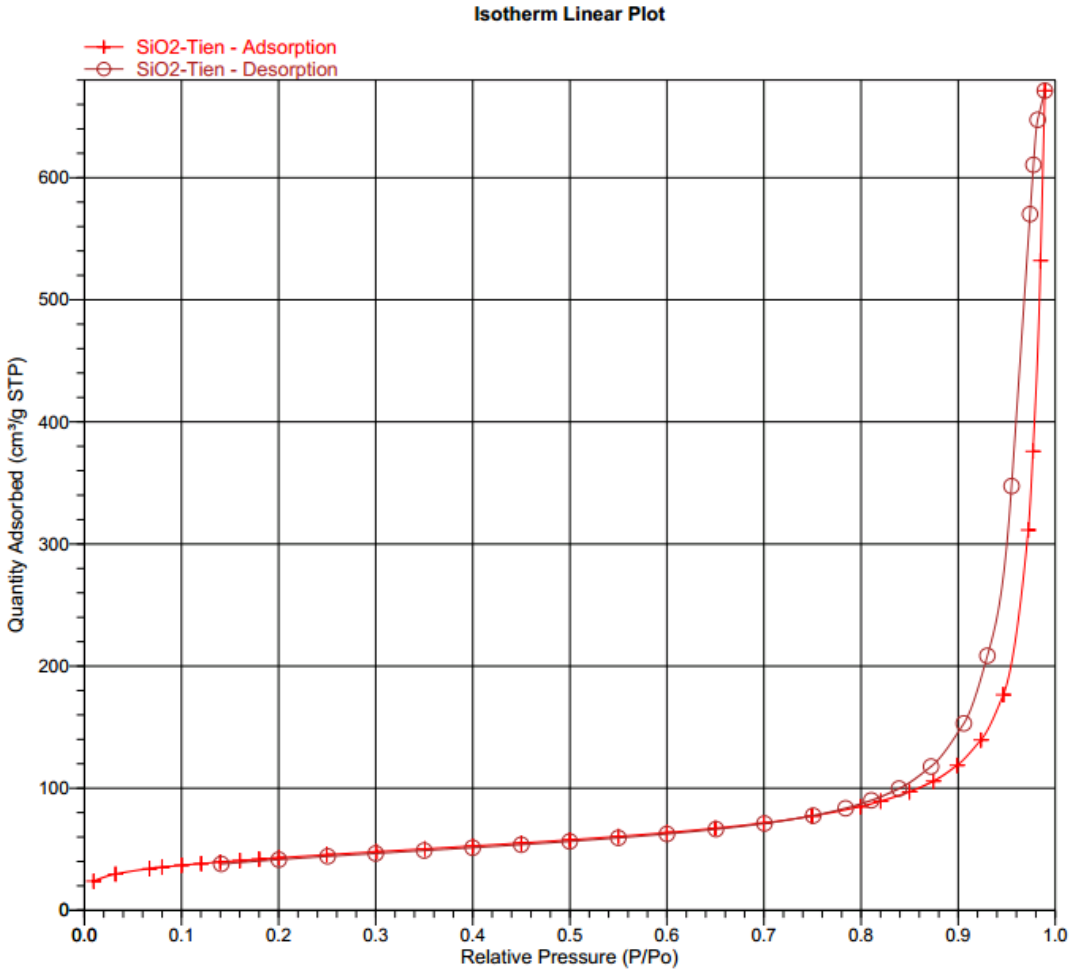

Figure B-10 Isotherm Linear plot of SiO_2

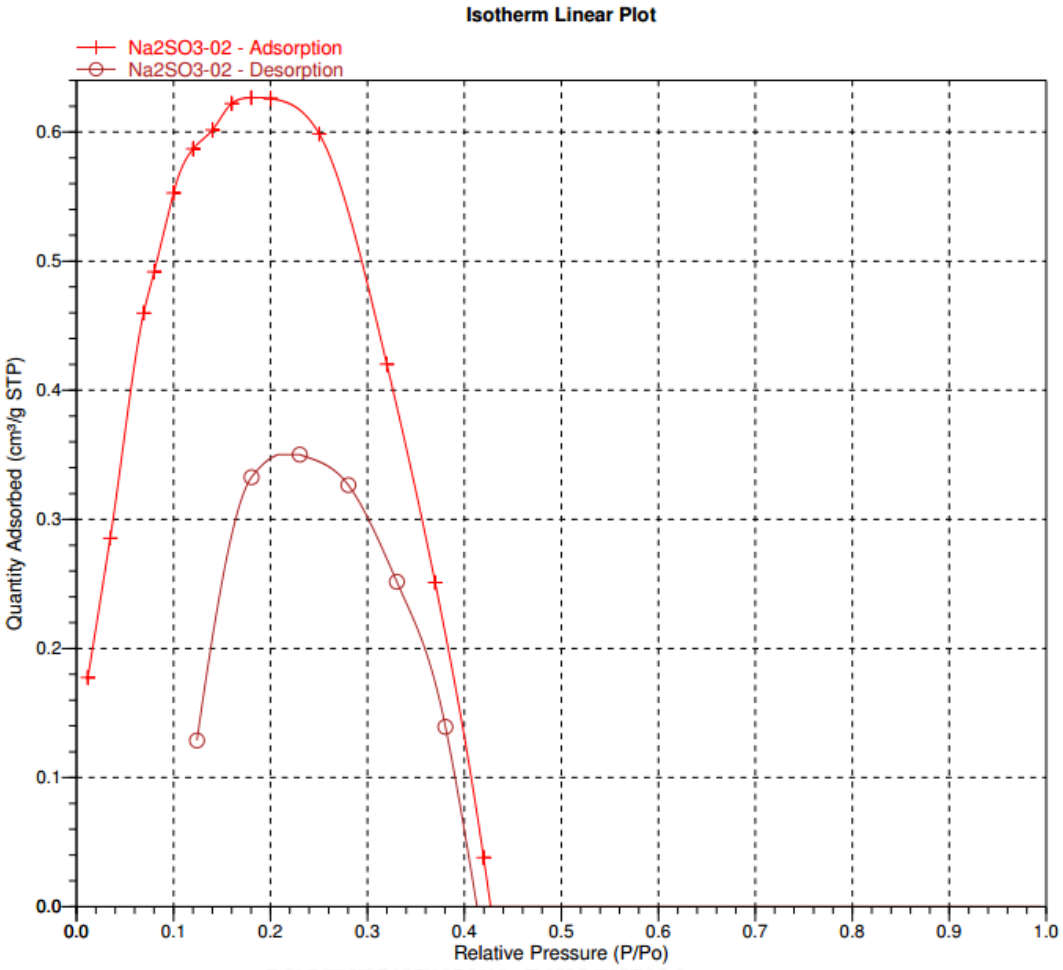

Figure B-11 Isotherm Linear plot of Na_2SiO_3

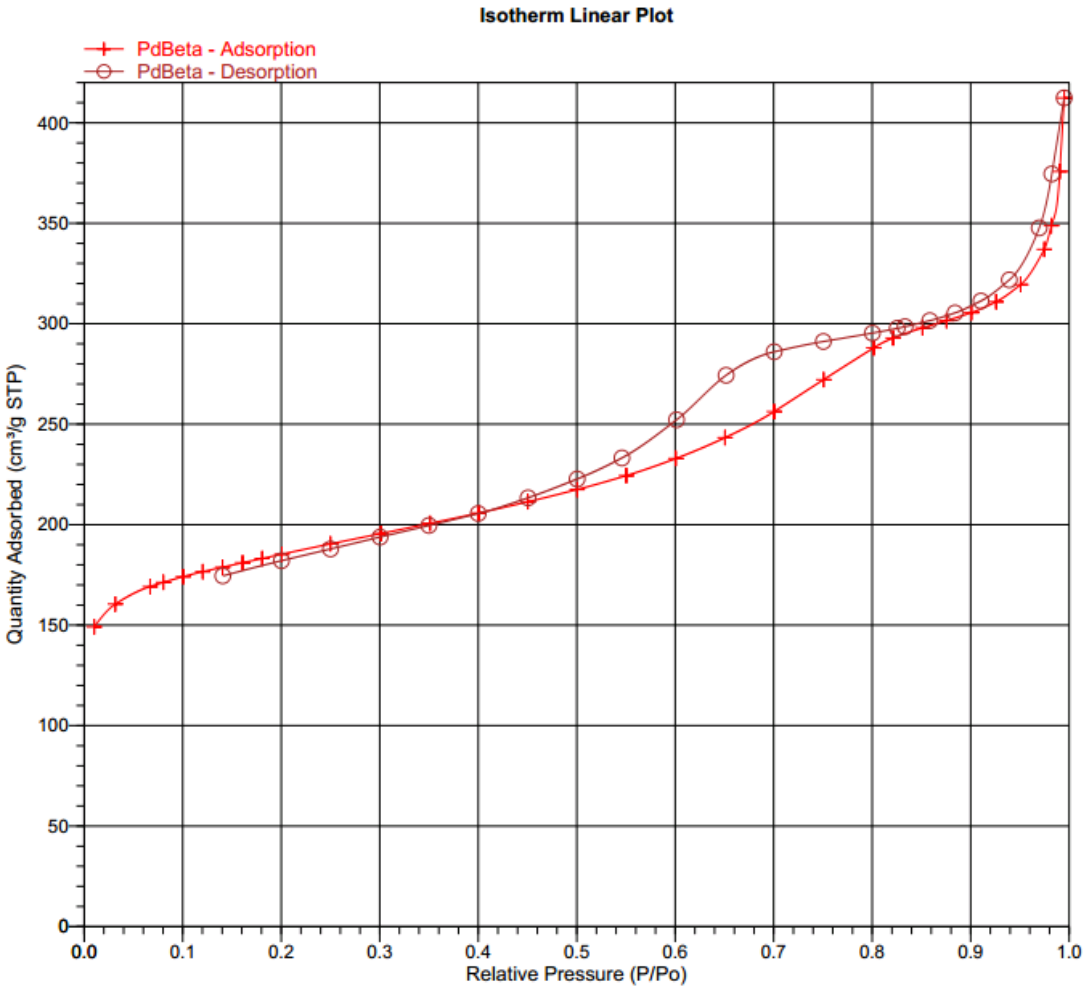

Figure B-12 Isotherm Linear plot of 0.5 wt%Pd/beta

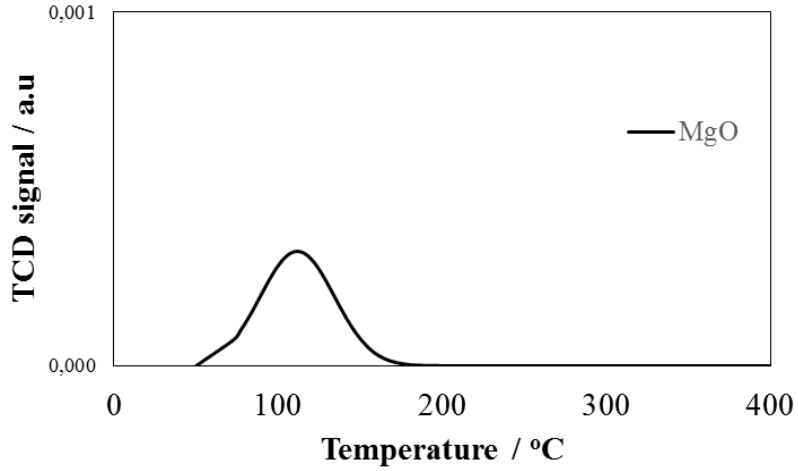

Figure B-13 CO_2-TPD profile of MgO

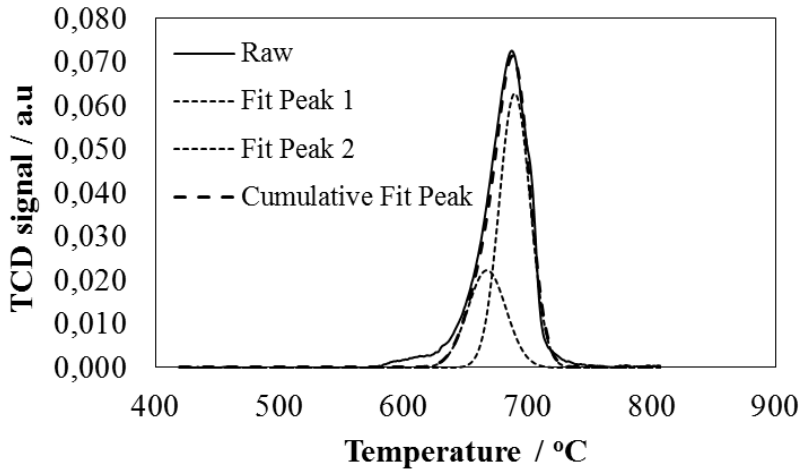

Figure B-13 CO_2-TPD profile of MgO

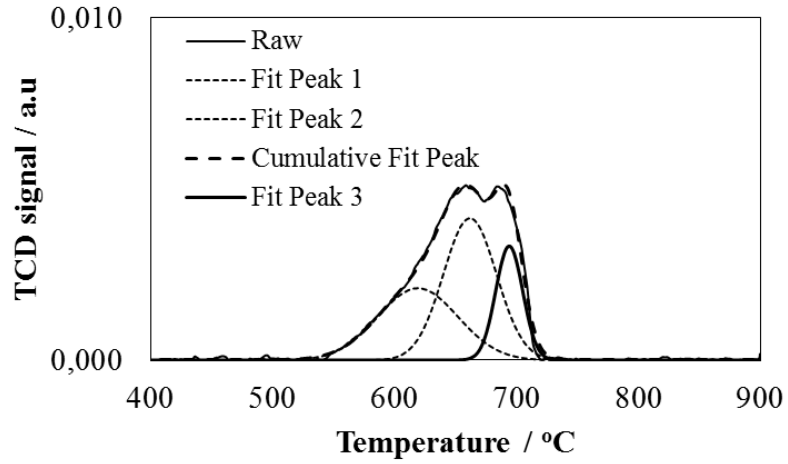

Figure B-14 CO_2-TPD profile of Na_2SiO_3

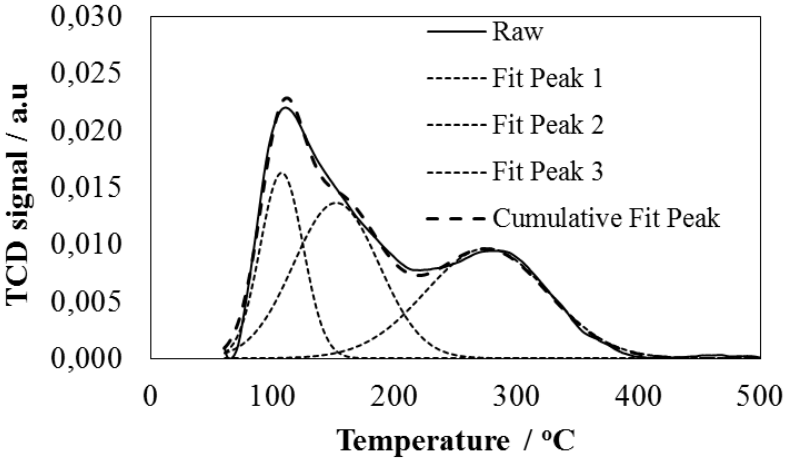

Figure B-15 NH_3-TPD profile of zeolite HY

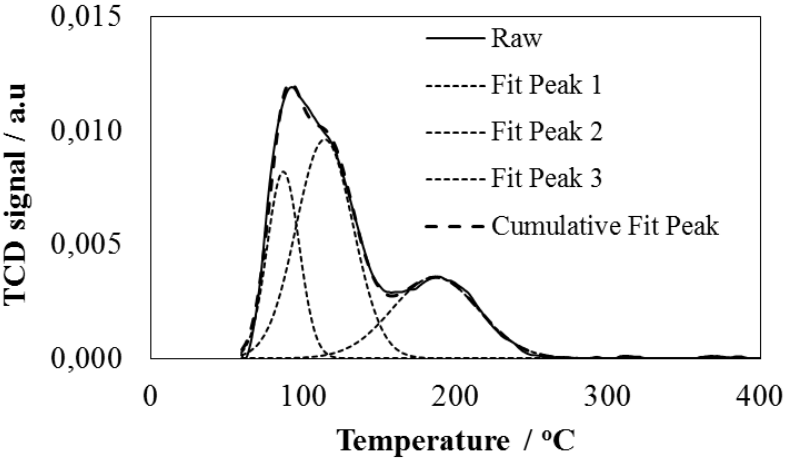

Figure B-16 NH_3-TPD profile of zeolite beta

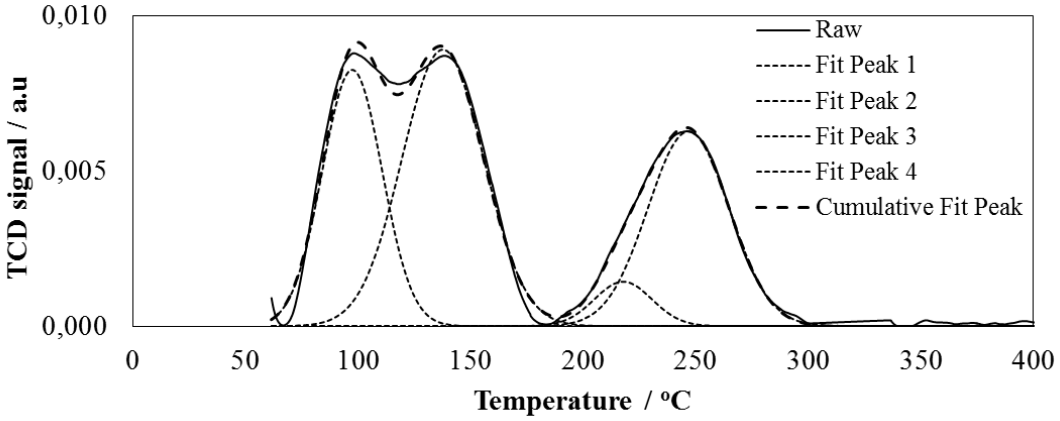

Figure B-17 NH_3-TPD profile of zeolite HZSM-5

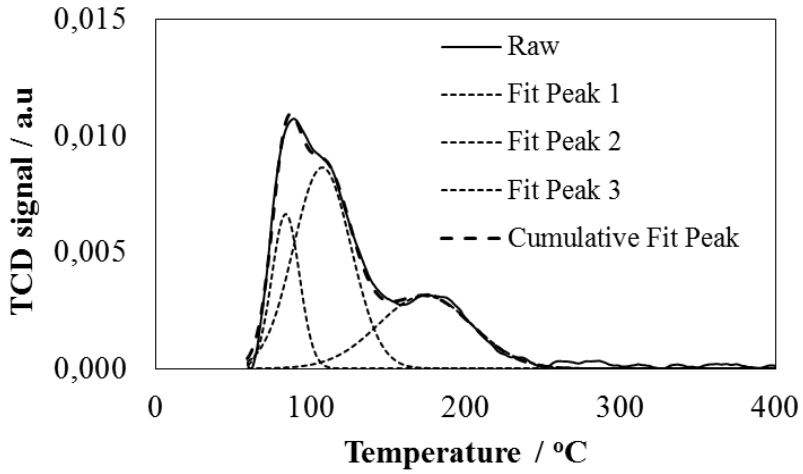

Figure B-18 NH_3-TPD profile of 0.5 wt% Pd/beta

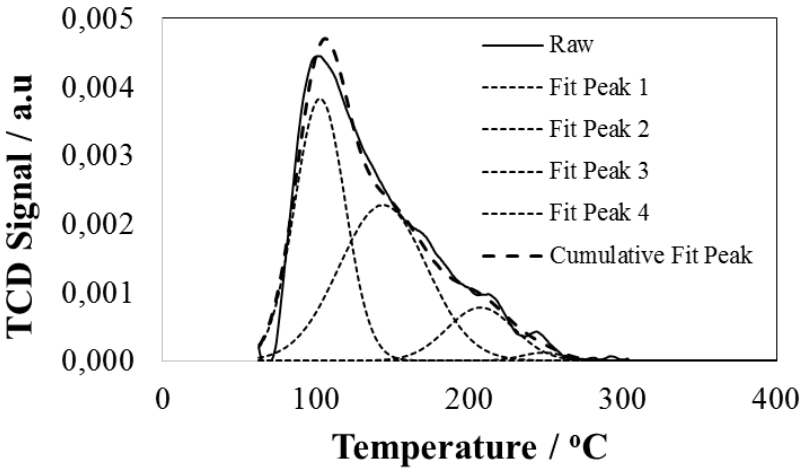

Figure B-18 NH_3-TPD profile of Al_2O_3

VITA

Mr Tieu Quang Trieu was born on July 20, 1986 in Travinh, Vietnam. He hold a bachelor degree in Chemical Engineering from Vietnam National University – Hochiminh City University of Technology in 2008 and he has finished the Master of Engineering from the same university in 2012. He has continued his study in PhD's degree in the field of chemical technology, Faculty of Science, Chulalongkorn University, Bangkok, Thailand since 2014.

Presentation:

Oral presentation at The International Congress on Advance Materials (AM 2016) in the topic of "Direct synthesize of iso-paraffin fuel from palm oil on mixed heterogeneous base and acid catalysts".

Publication:

1. Nguyen Tri, Luu Cam Loc*, Truong Phuong Thinh, Trieu Quang Tien, Hoang Tien Cuong, Dang Hoang Nam, Preparation of catalysts CuO/CeO2 modified by Pt for deep oxidation of carbon monoxide and p-xylene in the presence of water, Vietnam J. Chemistry, 51 (2013) 435 – 441.

2. Tien Quang Trieu, Guoqing Guan, Guoguo Liu, Noritatsu Tsubaki, Chanatip Samart, Prasert Reubroycharoen, Direct synthesis of isoparaffin fuel from palm oil on mixed heterogeneous acid and base catalysts, Monatsh Chem, DOI 10.1007/s00706-017-1963-3